

AD-A094 614

NAVAL POSTGRADUATE SCHOOL MONTEREY CA
NUMERICAL SOLUTION OF STEADY AND PERIODICALLY PULSED TWO-DIMENS--ETC(U)

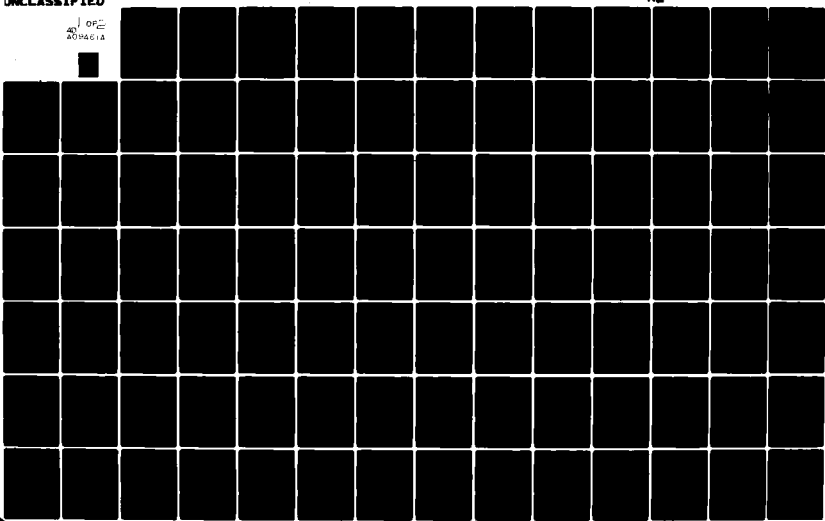
F/G 20/4

APR 80 J C LAI, J M SIMMONS

NL

UNCLASSIFIED

1 op²
A09461A



NPS67-80-015

AD A094614

NAVAL POSTGRADUATE SCHOOL
Monterey, California



LEVEL

DTIC
ELECT
FEB 5 1981

Numerical Solution of Steady and
Periodically Pulsed Two-Dimensional
Turbulent Free Jets,

by

Joseph C. S. Lai

and

J. M. Simmons

April 1980

Approved for public release; distribution
unlimited

Prepared for
Naval Air Systems Command
Washington, D.C. 20361

DDC FILE COPY

812 04 344

NAVAL POSTGRADUATE SCHOOL

Monterey, California

Rear Admiral J. J. Ekelund
Superintendent

Jack R. Borsting
Provost

The work reported herein was supported by the Naval Air Systems Command, Washington, DC.

Reproduction of all or part of this report is authorized.

This report was prepared by:

Joseph Lai
Joseph C. S. Lai
Visiting Research Associate

J. M. Simmons
J. M. Simmons
Senior Lecturer of
Mechanical Engineering
University of Queensland
Brisbane, Australia

Reviewed by:

M. F. Platzer
M. F. Platzer, Chairman
Department of Aeronautics

Released by:

William M. Tolles
W. M. Tolles
Dean of Research

UNCLASSIFIED

SECURITY CLASSIFICATION OF THIS PAGE (When Data Entered)

REPORT DOCUMENTATION PAGE		READ INSTRUCTIONS BEFORE COMPLETING THIS FORM
1. REPORT NUMBER NPS67-80-015	2. GOVT ACCESSION NO. <i>AD-A094 814</i>	3. RECIPIENT'S CATALOG NUMBER
4. TITLE (and Subtitle) Numerical Solution of Steady And Periodically Pulsed Two-Dimensional Turbulent Free Jets	5. TYPE OF REPORT & PERIOD COVERED Technical Report	
7. AUTHOR(S) Joseph C. S. Lai and J. M. Simmons	6. PERFORMING ORG. REPORT NUMBER	
9. PERFORMING ORGANIZATION NAME AND ADDRESS NAVAL POSTGRADUATE SCHOOL Monterey, CA 93940	10. PROGRAM ELEMENT, PROJECT, TASK AREA & WORK UNIT NUMBERS 61153N N00019-80-WR-01199	
11. CONTROLLING OFFICE NAME AND ADDRESS NAVAL POSTGRADUATE SCHOOL Monterey, CA 93940	12. REPORT DATE April 1980	
14. MONITORING AGENCY NAME & ADDRESS (if different from Controlling Office) NAVAL POSTGRADUATE SCHOOL Monterey, CA 93940	13. NUMBER OF PAGES 110	
15. SECURITY CLASS. (of this report)		
15a. DECLASSIFICATION OR DOWNGRADING SCHEDULE		
16. DISTRIBUTION STATEMENT (of this Report) Approved for public release, distribution unlimited		
17. DISTRIBUTION STATEMENT (of the abstract entered in Block 20, if different from Report)		
18. SUPPLEMENTARY NOTES		
19. KEY WORDS (Continue on reverse side if necessary and identify by block number) turbulent jets, viscous/inviscid interactions, shear flows, turbulence modelling, computational fluid dynamics, Cebeci-Keller box method		
20. ABSTRACT (Continue on reverse side if necessary and identify by block number) The flow fields of a steady and a periodically pulsed two-dimensional turbulent free jet have been studied by solving the thin shear layer equations by the Keller Box method in transformed variable form. A constant eddy-viscosity formulation was used to model the Reynolds shear stress term. For the steady jet, calculations agree well with documented experimental data. Computed results of the unsteady jet indicate that the mean flow characteristics follow closely those of the steady jet and compare well with		

DD FORM 1 JAN 73 EDITION OF 1 NOV 65 IS OBSOLETE
S/N 0102-014-6601

UNCLASSIFIED

SECURITY CLASSIFICATION OF THIS PAGE (When Data Entered)

UNCLASSIFIED

SECURITY CLASSIFICATION OF THIS PAGE/When Data Entered:

available experimental data. For sufficiently high frequency and amplitude of pulsation or at large streamwise distance, significant unsteady effects occur in the instantaneous quantities.

Accession For	
NTIS GRA&I	
DTIC TAB	
Unannounced	
Justification	
By _____	
Distribution/ _____	
Availability Codes	
Dist	Avail and/or
	Special
A	

DD Form 1473
1 Jan 73
S/N 0102-014-6601

UNCLASSIFIED

SECURITY CLASSIFICATION OF THIS PAGE/When Data Entered:

TABLE OF CONTENTS

	PAGE
Abstract	v
Acknowledgement	vi
Nomenclature	vii
1.0 Introduction	1
2.0 Governing Equations	4
2.1 Governing Equations in Non-dimensional Form	7
2.2 Turbulence Modelling	8
2.3 Governing Equations in Transformed Variable Form	12
3.0 Method of Solution	14
3.1 Finite Difference Form of the Governing Equations	15
3.2 Time-Varying Velocity Profile at the Nozzle Exit	19
3.3 Solution of the Finite Difference Equation	22
3.4 Convergence Criterion	24
3.5 Criterion for the Spreading of Jet . . .	25
3.6 Criterion for the Attainment of Steady State Solution	27
3.7 Mean Momentum Flux, Phase Angle and Peak to Peak Oscillation	29
3.7.1 Mean Momentum Flux	29
3.7.2 Phase Angle	29
3.7.3 Peak to Peak Oscillation	30

	PAGE
4.0 Results and Discussions	32
4.1 Steady Jet	33
4.2 Unsteady Jet	37
4.2.1 Sensitivity of the Solution to the Convergence Criterion	37
4.2.2 Validity of the Criterion for the Attainment of Steady State Solution	38
4.2.3 Sensitivity of the Solution to Time Step	38
4.2.4 Relaxation of the Criterion for Jet Spreading	38
4.2.5 Results	39
5.0 Concluding Remarks	43
6.0 References	45
Appendix A Structure and Listing of Computer Program	48
Appendix B Figures	79
Initial Distribution List	80

ABSTRACT

The flow fields of a steady and a periodically pulsed two-dimensional turbulent free jet have been studied by solving the thin shear layer equations by the Keller Box method in transformed variable form. A constant eddy-viscosity formulation was used to model the Reynolds shear stress term. For the steady jet, calculations agree well with documented experimental data. Computed results of the unsteady jet indicate that the mean flow characteristics follow closely those of the steady jet and compare well with available experimental data. For sufficiently high frequency and amplitude of pulsation or at large streamwise distance, significant unsteady effects occur in the instantaneous quantities.

ACKNOWLEDGEMENT

This work was supported by the Australian Research Grants Committee under Reference No. F77/15026 and by the Naval Air Systems Command, Code AIR 310 under contract No. N0001980WR01199, Job Order No. 57763 Segment 1385/4. The first author (JCSL) is grateful to Professor M. F. Platzer for his encouragement and support during his 6-months visit at the Naval Postgraduate School. Also, thanks are extended to Professor T. Cebeci for his valuable comments.

NOMENCLATURE

Unless otherwise stated, the symbols used in the text have the following meanings.

a	constant defined in Eq. (15a)
b	constant defined in Eq. (15b)
c	constant defined in Eq. (11)
F	% peak-to-peak oscillation of centre-line velocity
f	stream function in (ζ, t, η) coordinates defined in Eq. (15b)
h	nozzle width
M	mean momentum flux in streamwise direction
p*	mean pressure
p*	instantaneous pressure
Q	mean mass flow at any streamwise station
Q _E	mean mass flow at nozzle exit
T	period of pulsation
t	non-dimensional time = $U_{ci}^* t^*/h$
U	non-dimensional mean x-component velocity = U^*/U_{ci}^*
U _o (y)	non-dimensional mean velocity profile at the nozzle exit
u	non-dimensional instantaneous x-component velocity = u^*/U_{ci}^*
u'	non-dimensional x-component velocity fluctuation = u''/U_{ci}^*
v	non-dimensional mean y-component velocity = V^*/U_{ci}^*
v	non-dimensional instantaneous y-component velocity = v''/U_{ci}^*

v' non-dimensional y -component velocity fluctuation = v^*/U_{ci}^*
 x non-dimensional streamwise distance - x^*/h
 y non-dimensional transverse distance - y^*/h
 y_z value of y at which $U = \frac{1}{2}U_c$

GREEK SYMBOLS

Δ difference between two quantities
 ϵ amplitude of pulsation
 ν non-dimensional kinematic viscosity = $\nu^*/(U_{ci}^* h)$
 ν_t eddy-viscosity defined in Eq. (10)
 ν_{eff} Effective eddy viscosity defined in Eq. (13)
 ψ stream function in (ζ, t, y) coordinates defined in Eq. (15b)
 ϕ phase angle
 Φ function defined in Eq. (28)
 η transformed variable defined in Eq. (15b)
 ω non-dimensional angular frequency of pulsation = $\omega^* h / U_{ci}^*$
 ζ non-dimensional distance identical to x
 ζ_0 constant defined in Eq. (15a)

SUPERSCRIPT

* dimensional quantities

SUBSCRIPTS

c centerline
i initial
 ∞ jet edge
Overbar time-average quantities

1.0 Introduction

The steady two-dimensional turbulent jet has long been the subject of many theoretical and experimental investigations because of its important role in many different types of engineering applications such as fluidic and combustion systems and because of its significance in providing fundamental understanding to the physics of flow mechanisms such as turbulence and vortex structures. Owing to its simplicity in configuration, the steady two-dimensional turbulent jet has been studied in detail experimentally and is regarded as one of the most well-documented flows in the literature where sufficient data are available for many practical engineering purposes. However, despite such extensive investigations, for example Heskestad (1965), Gutmark and Wygnanski (1976) and Everitt and Robins (1978), considerable scatter is found to exist between the results of various workers even in the mean flow parameters such as centre-line velocity decay rate and jet spreading rate. Such discrepancies have been casually attributed to different effects such as Reynolds number, aspect ratio, nozzle geometry, initial conditions, upstream turbulence intensities and the uncertainties involved in the hot wire results in regions where reversed flow may occur. Nevertheless, no unified agreement on the effects of such factors and other flow mechanisms on the flow development has been reached. A

comprehensive review and evaluation of the experiemntal data on steady turbulent jets was given by Harsha (1971) and Rodi (1975).

The analytical solution of the fully-developed steady turbulent jet was first sought by Tollmien (1926) followed by Goertler (1942) and Schlichting (1965). With the advent of computer technology and the rapid development of numerical techniques, the steady turbulent jets have commonly been used for turbulence modelling and as standard test cases of turbulence models. Many numerical predictions of steady turbulent jets using various turbulence models have been attempted such as Rodi and Spalding (1970), Launder et al (1972) and Chen and Nikitopoulos (1979) to calculate the flow properties and to complement the experimental results.

Although almost inevitably unsteadiness of varying degrees occurs in practice either desirably to achieve certain favorable characteristics or undesirably due to the fluctuations in the surrounding fluid, very few results appear to have been reported on unsteady turbulent jets both theoretically and experimentally. Only until recently, because of the growing realization of the fundamental and practical implications of an improved understanding of unsteady effects, the excitation of turbulent jets by acoustic (Fiedler and Korschelt (1979)), mechanical (Bremhorst and Harch (1979)) and fluidic (Piatt and Viets (1979)) means has received considerable attention. On the other hand,

closed form solutions of the unsteady jets which adequately describe the flow development can hardly be obtained despite the efforts of Pai (1965) and McCormack et al (1966).

Numerical solution of unsteady laminar jets was obtained by Kent (1973). Although turbulence models have been developed to give sufficiently accurate predictions of a wide variety of steady flows, the applicability of such turbulence models to unsteady flows is uncertain.

The objectives of this study are to apply the transformation developed by Lai and Simmons (1978) to compute steady and unsteady turbulent jets, to add to the understanding of the steady and unsteady two-dimensional turbulent free jets, to investigate the validity of quasi-steady approximations and to evaluate the suitability of using turbulence models established for steady flows in unsteady flow calculations. The unsteady jet considered consists of an initially steady, two-dimensional, turbulent free jet with a sinusoidal mass flow variation superimposed on it at the nozzle exit. The steady-state oscillatory flow characteristics at any location downstream of the nozzle are obtained by solving the thin shear layer equations in two spatial (ζ, n) and one time (t) transformed coordinates.

2.0 Governing Equations

The Navier-Stokes equations for two-dimensional incompressible flow in tensor notations are given by (see, e.g., Hinze (1975))

$$\frac{\partial U_i^*}{\partial t^*} + u_j^* \frac{\partial U_i^*}{\partial x_j^*} = - \frac{1}{\rho} \frac{\partial p^*}{\partial x_i^*} + v^* \frac{\partial^2 U_i^*}{\partial x_j^* \partial x_j^*} \quad (1)$$

with the continuity equation being given by

$$\frac{\partial u_i^*}{\partial x_i^*} = 0 \quad (2)$$

By applying Reynolds decomposition

$$u_i^* = U_i^* + u_i^{*'}, \text{ etc.}$$

to equation (1) and taking time average with a time scale large compared with that of the turbulent motions but small compared with the periodicity of the flow, the time-averaged Reynolds equations can then be given by

$$\begin{aligned} \frac{\partial U_i^*}{\partial t^*} + U_j^* \frac{\partial U_i^*}{\partial x_j^*} &= \frac{1}{\rho} \frac{\partial}{\partial x_j^*} (-P^* + \frac{\partial U_i^*}{\partial x_j^*} + \frac{\partial U_j^*}{\partial x_i^*} \\ &\quad - \overline{\rho u_i^{*' u_j^{*'}}}) \end{aligned} \quad (3)$$

Consider an unsteady, two-dimensional, constant property, turbulent free jet issuing into a stationary medium. The instantaneous configuration is shown schematically in Fig. 1.

Assuming the thin shear layer approximations as in Cebeci and Bradshaw (1977), the governing equations can be obtained from equations (2) and (3) to yield in rectangular coordinate system

$$\frac{\partial U^*}{\partial x^*} + \frac{\partial V^*}{\partial y^*} = 0 \quad (4a)$$

and $\frac{\partial U^*}{\partial t^*} + U^* \frac{\partial U^*}{\partial x^*} + V^* \frac{\partial U^*}{\partial y^*} = \frac{\partial}{\partial y^*} (v^* \frac{\partial U^*}{\partial y^*} - \overline{u^* v^*}) \quad (4b)$

The boundary conditions on the centre-line and at the edge of the jet can be expressed respectively by

$$t^* \geq 0 \quad \begin{cases} y^* = 0 & \frac{\partial U^*}{\partial y^*} = V^* = 0 \\ y^* = y_\infty & U^* = 0 \end{cases} \quad (5a)$$

$$(5b)$$

The time-varying boundary condition at the nozzle exit is given by

$$t^* \geq 0 \quad x^* = 0 \quad U^* = U_0^*(y^*) (1 + \epsilon \sin \omega^* t^*) \quad (6a)$$

where $U_0^*(y^*)$ is the mean velocity profile at the nozzle exit, ϵ is the amplitude of pulsation and ω^* is the angular frequency of pulsation.

For all locations downstream of the nozzle, the initial conditions are given by

$$t^* = 0 \quad x^* \geq 0 \quad U^* = U_i^*(x^*, y^*) \quad (6b)$$

where $U_i^*(x^*, y^*)$ is the steady state solution of equation (4) with the boundary condition at the nozzle exit given by equation (6a) with $t^* = 0$.

2.1 Governing Equations in Non-Dimensional Form:

In order to enable the solution obtained to be valid for a family of velocity profiles which have the same normalized shape at the nozzle exit, the following non-dimensional variables are used: -

$$U(x, y, t) = \frac{U^*(x^*, y^*, t^*)}{U_{ci}^*}, \quad V(x, y, t) = \frac{V^*(x^*, y^*, t^*)}{U_{ci}^*}$$

$$x = \frac{x^*}{h} \quad y = \frac{y^*}{h} \quad t = \frac{U_{ci}^*}{h} t^* \quad \omega = \frac{h}{U_{ci}^*} \omega^*$$

$$v = \frac{v^*}{U_{ci}^* h} \quad \bar{u}' v' = \frac{\bar{u}^* v^*}{U_{ci}^{*2}}$$

where U_{ci}^* is the centre-line velocity at the nozzle exit at $t^* = 0$.

Equation (4) can now be written as

$$\frac{\partial U}{\partial x} + \frac{\partial V}{\partial y} = 0 \quad (7a)$$

$$\frac{\partial U}{\partial t} + U \frac{\partial U}{\partial x} + V \frac{\partial U}{\partial y} = \frac{\partial}{\partial y} (v \frac{\partial U}{\partial y} - \bar{u}' v') \quad (7b)$$

subject to the following boundary and initial conditions

$$t \geq 0 \quad \begin{cases} y = 0 & \frac{\partial U}{\partial y} = V = 0 \\ y = \infty & U = 0 \end{cases} \quad (8a)$$

$$t \geq 0 \quad x = 0 \quad U = U_o(y)(1 + \epsilon \sin \omega t) \quad (9a)$$

$$t = 0 \quad x \geq 0 \quad U = U_i(x, y) \quad (9b)$$

2.2 Turbulence Modelling

The Navier-Stokes equations constitute a complete set of equations of motion which can in theory be solved to yield a solution for any laminar or turbulent flow field. However, turbulence comprises a wide range of length scales bounded from above by the dimensions of the flow field and bounded from below by the diffusive action of molecular viscosity. The resolution scale of the smaller eddies which are responsible for the decay of turbulence is too small that it precludes the use of any existing computer. Furthermore, very often only the time-averaged properties are of interest in engineering applications even if the flow is time dependent. Hence, the Navier-Stokes equations are time-averaged first before being solved. This avoids not only the difficulty in representing all the characteristic turbulence scales but also unnecessary computations of transients if only the time-averaged properties are required. The process of time-averaging such as the Reynolds time-averaging described in section 2.0 causes the loss of certain information contained in the original equations and results in more unknowns than the governing equations through the introduction of statistical correlations of fluctuating velocities such as the $\overline{u'v'}$ term in equation (7b) which are known as apparent Reynolds stresses and are responsible for the actual momentum

transfer. Attempts to derive additional equations for those Reynolds stresses will only result in additional unknowns. Thus the time-averaging process presents a closure problem which is to reduce the number of unkownws to equal the number of governing equations. In order to achieve this, the additional unknown quantities must be modelled or approximated in terms of known quantities through a set of equations which, when solved with the mean-flow equations, simulate the actual flow situation. This process is generally termed "turbulence modelling."

Turbulence models can broadly be classified into "first-order" models in which the mean flow equations are solved without additional partial differential equations for the velocity fluctuation terms and "higher-order" models in which transport equations for higher-order velocity correlations are solved with the mean flow equations. Since in the "first-order" models additional partial differential equations are not solved for the turbulence quantities which are expressed in terms of known quantities through certain algebraic formulation, they are known as zero-equation models and "higher-order" models which involve at least one partial differential equation for the turbulence quantities can thus be termed one-equation or two-equation models, etc. A description of the various types of turbulence models can be found in Launder and Spalding (1972) and a comprehensive review of the state-of-art is given by Reynolds and Cebeci (1978).

Zero-equation models which are based on empirical correlations of the extensive available experimental data and mostly on the eddy-viscosity and mixing-length concepts such as the Cebeci-Smith eddy viscosity model (1974) have been widely used and proved to be very successful in obtaining very accurate predictions of non-separating flows. For more complex flows which involve recirculation and separation, the more refined two-equation $k-\epsilon$ model described by Launder and Spalding (1976) is the most well-developed among all other "high-order" models. It has been recognized that although "higher-order" models contain more information and hence simulate the flow situation more realistically than the "first-order" models, they are more difficult to solve and require generally an order-of magnitude more computing storage and time while in non-separating and simple flow situations, the first-order models can yield predictions to the same degree of accuracy as the "higher-order" models. It is in the light of this philosophy that in this study, a constant-eddy viscosity model due to Prandtl (1942) is used.

By employing the eddy-viscosity concept of Boussinesq, the fluctuating-velocity correlation term $\overline{u'v'}$ in equation (7b) is related to the mean velocity gradient through the eddy viscosity v_t as follows:

$$\overline{u'v'} = - v_t \frac{\partial U}{\partial y} \quad (10)$$

The eddy viscosity v_t can then be obtained from the constant eddy-viscosity model as

$$v_t(t) = c y_{1/2} U_c(t) \quad (11)$$

where c is a constant, and $y_{1/2}$ is the jet half-width.

In this model, two constants c_1 and c_2 are used for the free jet as it emerges from developing to fully developed form. Hence c is given by

$$c = \begin{cases} c_1 & \text{if } \bar{U}_c \geq 0.95 \\ c_2 & \text{if } \bar{U}_c < 0.95 \end{cases} \quad (12)$$

By defining an effective eddy viscosity v_{eff} such that

$$v_{eff} = v_t + v \quad (13)$$

and using equation (10), equation (7b) can then be written as

$$\frac{\partial U}{\partial t} + U \frac{\partial U}{\partial x} + V \frac{\partial U}{\partial y} = \frac{\partial}{\partial y} (v_{eff} \frac{\partial U}{\partial y}) \quad (14)$$

Hence the flow development of a periodically pulsed turbulent free jet is governed by equations (7a) and (14) subject to the boundary and initial conditions of equations (8) and (9) with the constant eddy viscosity model of (11)

2.3 Governing Equation in Transformed Variable Form

It has been shown by Lai and Simmons (1978) that transformations based on the similarity solutions are successful in reducing substantially the rate of spread of an unsteady laminar jet, hence enabling the use of variable grid sizes over predetermined regions. In this study, similar transformations are employed. A dimensionless transverse distance η and a dimensionless stream function ψ are defined by

$$\eta = ay/(\zeta + \zeta_0) \quad (15a)$$

$$\psi(\zeta, y, t) = b(\zeta + \zeta_0)^{1/2} f(\zeta, \eta, t) \quad (15b)$$

where a , b and ζ_0 are arbitrary constants which can be varied to facilitate computation and x is renamed as ζ .

The function f automatically satisfies the continuity equation (7a) and equation (14) can be re-written in the transformed coordinates as

$$(\zeta + \zeta_0)^{-1/2} [v_{eff} f''']' + (f')^2 + ff'' = 2(\zeta + \zeta_0) [f' \frac{\partial f'}{\partial \zeta} - f'' \frac{\partial f}{\partial \zeta} + \frac{(\zeta + \zeta_0)^{1/2}}{ab} \frac{\partial f'}{\partial t}] \quad (16)$$

where prime denotes differentiation with respect to n ,

$$f' = (\zeta + \zeta_0)^{1/2} U/ab \quad (17)$$

and a and b are chosen for convenience such that
 $a/b = \frac{1}{2}$.

The boundary conditions in equation (8) become

$$t > 0 \quad \begin{cases} n = 0 & f'' = 0 & f + 2(\zeta + \zeta_0) \frac{\partial f}{\partial \zeta} = 0 \\ n = n_\infty & f' = 0 & \end{cases} \quad (18a)$$

$$(18b)$$

The initial conditions at $\zeta = 0$ in the (n, t) plane is obtained by writing equation (9a) with equation (17) as

$$f' = f'_0(n)(1 + \epsilon \sin \omega t) \quad (19a)$$

The initial conditions at $t = 0$ in the (ζ, n) plane are generated by the solutions $U_i(\zeta, n)$ of the following steady jet equation obtained from equation (16)

$$(\zeta + \zeta_0)^{-\frac{1}{2}} [v_{eff} f''']' + (f')^2 + ff'' = 2(\zeta + \zeta_0) [f' \frac{\partial f'}{\partial \zeta} - f'' \frac{\partial f}{\partial \zeta}] \quad (19b)$$

The effective eddy-viscosity can be obtained from equation (13) using equations (11) and (15) to give

$$v_{eff}(t) = cb(\zeta + \zeta_0)^{1/2} n^{1/2} f_c'(t) + v \quad (20)$$

where c is subject to the conditions specified in equation (12).

3.0 Method of Solution

Since the initial conditions in the (ζ, n) plane are generated by solving the steady jet equation (19b) subject to the boundary conditions in equation (18), the flow development of the steady jet is first studied. For computer programme development purpose, two separate computer programs were written for the steady and unsteady jet respectively with the solutions of the steady jet stored on disk for use in the unsteady jet program. However, if necessary, the steady jet program can easily be incorporated into the unsteady one. Both equations (16) and (19b) are parabolic and can be solved by a marching procedure. The finite difference scheme employed is the Box Method developed by Keller (1970), and described in detail by Cebeci and Bradshaw (1977). The scheme has been applied successfully to a wide range of boundary-layer type of flows including both time-dependent and separating flows by Cebeci and his co-workers (e.g., see Bradshaw et al (1980)).

3.1 Finite Difference Form of the Governing Equations

Equation (16) is rewritten as a system of first order parital differential equations -

$$f' = g \quad (21a)$$

$$g' = q \quad (21b)$$

$$(\zeta + \zeta_0)^{-1/2} [v_{\text{eff}} q]' + g^2 + fq = 2(\zeta + \zeta_0) [g \frac{\partial g}{\partial \zeta} - q \frac{\partial f}{\partial \zeta}] + (\frac{\zeta + \zeta_0}{ab})^{1/2} \frac{\partial g}{\partial t} \quad (21c)$$

Consider the net cube shown in Fig. 2 and denote the grid points by

$$\zeta_0 = 0 \quad \zeta_{i+1} = \zeta_i + r_i \quad i = 1, 2, \dots, I$$

$$t_0 = 0 \quad t_n = t_{n-1} + k_n \quad n = 1, 2, \dots, N$$

$$n_0 = 0 \quad n_j = n_{j-1} + h_j \quad j = 1, 2, \dots, J$$

$$n_J = n_\infty$$

where i, n, j are just sequence numbers and the variable net spacings r_i , k_n and h_j are completely arbitrary.

In the study of jets, a coarse grid spacing h_j can be used in the vicinity of the centre line and the edge of the jet as the transverse (n) gradients of f are small in those regions. The quantities (f, g, q) at points (ζ_i, t_n, n_j) are approximated by the grid functions $(f_j^{i,n}, g_j^{i,n}, q_j^{i,n})$. Hence by using central differencing and averaging about the mid-point $(\zeta_i, t_n, n_{j-\frac{1}{2}})$, Eqs. (21a) and (21b) can be written in the following finite difference forms

$$(f_j^{i,n} - f_{j-1}^{i,n})/h_j = g_{j-\frac{1}{2}}^{i,n} \quad (22a)$$

$$(g_j^{i,n} - g_{j-1}^{i,n})/h_j = q_{j-\frac{1}{2}}^{i,n} \quad (22b)$$

where, for example, the shorthand notation $g_{j-\frac{1}{2}}^{i,n}$ has been used for $\frac{1}{2}(g_j^{i,n} + g_{j-1}^{i,n})$

Shorthand notations are introduced, for example,

$$\bar{f}_i = \frac{1}{4}(f_j^{i,n} + f_j^{i,n-1} + f_{j-1}^{i,n} + f_{j-1}^{i,n-1}) = \frac{1}{4}(f_{j-\frac{1}{2}}^{i,n} + f_{j-\frac{1}{2}}^{i,n-1})$$

$$\bar{f}_j = \frac{1}{4}(f_j^{i,n} + f_j^{i-1,n} + f_j^{i,n-1} + f_j^{i-1,n-1}) = \frac{1}{4}(f_j^{i,n} + f_j^{234})$$

$$\bar{f}_n = \frac{1}{4}(f_j^{i,n} + f_j^{i-1,n} + f_{j-1}^{i,n} + f_{j-1}^{i-1,n}) = \frac{1}{4}(f_{j-\frac{1}{2}}^{i,n} + f_{j-\frac{1}{2}}^{i-1,n})$$

$$f_j^{234} = f_j^{i,n-1} + f_j^{i-1,n} + f_j^{i-1,n-1}$$

Eq. (21c) can be approximated using central differencing at $(\zeta_{i-\frac{1}{2}}, t_{n-\frac{1}{2}}, \eta_{j-\frac{1}{2}})$ by

$$\begin{aligned} (Bq)_j - (Bq)_{j-1} + h_j \{(g^2)_{j-\frac{1}{2}} + (fq)_{j-\frac{1}{2}} - \alpha [g_{j-\frac{1}{2}}(g_{j-\frac{1}{2}} + \\ g_{j-\frac{1}{2}}^{i,n-1} + g_{j-\frac{1}{2}}^{234} - 2\bar{g}_{i-1}) - q_{j-\frac{1}{2}}(f_{j-\frac{1}{2}} + \\ f_{j-\frac{1}{2}}^{i,n-1} - 2\bar{f}_{i-1}) - f_{j-\frac{1}{2}}q_{j-\frac{1}{2}}^{234}] - \\ \alpha_i g_{j-\frac{1}{2}}\} = T_{j-\frac{1}{2}}^{i-1,n-1} \end{aligned} \quad (22c)$$

where $B = (\zeta + \zeta_0)^{-\frac{1}{2}} v_{eff}$

$$\alpha = \frac{m_1^{i-\frac{1}{2}}}{2r_i}$$

$$m_1 = 2(\zeta + \zeta_0)$$

$$\alpha_1 = \frac{4[(\zeta + \zeta_0)^{3/2}]^{i-\frac{1}{2}}}{ab k_n}$$

$$T_{j-\frac{1}{2}}^{i-1, n-1} = (Bq)_{j-1}^{234} - (Bq)_j^{234} + h_j \{ - (g^2)_{j-\frac{1}{2}}^{234} - (fq)_{j-\frac{1}{2}}^{234} + \\ a[\beta_2 g_{j-\frac{1}{2}}^{234} - \beta_1 q_{j-\frac{1}{2}}^{234}] + \alpha_1 \beta_3 \}$$

$$\beta = g_{j-\frac{1}{2}}^{i,n-1} + g_{j-\frac{1}{2}}^{234} - 2 \bar{g}_{i-1}$$

$$\beta_1 = f_{j-\frac{1}{2}}^{i,n-1} + 2 \bar{f}_{i-1}$$

$$\beta_2 = g_{j-\frac{1}{2}}^{i,n-1} - 2 \bar{g}_{i-1}$$

$$\beta_3 = g_{j-\frac{1}{2}}^{i-1,n} - 2 \bar{g}_{n-1}$$

In the above equation (22c), the superscripts i, n have been dropped for simplicity.

It has been pointed out by Keller (1978) that in approximating non-linear terms such as $(fq)_{j-\frac{1}{2}}$ in equation (22c) with the Box scheme, there exists several choices which should not have serious effect on accuracy or stability as long as the proper centering is maintained. However, in jet calculations, it has been found in this study that the approximation of terms such as (fq) in the form of $(f)_{j-\frac{1}{2}}(q)_{j-\frac{1}{2}}$

results in better numerical stability at the jet edge.

The boundary conditions in Eq. (18) become

$$q_0^{i,n} = 0 \quad (23a)$$

$$f_0^{i,n} = (1 + \frac{2m_1}{r_i})^{-1} (\frac{2m_1}{r_i} - 1) f_0^{i-1,n} \quad (23b)$$

$$g_J^{i,n} = 0 \quad (23c)$$

The initial conditions at $\zeta = 0$ in the (n, t) plane in Eq (19a) are given by

$$(f')_j^n = (f'_{\infty})_j^n [1 + \epsilon \sin \omega(n\Delta t)] \quad (24)$$

where Δt is the temporal grid size.

The initial conditions at $t = 0$ in the (ζ, n) plane correspond to the steady jet solutions of equation (19b). The finite difference equations can be obtained similar to the above derivation for the unsteady jet except terms in equation (22) at $t = t_{n-1}$ are equal to those at $t = t_n$ and $\alpha_1 = 0$.

3.2. Time Varying Velocity Profile at the Nozzle Exit

Because of symmetry, only half of the jet needs to be computed. The time-varying velocity profile considered at the nozzle exit is the commonly assumed "top-hat" profile which is given by

$$U(y, t) = \begin{cases} 1 + \epsilon \sin \omega t & \text{for } 0 \leq y \leq 1/2 \\ 0 & \text{for } 1/2 < y \end{cases} \quad (25)$$

In terms of the transformed coordinates, equation (25) can be rewritten using equation (17) as

$$f' = \begin{cases} \frac{(\zeta + \zeta_0)^{1/2}}{ab} (1 + \epsilon \sin \omega t) & \text{for } 0 \leq n \leq (n_\infty)_i \\ 0 & \text{for } (n_\infty)_i \leq n \end{cases}$$

$$\text{where } (n_\infty)_i = 0.5 a/\zeta_0 \quad (26)$$

Since a discontinuity exists in f' at $n = (n_\infty)_i$ and will cause computational problems, the top-hat profile has to be approximated by

$$f' = \frac{(\zeta + \zeta_0)^{1/2}}{ab} \Phi_1(n)(1 + \epsilon \sin \omega t) \quad (27)$$

where

$$\Phi_1(n) = \begin{cases} 1 & \text{for } 0 \leq n \leq n_a \\ (1 - n_N^2)(1 + 2n_N) & \text{for } n_a \leq n \leq (n_\infty)_i \\ 0 & \text{for } (n_\infty)_i \leq n \end{cases} \quad (28)$$

$$n_N = \frac{n - n_a}{(n_\infty)_i - n_a}$$

and η_a is some point in the interval $[0, (\eta_\infty)_i]$.

The function $(1 - \eta_N^2)(1 + 2\eta_N)$ was obtained by matching the velocity and velocity gradient profiles at $\eta = (\eta_\infty)_i$ and $\eta = \eta_a$ through the following boundary conditions to ensure continuity:

$$\eta_N = 0 \quad \Phi_1 = 1 \quad \Phi'_1 = 0 \quad (29a)$$

$$\eta_N = 1 \quad \Phi_1 = 0 \quad \Phi'_1 = 0 \quad (29b)$$

f and f'' can be obtained by respectively integrating and differentiating equation (27) with respect to η to yield

$$f = \frac{(\zeta + \zeta_0)^{1/2}}{ab} \quad \Phi_0(\eta)(1 + \epsilon \sin \omega t) \quad (30)$$

$$\text{and } f'' = \frac{(\zeta + \zeta_0)^{1/2}}{ab} \quad \Phi_2(\eta)(1 + \epsilon \sin \omega t) \quad (31)$$

$$\Phi_0(\eta) = \begin{cases} 1 & \text{for } 0 \leq \eta \leq \eta_a \\ [(\eta_\infty)_i - \eta_a]\eta_N(1 - \eta_N^2 + 0.5\eta_N^3) & \text{for } \eta_a \leq \eta \leq (\eta_\infty)_i \\ 0 & \text{for } (\eta_\infty)_i \leq \eta \end{cases} \quad (32)$$

and

$$\Phi_2(\eta) = \begin{cases} 1 & \text{for } 0 < \eta < \eta_a \\ -6\eta_N(1 - \eta_N)/[(\eta_\infty)_i - \eta_a] & \text{for } \eta_a \leq \eta < (\eta_\infty)_i \\ 0 & \text{for } (\eta_\infty)_i \leq \eta \end{cases} \quad (33)$$

The value of η_a can be determined to match the experimental top-hat profile as close as possible and in this study it is chosen to be the point such that the velocity profile is uniform over 97.5% of the nozzle.

Adopting similar procedure given in Lai and Simmons (1978),
a and ξ_0 are given the values 0.3 and 3.75 respectively
such that $(\eta_\infty)_i = 0.04$ and $\eta_a = 0.039$.

3.3 Solution of the Finite Difference Equation

With $(f_j^{n-1}, g_j^{n-1}, q_j^{n-1})$ known from the solution of Eq (19b) and $(f_j^{i-1}, g_j^{i-1}, q_j^{i-1})$ specified by Eqs. (27), (30) and (31), Eq. (22) for $1 \leq j \leq J$ and Eq. (23) yield an implicit non-linear algebraic system of $3J + 3$ equations. This system is linearized by Newton's Method by introducing the perturbed quantities $(\delta f, \delta g, \delta q)$ to yield after considerable algebra

$$\delta f_j - \delta f_{j-1} - \frac{h_j}{2}(\delta g_j + \delta g_{j-1}) = (r_1)_j \quad (34a)$$

$$\delta g_j - \delta g_{j-1} - \frac{h_j}{2}(\delta q_j + \delta q_{j-1}) = (r_3)_{j-1} \quad (34b)$$

$$(s_1)_j \delta q_j + (s_2)_j \delta q_{j-1} + (s_3)_j \delta f_j + (s_4)_j \delta f_{j-1} \\ + (s_5)_j \delta g_j + (s_6)_j \delta g_{j-1} = (r_2)_j \quad (34c)$$

where

$$(s_1)_j = B_j + \frac{h_j}{2}(f_j + \alpha f_{j-\frac{1}{2}} + \alpha \beta_1)$$

$$(s_2)_j = B_{j-1} + \frac{h_j}{2}(f_{j-1} + \alpha f_{j-\frac{1}{2}} + \alpha \beta_1)$$

$$(s_3)_j = \frac{h_j}{2}(q_j + \alpha q_{j-\frac{1}{2}} + \alpha q_{j-\frac{1}{2}}^{234})$$

$$(s_4)_j = \frac{h_j}{2}(q_{j-1} + \alpha q_{j-\frac{1}{2}}^{234})$$

$$(s_5)_j = h_j(g_j - \alpha g_{j-\frac{1}{2}} - \frac{\alpha \beta}{2} - \frac{\alpha_1}{2})$$

$$(s_6)_j = h_j(g_{j-1} - \alpha g_{j-\frac{1}{2}} - \frac{\alpha \beta}{2} - \frac{\alpha_1}{2})$$

$$(r_1)_j = f_{j-1} - f_j + h_j g_{j-\frac{1}{2}}$$

$$\begin{aligned}
 (r_3)_{j-1} &= g_{j-1} - g_j + h_j q_{j-\frac{1}{2}} \\
 (r_2)_j &= T_{j-\frac{1}{2}}^{i-1, n-1} + (Bq)_{j-1} - (Bq)_j - h_j \{g_{j-\frac{1}{2}}^2 (fq)_{j-\frac{1}{2}} \\
 &\quad - \alpha [\frac{1}{2}(g_{j-\frac{1}{2}}^2 + g_j g_{j-1}) + \beta g_{j-\frac{1}{2}} - f_{j-\frac{1}{2}} g_{j-\frac{1}{2}}] \\
 &\quad - \beta_1 q_{j-\frac{1}{2}} - q_{j-\frac{1}{2}}^{234} f_{j-\frac{1}{2}}] - \alpha_1 g_{j-\frac{1}{2}}\}
 \end{aligned}$$

The boundary conditions are given by

$$\begin{aligned}
 \delta f_0 &= 0 \\
 \delta q_0 &= 0 \\
 \delta g_j &= 0
 \end{aligned} \tag{35}$$

The above derivation is similar to that outlined in Appendix C in Lai & Simmons (1978). The linear system Eq. (3.10) is then solved very effectively by the Block Elimination Method discussed by Cebeci and Bradshaw (1977).

The linearized form of the steady jet equation can similarly be obtained and solved with quantities at $t = t_{n-1}$ equal to those at $t = t_n$ and $\alpha_1 = 0$.

3.4 Convergence Criterion

As the governing equations for both the steady and unsteady jet are parabolic, they are solved by marching along the t -direction in the case of the unsteady jet and along the ζ -direction in the case of the steady jet. At a given streamwise (ζ) station, the linearized system Eq. (34) is solved by iterating at each t -station until some convergence criterion is satisfied. Iterations are terminated at each t -station if

$$|f'(i+1) - f'(i)| < \epsilon_1, \text{ at } n = n_{\text{con}} \quad (36)$$

where the value of ϵ_1 is prescribed;

$f'(i)$ and $f'(i+1)$ are the i th and $(i+1)$ th iterates of f' respectively; and n_{con} is some point where the convergence criterion is applied. In practice, it is adequate to set ϵ_1 to be 10^{-3} .

3.5 Criterion for the Spreading of Jet

Since the mass flow varies sinusoidally with time, and because of the initially steep velocity gradient, the jet width will be changing with time at a given streamwise (ζ) station. A criterion must therefore be set to determine n_∞ at each t-station, noting that $n_\infty^{(i)} \geq n_\infty^{(i-1)}$. Here $n_\infty^{(i)}$ and $n_\infty^{(i-1)}$ are the jet width for the i th and $(i-1)$ th iterations. The edge of the jet is defined by the following two conditions -

$$|f'_{J-1}| \leq \epsilon_2 \quad (37a)$$

$$|f''_j| \leq \epsilon_3 \quad (37b)$$

where the values of ϵ_2 and ϵ_3 are prescribed and J denotes the point at the jet boundary. Experience indicates that it is sufficient to choose

$$\epsilon_2 = 10^{-2} \text{ and } \epsilon_3 = 10^{-1}$$

If the criteria set out in Eq. (37) are satisfied then $n_\infty^{(i+1)} = n_\infty^{(i)}$. Otherwise n_g points have to be added so that $J_{\text{new}} = J_{\text{old}} + n_g$ and the values of $(f_j^{i,n}, g_j^{i,n}, q_j^{i,n})$ for the new n_j points are obtained as follows -

$$f_j^{i,n} = (n_j - n_\infty) g_J^{i,n} + f_J^{i,n} \quad (38a)$$

$$g_j^{i,n} = g_J^{i,n} \quad (38b)$$

$$q_j^{i,n} = 0 \quad (38c)$$

$$B_j^{i,n} = B_J^{i,n} \quad (38d)$$

The same procedure is also applied to $f_j^{i,n-1}$, $g_j^{i,n-1}$,
 $q_j^{i,n-1}$, $B_J^{i,n-1}$, $f_j^{i-1,n}$, $g_j^{i-1,n}$, $q_j^{i-1,n}$, $B_j^{i,n-1}$, $f_j^{i-1,n-1}$,
 $q_j^{i-1,n-1}$, $B_j^{i-1,n-1}$

3.6 Criterion for the Attainment of Steady State Solution

As the mass flow at the nozzle varies sinusoidally with time, the steady state solution at any streamwise (ζ) station downstream must vary periodically and can be expressed in the form

$$f'(\zeta, t, n) = f'_0(\zeta, t, n) + \lim_{L \rightarrow \infty} \sum_{\ell=1}^L \epsilon_\ell f_\ell(\zeta, n) \sin(\ell \omega t + \phi_\ell) \quad (39)$$

In general, for a periodically pulsed flow, the steady state solution at a given streamwise (ζ_i) station, is said to be reached if

$$f'(\zeta, t + nT, n) = f'(\zeta, t, n) \quad \text{for } n = 1, 2, \dots$$

where T is the period of oscillation.

This entails velocity profiles to agree over a few cycles and thus requires unnecessary and uneconomic computations extending for a few periods in order to ascertain that steady state has been attained. However, if all the three parameters, f , f' and f'' are considered, it is adequate to regard that the steady state solution has been reached if at some point n_s , the following criteria are satisfied -

$$|[f(\zeta, t_n + T, n_s) - f(\zeta, t_n, n_s)]/(f(\zeta, t_n, n_s))| \leq \epsilon_4$$

$$|[f'(\zeta, t_n + T, n_s) - f'(\zeta, t_n, n_s)]/f'(\zeta, t_n, n_s)| \leq \epsilon \quad n = 1, 2 \quad (40)$$

$$|[f''(\zeta, t_n + T, n_s) - f''(\zeta, t_n, n_s)]/f''(\zeta, t_n, n_s)| \leq \epsilon_6$$

where the values of ϵ_4 , ϵ_5 and ϵ_6 are prescribed and
 $t_2 - t_1 = \Delta t$.

The sensitivity of the steady-state test varies with the point n_s to which it is applied. In practice, the point n_s should be so chosen such that reasonable sensitivity is achieved without excessive computations.

Since f' and f'' are the first and second order derivatives of f , discrepancies between results separated by one period T are more pronounced in f'' . Hence, in general ϵ_4 , ϵ_5 and ϵ_6 must be so chosen that $\epsilon_4 < \epsilon_5 < \epsilon_6$. Otherwise, if $\epsilon_6 > \epsilon_5 > \epsilon_4$ and if ϵ_6 is very small, the criteria in Eq. (40) might never be satisfied although the steady state solution has long been attained within practical limits.

As a further check of the attainment of the steady-state condition, the following condition is imposed on f' at the centre-line -

$$|[f'(\zeta, t_n + T, 0) - f'(\zeta, t_n, 0)]/f'(\zeta, t_n, 0)| < \epsilon_7 \quad (41)$$

for $n = 1, 2$

where the value of ϵ_7 is prescribed.

It has been chosen that $\epsilon_4 = \epsilon_5 = \epsilon_6 = \epsilon_7 = 10^{-2}$

3.7 Mean Momentum Flux, Phase Angle and Peak-to-Peak Oscillation

3.7.1 Mean Momentum Flux

The instantaneous momentum at a specified streamwise (ζ_i) station is given by

$$M_i = 2hU_{ci}^2 \int_0^{n_\infty} [f'(\zeta, t_i, n)]^2 dn \quad (42)$$

M_i is evaluated by Simpson's rule for unequally spaced points derived in Appendix D in Lai & Simmons (1978).

The mean momentum flux in the streamwise direction is defined by

$$M = \frac{1}{T} \int_{t_0}^{t_0 + T} M_i dt \quad (43)$$

and the integral is approximated by

$$M = \frac{1}{N} \sum_{i=1}^N M_i \quad (44)$$

The quantity M can be served as an additional check on the overall results by testing for its constancy with ζ .

3.7.2. Phase Angle

The phase angle between the fundamental component of the centre-line velocity at any downstream station and that at the nozzle can readily be obtained by cross-correlating the steady-state instantaneous centre-line velocity at that station with a reference sine and cosine signal respectively.

Consider

$$S_1 = \sin \omega t \quad (45)$$

$$S_2 = \cos \omega t \quad (46)$$

From Eq. (39),

$$f'_c \equiv f'(\zeta, t, 0) = f'_0(\zeta, t, 0) + \lim_{L \rightarrow \infty} \sum_{\ell=1}^L \epsilon^\ell f_\ell(\zeta, 0) \sin(\ell \omega + \phi_\ell) \quad (47)$$

Multiplying Eq. (45) with Eq. (47) and taking time average yields

$$\overline{S_1 f'_c} = A \cos \phi_1 \quad (48)$$

where A is a constant.

Multiplying Eq. (46) with Eq. (47) and taking time average gives

$$\overline{S_2 f'_c} = A \sin \phi_1 \quad (49)$$

From Eqs. (48) and (49),

$$\phi_1 = \tan^{-1} \frac{\overline{S_2 f'_c}}{\overline{S_1 f'_c}} \quad (50)$$

3.7.3. Peak-to-Peak Oscillation

The percentage peak to peak variation of the centre-line velocity at any downstream station is defined by

$$F = \frac{(f'_c)_{\max} - (f'_c)_{\min}}{f'_c} \times 100\% \quad (51)$$

The quantities $(f'_c)_{\max}$ and $(f'_c)_{\min}$ are obtained by quadratic interpolation of the form

$$f'_c = a_0 t^2 + a_1 t + a_2 \quad (52)$$

through three points $(f'_c(t_1), t_1)$, $(f'_c(t_2), t_2)$ and $(f'_c(t_3), t_3)$

where for $(f'_c)_{\max}$, $f'_c(t_1) \leq f'_c(t_2)$

$$f'_c(t_3) \leq f'_c(t_2)$$

and for $(f'_c)_{\min}$ $f'_c(t_1) > f'_c(t_2)$

$$f'_c(t_3) > f'_c(t_2)$$

Eq. (52) can be solved for a_0 , a_1 and a_2 by substituting $f'_c(t_1)$, $f'_c(t_2)$ and $f'_c(t_3)$. With a_0 , a_1 and a_2 known, $(f'_c)_{\max}$ or $(f'_c)_{\min}$ can be obtained from Eq. (52) with t given by $-a_1/2a_0$.

4.0 Results and Discussions

The structure and listing of the computer programs for both the steady and unsteady jet are described in Appendix A. Calculations were performed on the University of Queensland PDP1055 and the U.S. Naval Postgraduate School IBM 360/67 computers. The computer program for the steady jet occupies a core memory of 16K words and that of the unsteady jet occupies a core memory of 67K words. It must be pointed out here that the unsteady jet program can actually be reduced to about 25K words of core memory since at any one time instant, only calculations involving two time levels are required in core whereas all the quantities at other time levels can be stored on disk and retrieved when required. However, in this case, the computer core storage is not a problem with the computing facility available whereas the computing time is important and as such a trade-off is made such that quantities at all time levels are retained in core in order to save computing time of writing to and reading from disk. Moreover, although a constant eddy viscosity model was used, the programs were written to accept variable eddy viscosity. A very straightforward modification of the program by incorporating a routine to read from and write to a disk can reduce its size to enable it to be run on any mini-computer with available core memory of about 25K words.

4.1 Steady Jet

Owing to the nature of the initially top-hat velocity profile, the initial velocity gradient is very steep and the velocity profile changes vary appreciably over a very short streamwise distance. Since the solution of the finite difference equations is obtained through linearization by Newton's method as described in section 3.3, an initial guess at any streamwise station must be close to the solution. Consequently, a fine grid has also to be used initially but as the computation proceeds and as the velocity profiles start to appear in similar form, a coarser grid can be used by dropping every other point. The initial grid used in the transverse (η) direction is specified as follows:

$$\Delta\eta = \begin{array}{ll} 0.005 & 0 \leq \eta \leq 0.01 \\ 0.002 & 0.01 \leq \eta \leq 0.036 \\ 0.0002 & 0.036 \leq \eta \leq 0.039 \\ 0.0001 & 0.039 \leq \eta \leq 0.04 \\ 0.00025 & 0.04 \leq \eta \leq 0.045 \\ 0.001 & 0.045 \leq \eta \leq 0.06 \\ 0.002 & 0.06 \leq \eta \leq 0.02 \\ 0.01 & \eta \leq 0.12 \end{array} \quad (53)$$
$$(\eta_\infty)_i = 0.04$$

The grid-sizes in the streamwise (ζ) direction are specified as follows:

	0.0005	$0 \leq \zeta \leq 0.007$	
	0.005	$0.007 \leq \zeta \leq 0.032$	
	0.025	$0.032 \leq \zeta \leq 0.132$	
	0.1	$0.132 \leq \zeta \leq 1.032$	
$\Delta\zeta =$	1	$1.032 \leq \zeta \leq 20.032$	(54)
	2	$20.032 \leq \zeta \leq 40.032$	
	5	$40.032 \leq \zeta$	

The constants c_1 and c_2 in equation (12) in the constant eddy viscosity model are varied to match the experimental data. The sensitivity of the solutions to various values of c_1 and c_2 was tested. No significant difference was found when c_1 was varied from 0.009 to 0.012 and c_2 from 0.032 to 0.037. The final values of $c_1 = 0.009$ and $c_2 = 0.034$ were chosen.

As shown in Fig. 3, the non-dimensional self-preserved velocity profiles of various workers agree very well with each other and with the Goertler solution except near the jet edge where conventional hot-wire measurements are dubious. However, the results of Heskestad (1965) follow very closely the Goertler solution and those of Robins (1971) which have been recommended by Rodi (1975) as reliable agree very well with the results of Heskestad (1965). The computed development of the non-dimensional velocity profiles of the steady jet with y normalized with respect to the jet half-width $y_{1/2}$ are depicted in Fig. 4 and at streamwise station $\zeta = 22.032$, the mean velocity profile differs insignificantly from

the Goertler solution, indicating that self-preservation in mean velocity profile is attained.

The variation of the non-dimensional centre-line velocity with streamwise distance is plotted in Fig. 5. The results agree well with the experimental data of Lai and Simmons (1979) and Zijnen (1958). The variation of the jet half-width with streamwise distance is compared with the result of Kotsovinos (1976) and Lai and Simmons (1979) in Fig. 6 and is found to give reasonably good agreement for streamwise distance less than about 40 nozzle widths. The discrepancy which exists at larger streamwise distance is not as significant as it appears because the results of Kotsovinos (1976) were obtained by fitting a third-order polynomial through the scattered data in the literature and most of the experimental data were not available for streamwise distance larger than 50 nozzle widths. Furthermore, uncertainty in the hot-wire data increases as the streamwise distance increases because of the decay of the velocity profile and possible three-dimensional and reversed flow effects. The rate of decay of the centre-line velocity $d\bar{U}_c^2/d(x/h)$ of 0.165 and the spreading rate $d(y_{1/2}/h)/d(x/h)$ of 0.106 obtained from Figs. 5 and 6 respectively fall within the range of values reported in the literature. As pointed out by Goldschmidt and Bradshaw (1980), exact self-preservation in mean quantities requires the kinematic virtual origin, obtained from the centre-line velocity decay curve, be equal to the geometric virtual origin obtained from the jet spreading curve. However, most

experimental data do not confirm this. In this study, the computed kinematic virtual origin agrees with the geometric virtual origin and is found to be $0.8h$.

The development of the normalized shear stress profiles is shown in Fig. 7. The agreement between the computed shear stress profile at $\zeta = 95.032$ and the experimental results of Gutmark and Wygnanski (1976) is good considering that the shear stress term is the most difficult to be measured with sufficient accuracy and a scatter of at least 20% exists in the available experimental data in the literature. The maximum value of the computed non-dimensional shear stress term $\bar{u}'\bar{v}'/U_c^2$ is 0.023 which agrees well with most measured values reported in Rodi (1975).

In jet computations, numerical errors introduced at the jet edge normally have little overall influence on the calculations as noted by McGuirk and Rodi (1979). The momentum integral in this study varies by less than 1% over a streamwise distance of 100 nozzle widths.

4.2 Unsteady Jet

The constant eddy-viscosity model which was found to give good agreement with experimental data was used in the computation of the periodically pulsed jet. Results were obtained for three frequencies of pulsation, $\omega = 0.000871$, 0.00871 and 0.0871 which for a jet exit Reynolds number of 10^4 and a jet width h of 5mm correspond to 1, 10 and 100 Hz respectively. Two values of amplitude of pulsation were studied, namely $\epsilon = 0.1$ and 0.15. The results were compared with the experimental data of Lai and Simmons (1979) and solutions for steady jets. The grid-sizes used in the streamwise (ζ) and transverse (n) directions are the same as those of the steady jet given in section 4.1.

4.2.1 Sensitivity of the Solution to the Convergence Criterion

Results show that solutions are very sensitive to the convergence criterion applied to points very near to the edge of the jet. Normally, the closer the point n_{con} is to the edge of the jet, the more difficult it will be for the solution to converge. It was found by Lai and Simmons (1979) that the convergence criterion can be applied to a point in the jet which varies with streamwise distance and is defined by

$$n_{con} = \begin{cases} (n_\infty)_i - 3 & \text{for } \zeta \leq 0.1 \\ 6(n_\infty)_{\min}/10-1 & \text{for } \zeta \geq 0.1 \end{cases} \quad (55)$$

This allows a comparatively sensitive measure of the convergence of the solution and yet maintains a reasonably

fast convergence without affecting the overall accuracy of the solution.

A fixed point arbitrarily defined by $n_{con} = n_\infty - 6$ may also be sufficient.

4.2.2 Validity of the Criterion for the Attainment of Steady State Solution

The criterion for the attainment of steady state solution described in section 3.6 is found to be adequate. The point n_s to which the steady state tests are applied has been chosen to coincide with n_{con} specified in equation (53).

4.2.3 Sensitivity of the Solution to Time Step

The sensitivity of the solution to time step has been tested for various frequencies. Calculations have been carried out with the period of pulsation divided into 12, and 49 intervals respectively. Results indicate that although division of a period into 12 time intervals seems to be too coarse, they differ insignificantly from each other. It is therefore sufficient to use 12 time intervals in the present study.

4.2.4 Relaxation of the Criterion for Jet Spreading

As pointed out in section 3.5, the jet spreads rapidly initially due to a steep velocity gradient. As the computations proceed downstream, the velocity profile becomes wider with a long tail at the jet edge. Because of the very low velocities at the jet edge, small numerical errors introduced there might cause instabilities and the criteria set out in equation (37) for the definition of the jet edge will not be satisfied resulting in continuous addition of unnecessary grid points. Furthermore, the number n_g of grid points which can

be added each time imposes a trade-off between the accuracy of the solution and the computing time required. This is because less computing time will be required if more points are added but since the quantities at the new points are obtained by extrapolation and the jet edge is particularly sensitive to small numerical errors, instability or inaccurate solution may result. The program provides choices of two different number of added grid points as the calculations are marched downstream and if the jet spreads beyond a certain η value which can be obtained from the Goertler solution, a new definition for the jet edge is applied to terminate the jet at the point where the velocity starts increasing or changes sign.

4.2.5 Results

Non-dimensional mean and instantaneous velocity profiles at various time delay intervals are plotted in Fig. 8 for the various frequencies and amplitudes of pulsation and $\zeta = 40.032$. The mean velocity profiles follow closely the steady jet curve. The instantaneous profiles also collapse into the steady jet curve except in Figs. 8(e) and (f) where a slight discrepancy occurs for $\omega = 0.00871$ and 0.0871 and $\epsilon = 0.15$. This agrees with the trend observed in the experimental data of Lai and Simmons (1979), in which a slight departure of the non-dimensional instantaneous velocity profiles from the steady jet curve exists.

The mean centre-line velocity U_c obtained by time-averaging the steady state instantaneous centre-line velocity U_c over a period is shown in Fig. 9 to agree well with the centre-line velocity

decay curve for the steady jets for all the computed cases.

Fig. 10 shows the variation of the jet half-width of the mean velocity profile with streamwise distance. For all cases, the mean jet half-width of the unsteady jet collapses on the steady jet spreading curve. A plot of Q/Q_E , a measure of mean entrainment, versus ζ for various frequencies and amplitudes of pulsation indicates that the mean entrainment rate does not differ from that of the steady jet, which is consistent with the trend associated with the mean centre-line velocity decay and jet spreading. In all the computed cases, the mean momentum flux M is conserved to within 1% over a streamwise distance of 100 nozzle widths, thus confirming the accuracy of the solutions.

With reference to Fig. 12, the non-dimensional mean shear stress profiles of the unsteady jet at $\zeta = 40.032$ agrees very well with that of the steady jet. The non-dimensional instantaneous shear stress profiles can also be collapsed into the steady jet profile except for $\omega = 0.0871$ in Figs. 12(c) and (f) where significant discrepancies are noted. This is consistent with the behavior of the instantaneous velocity profiles where a slight disagreement will be amplified in the velocity gradient term which is shown up in the shear stress profile.

Fig. 13 shows the variation of the steady-state instantaneous centre-line velocity with time for various frequencies and amplitudes of pulsation at three different streamwise distances. The reference signal is given by

$U_c (1 + \epsilon \sin \omega t)$. It can be noted that as the frequency and amplitude increases and for large streamwise distance, distortions in the waveform of the centre-line velocity exist, an indication of the importance of higher harmonics. Such a trend was also observed by Lai and Simmons (1979) in their experimentally pulsed jet. The variation of the phase angle ϕ between the steady-state fundamental component of the centre-line velocity at any streamwise station and that at the nozzle exit with ζ is depicted in Fig. 14. The phase angle is a lag which increases with both frequency and streamwise distance. However, the amplitude of pulsation does not have any significant effect on the phase lag variation. For a region sufficiently close to the nozzle, the flow varies with time in a quasi-steady manner. That is, the solution over the region of interest can be approximated by a sequence of steady jet solutions, each of which corresponds to the instantaneous conditions at the nozzle. The region over which quasi-steady approximations can be applied to an unsteady jet can readily be determined by using the phase plot in Fig. 14. It is taken arbitrarily here that a phase lag of 5 degrees defines the downstream limit to quasi-steady solutions. This definition enables the quasi-steady approximations to U_c to be accurate to within 1%. From Fig. 14 it is apparent that the region over which quasi-steady approximations can be used decreases with increasing frequency. The quasi-steady region for the computed frequencies and for $\epsilon = 0.1$ or 0.15 is as follows -

$$\omega = 0.000871 \quad 0 \leq \zeta \leq 60$$

$$\omega = 0.00871 \quad 0 \leq \zeta \leq 10$$

$$\omega = 0.0871 \quad 0 \leq \zeta \leq 1$$

The variation of the percentage peak-to-peak oscillation, F , of the steady-state instantaneous centre-line velocity expressed as a percentage of the mean value with streamwise distance is plotted in Fig. 15. Although for $\omega = 0.0871$, F differs quite significantly from its initial value of 20% or 30%, it varies very little for other tested frequencies and amplitudes of pulsation. In the experimental data of Lai and Simmons (1979), it was shown that for frequencies between 1 and 10 Hz, which correspond to $\omega = 0.000871$ and 0.00871 here, the general trend indicates that F increases to a maximum at 10 nozzle widths and drops off beyond that point and F increases by almost 40% over the initial value even for 1Hz case. The present computations using the constant eddy viscosity model fail to predict this trend.

5.0 Concluding Remarks

A method which employs a transformation to solve the thin shear layer equations for the steady and unsteady, two-dimensional turbulent free jet issuing into stationary air has been presented. A Prandtl type constant eddy viscosity formulation was used to model the Reynolds shear stress term. The transformation reduces the rate of spread of the jet and enables the use of variable grid sizes over predetermined regions leading to accurate predictions.

In the steady jet, the mean velocity profiles, the mean centre-line velocity decay rate, the spreading rate of the jet and the normalized shear stress profiles all show good agreement with experimental data.

In the unsteady jet, the mean flow characteristics, such as the mean velocity and shear stress profiles, the mean centre-line velocity decay, the mean jet spreading and entrainment all follow closely those of the steady jet for the range of tested frequencies and amplitudes of pulsation. This is in agreement with the only available experimental data of this type which are available in Lai & Simmons (1979). However, unsteady effects are apparent in the distortion of the waveform for the variation of the instantaneous centre-line velocity with time and in the increase in the phase lag with streamwise distance. For high frequencies and amplitude of pulsation or at large streamwise distance from the nozzle, instantaneous quantities depart from quasi-steady values. The flow region over which quasi-steady approximations are applicable has been established for various frequencies.

Although the constant-eddy viscosity model used gives good predictions for the steady jet and the mean quantities for the unsteady jet, it fails to predict accurately the instantaneous quantities especially the percentage peak to peak oscillation of the steady-state instantaneous centre-line velocity. This suggests that if only mean flow quantities are required and if the frequencies and amplitudes of pulsation are of the order of those in this study, the constant eddy-viscosity model is adequate. However, if instantaneous quantities are critical and if frequencies and amplitudes of pulsation are an order of magnitude higher than those in this study, a more refined turbulence model has to be sought and tested.

6.0 References

1. BRADBURY, L. J. S., 1965, "The Structure of a Self-Preserving Turbulent Plane Jet" *J. Fluid Mech.*, vol. 23, part 1, pp. 31-64.
2. BRADSHAW, P., CEBECI, T. and WHITELAW, J. H., 1980, "Lecture Series on Engineering Calculation Methods for Turbulent Flows." Calif State Univ, Long Beach, CA.
3. BREMHORST, K. and HARCH, W. H., 1979, "Near Field Velocity Measurements in a Fully Pulsed Subsonic Air Jet," in *Turbulent Shear Flows I*, ed., by Durst, F., Launder, B. E., Schmidt, F. W. and Whitelaw J. H., Springer-Verlag, Berlin, Heidelberg, pp. 37-54.
4. CEBECI, T. and BRADSHAW, P., 1977, "Momentum Transfer in Boundary Layers", McGraw Hill, New York.
5. CEBECI, T. and SMITH, A. M. O., 1974, "Analysis of Turbulent Boundary Layers", *Applied Math. and Mech.*, 15, Academic Press, New York.
6. CHEN, J. C. and NIKITOPOULOS, C. P., 1979, "On the Near Field Characteristics of Axisymmetric Turbulent Buoyant Jets in a Uniform Environment" *Int. J. Heat Mass Transfer*, vol 22, pp. 245-255.
7. EVERITT, K. W. and ROBINS, A. G., 1978, "The Development and Structure of Turbulent Plane Jets", *J. Fluid Mech.*, vol. 88, part 3, pp. 563-583.
8. FIEDLER, H. and KORSCHELT, D., 1979, "The Two-Dimensional Jet with Periodic Initial Condition," 2nd Symposium on Turbulent Shear Flows, Imperial College, July.
9. GOERTLER, H., 1942, "Berechnung von Aufgaben der freien Turbulenz auf Grund eines neuen Naherungsansatzes" *Z.A.M.M.*, 22, pp. 244-254.
10. GOLDSCHMIDT, V. W. and BRADSHAW, P., 1980, "Upstream Effects on the Widening Rate of Plane Free Jets", To appear.
11. GUTMARK, E. and WYGNANSKI, 1976, "The Planar Turbulent Jet", *J. Fluid Mech.*, vol. 73, part 3, pp. 465-495.
12. HARSHA, P. T., 1971, "Free Turbulent Mixing: A Critical Evaluation of Theory and Experiment" Arnold Engineering Development Center, Report No. AEDC-TR-71-36.

13. HESKESTAD, G., 1965, "Hot-Wire Measurements in a Plane Turbulent Jet", J. Applied. Mech. ASME, Dec., pp. 721-734.
14. HINZE, J. O., 1975, "Turbulence" 2nd Edition, McGraw-Hill, New York.
15. KELLER, H. B., 1970, "A New Difference Scheme for Parabolic Problems", in Numerical Solutions of Partial Differential Equations, vol. II, ed. by J. Bramble, Academic Press, New York.
16. KELLER, H. B., 1978, "Numerical Methods in Boundary-Layer Theory", Ann Rev. Fluid Mech., vol. 10, pp. 417-433.
17. KENT, J. C., 1973, "Unsteady Viscous Jet Flow into Stationary Surroundings" Computers and Fluids, vol. 1, pp. 101-117.
18. KOTSOVINO, N. E., 1976, "A Note on the Spreading Rate and Virtual Origin of a Plane Turbulent Jet", J. Fluid Mech., vol 77, part 2, pp. 305-311.
19. LAI, J. C. S., and SIMMONS, J. M., 1978, "Numerical Solution of the Steady Two-Dimensional Laminar Free Jet" Univ. Queensland, Brisbane, Australia, Department of Mechanical Engineering, Rep. No. 5/78.
20. LAI, J. C. S. and SIMMONS, J. M., 1978, "Numerical Solution of a Periodically Pulsed, two-Dimensional Laminar Free Jet", Univ. Queensland, Brisbane, Australia, Dept. of Mech. Eng., Rep. No. 8/78.
21. LAI, J. C. S., and SIMMONS, J. M., 1979, "Instantaneous Velocity Measurements in a Periodically Pulsea Two-Dimensional Turbulent Jet", Univ. Queensland, Brisbane, Australia, Dept. of Mech. Eng. Rep. No. 13/79.
22. LAUNDER, B. E. and SPALDING, D. B., 1972, "Lectures in Mathematical Models of Turbulence", Academic Press, London.
23. LAUNDER, B. E., MORSE, A., RODI, W. and SPALDING, D. B., 1972, "Prediction of Free Shear Flows-A Comparison of the Performance of Six Turbulence Models", Free Turbulent Shear Flows, vol. 1, NASA SP-321, pp. 361-426.
24. LAUNDER, B. E. and SPALDING, D. B., 1974, "The Numerical Computation of Turbulent Flows" Computer Methods in Applied Mech. and Eng., vol. 3, pp. 269-289.
25. McCORMACK, P. D., COCHRAN, D. and CRANE, L., 1966, "Periodic Vorticity and Its Effect on Jet Mixing" Physics of Fluids, vol. 9, pp. 1555-1560.

26. MCGUIRK, J. J. and RODI, W., 1979, "Mathematical Modelling of Three-Dimensional Heated Surface Jets", *J. Fluid Mech.*, vol. 95, part 4, pp. 609-633.
27. PAI, S. I., 1965, "Unsteady Three-Dimensional Laminar Jet Mixing of a Compressible Fluid", *AIAA J.*, March, pp. 617-621.
28. PIATT, M. and VIETS, H., 1979, "Conditional Sampling in an Unsteady Jet", Paper No. 79-1857, *AIAA Aircraft Systems and Technology Meeting*, August 20-22.
29. PRANDTL, L., 1942, "Bemerkungen zur Theorie der freien Turbulenz" *ZAMM* 22, pp. 241-243.
30. REYNOLDS, W. C and CEBCI, T., 1978, "Calculation of Turbulent Flows" in *Turbulence, Topics in Applied Physics*, vol. 12, ed. by Bradshaw, P., 2nd edition, Springer-Verlag, New York.
31. ROBINS, A. G., 1973, Ph.D. Thesis, London University (As quoted in Rodi, W., 1975).
32. RODI, W., 1975, "A Review of Experimental Data of Uniform Density Free Turbulent Boundary Layers" in *Studies in Convection*, vol. 1, ed. by Launder, B. E., Academic Press, New York.
33. RODI, W. and SPALDING, D. B., 1970, "A Two-Parameter Model of Turbulence and its Applications to Free Jets" *Wärme-und Stoffübertragung Bd. 3*, pp. 85-95.
34. SCHLICHTING, H., 1966, "Boundary-Layer Theory," McGraw-Hill, New York.
35. TOLLMIEN, W., 1926, "Berechnung Turbulenter Ausbreitungsvorgänge" *Z. A. M. M.* vol. 6, pp. 468-478.
36. ZIJNEN, B. G., Van der Hegge, 1958, "Measurements of the Velocity Distribution in a Plane Turbulent Jet of Air", *Appl. Sci., Res., Sect. A*, vol. 7, pp. 256-276.

Appendix A Structure and Listings of Computer Program

A.1 Sturcture of the Steady Jet Program

The structure of the input data is as follows:

CARD 1	NRG, (RG(I), I = 1, NRG), DEGR
FORMAT	I5, 6F10.6
CARD 2	PROD , CONST 1, CONST 2
FORMAT	3F10.6
CARD 3	CO, XO, AA, BB, NPG, INC, IFREQ, NXI
FORMAT	4F10.6, 4I4
CARD 4	(NXTT(I), I = 2, NXII)
FORMAT	10I4
CARD 5	(DELX(I), I=1,NXI), X(1)
FORMAT	8F10.6
CARD 6	(DETAC(I), I = 1,8)
FORMAT	8F10.6
CARD 7	(VC(I), I = 1,7), ETAE
FORMAT	8F10.6
CARD 8	E1, E2, E3
FORMAT	3F10.6
CARD 9	OUTDSK, LN
FORMAT	L1, I3
CARD 10	ETAG
FORMAT	F10.6

The symbols used have the following meaning:

NRG	No. of times grid points have to be rearranged
RG(I)	Upper η value above which grid points will not be dropped
DEGR	Lower η value below which grid points will not be dropped.
PROD	ν defined in section 2.1 (Jet Exit Reynolds Number)
CONST 1, CONST 2	c_1 and c_2 defined in Eq. (12)
CO	$\zeta_0^{1/2}/(ab)$
XO	ζ_0
AA	a defined in Eq. (15a)
BB	b defined in Eq. (15b)
NPG	n_g , No. of grid points to be added if the jet spreads
INC	interval, in terms of the number of transverse grid points, at which a value of the velocity profile is required
IFREQ	interval, in terms of the number of streamwise stations, at which velocity profile is required
NXI	No. of different grid sizes in streamwise direction
NXTT(I)	Streamwise station number at which a different grid size is used.
DELX (I)	Streamwise grid size $\Delta\zeta_i$
X(1)	Value of ζ at initial streamwise station (zero at nozzle exit)
DETAC(I)	Transverse grid size $\Delta\eta$
VC(I)	Values of η for each sub-region
ETAE	$(\eta_\infty)_i$
E1	Convergence limit defined in Eq. (36)
E2, E3	Jet edge definition defined in Eq. (37)

OUTDSK Assumes logical value TRUE if solutions are
 written to disk

LN Device number of writing to disk

ETAG n_a defined in Eq. (28)

A.2. Listing of Steady-Jet Programs

FACSIMILE 1211

卷之三

A.3 Structure of the Unsteady Jet Program

The structure of the input data is as follows:

CARD 1	NRG, (RG(I), I = 1, NRG), DEGR
FORMAT	I5, 6F10.6
CARD 2	(NXG(I), I - 1, NRG)
FORMAT	5I5
CARD 3	NPG, NPG2, START, LN, NEW, NTRANS, NPRINT
FORMAT	7I5
CARD 4	CONST 1, CONST 2
FORMAT	2F10.4
CARD 5	CO, XO, EPS, OMG, NT, INC
FORMAT	4F10.4, 2I5
CARD 6	IFREQ, IFR, IFA, NXI
FORMAT	4I5
CARD 7	(NXTT(I), I=2, NXII)
FORMAT	10I5
CARD 8	(DELX(I), I = 1, NXI), X(1)
FORMAT	8F10.4
CARD 9	(DETAC(I), I = 1,8)
FORMAT	8F10.4
CARD 10	(VC(I), I = 1.7), GTAG
FORMAT	8F10.4
CARD 11	E1, E2, E3, E4, E5, AA, BB, PROD
FORMAT	8F10.4
CARD 12	ETAG
FORMAT	F10.4

Symbols which appear also in the steady jet program have the same meanings here. All other symbols are defined as follows: -

NXG(I)	Streamwise station at which grid has to be rearranged.
NPG 2	Second choice of number of transverse grid points to be added if jet spreads as discussed in section 4.2.4
START	Streamwise station number at which computations start
NEW	See below
NTRANS	Streamwise station number at and beyond which constant c_2 is used.
NPRINT	Streamwise station number at and beyond which velocity profiles are required
EPS	ϵ , amplitude of pulsation
OMG	ω , angular frequency of pulsation
NT	Number of time intervals in a period + 1
IFR	interval, in terms of the number of streamwise stations, at which instantaneous velocity profiles are required.
IFA	interval, in terms of the number of streamwise stations, at which mean quantities are required
E4	ϵ_4 , ϵ_5 and ϵ_7 defined in Eq. (40) and (41)
E5	ϵ_6 defined in Eq. (40)

Because of the initially steep velocity gradient, the velocity gradient curve behaves erratically at the region around the initial jet edge which constitutes about 3% of the total jet-width. To eliminate such numerical erratic behavior, a first-order smoothing function can be applied and is supplied through the Subroutine SMOOTH. The use of the

smoothing function does not affect the overall results and is optional. The parameter NEW specifies the streamwise station number where smoothing function starts to be used. If smoothing function is not required, NEW can assume the value of the final streamwise station number.

A.4 Listing of Unsteady Jet Program

FPC = 2011

200 CONTINUE
 IF(NT.LT.1) GO TO 201
 CALL FOUT
 C1=PI/2.0
 C2=PI/4.0
 C3=PI/3.0
 C4=PI/6.0
 C5=PI/12.0
 C6=PI/24.0
 C7=PI/48.0
 C8=PI/96.0
 C9=PI/192.0
 C10=PI/384.0
 C11=PI/768.0
 C12=PI/1536.0
 C13=PI/3072.0
 C14=PI/6144.0
 C15=PI/12288.0
 C16=PI/24576.0
 C17=PI/49152.0
 C18=PI/98304.0
 C19=PI/196608.0
 C20=PI/393216.0
 C21=PI/786432.0
 C22=PI/1572864.0
 C23=PI/3145728.0
 C24=PI/6291456.0
 C25=PI/12582912.0
 C26=PI/25165824.0
 C27=PI/50331648.0
 C28=PI/100663296.0
 C29=PI/201326592.0
 C30=PI/402653184.0
 C31=PI/805306368.0
 C32=PI/1610612736.0
 C33=PI/3221225472.0
 C34=PI/6442450944.0
 C35=PI/12884901888.0
 C36=PI/25769803776.0
 C37=PI/51539607552.0
 C38=PI/103079215104.0
 C39=PI/206158430208.0
 C40=PI/412316860416.0
 C41=PI/824633720832.0
 C42=PI/164926741664.0
 C43=PI/329853483328.0
 C44=PI/659706966656.0
 C45=PI/131941393312.0
 C46=PI/263882786624.0
 C47=PI/527765573248.0
 C48=PI/105553114696.0
 C49=PI/211106229392.0
 C50=PI/422212458784.0
 C51=PI/844424917568.0
 C52=PI/1688849835136.0
 C53=PI/3377699670272.0
 C54=PI/6755399340544.0
 C55=PI/1351079868108.0
 C56=PI/2702159736216.0
 C57=PI/5404319472432.0
 C58=PI/10808638944864.0
 C59=PI/21617277889728.0
 C60=PI/43234555779456.0
 C61=PI/86469111558912.0
 C62=PI/17293822311784.0
 C63=PI/34587644623568.0
 C64=PI/69175289247136.0
 C65=PI/138350578494272.0
 C66=PI/276701156988544.0
 C67=PI/553402313977088.0
 C68=PI/1106804627954176.0
 C69=PI/2213609255908352.0
 C70=PI/4427218511816704.0
 C71=PI/8854437023633408.0
 C72=PI/17708874047266816.0
 C73=PI/35417748094533632.0
 C74=PI/70835496189067264.0
 C75=PI/141670992378134528.0
 C76=PI/283341984756269056.0
 C77=PI/566683969512538112.0
 C78=PI/113336793902517624.0
 C79=PI/226673587805035248.0
 C80=PI/453347175610070496.0
 C81=PI/906694351220140992.0
 C82=PI/1813388702440281984.0
 C83=PI/3626777404880563968.0
 C84=PI/7253554809761127936.0
 C85=PI/14507109619522255872.0
 C86=PI/29014219238544511744.0
 C87=PI/58028438477089023488.0
 C88=PI/11605687695417804696.0
 C89=PI/23211375390835609392.0
 C90=PI/46422750781671218784.0
 C91=PI/92845401563342437568.0
 C92=PI/185690803126684875136.0
 C93=PI/371381606253369750272.0
 C94=PI/742763212506739500544.0
 C95=PI/1485526425013479001088.0
 C96=PI/2971052850026958002176.0
 C97=PI/5942105700053916004352.0
 C98=PI/1188421140000783200870.0
 C99=PI/2376842280001566401740.0
 C100=PI/4753684560003132803480.0
 C101=PI/9507369120006265606960.0
 C102=PI/19014738240012531213920.0
 C103=PI/38029476480025062427840.0
 C104=PI/76058952960050124855680.0
 C105=PI/15211790592010024911360.0
 C106=PI/30423581184020049822720.0
 C107=PI/60847162368040099645440.0
 C108=PI/12169432473608019890880.0
 C109=PI/24338864947216039781760.0
 C110=PI/48677729894432079563520.0
 C111=PI/97355459788864159127040.0
 C112=PI/194710919577728318254080.0
 C113=PI/389421839155456636508160.0
 C114=PI/778843678310913373016320.0
 C115=PI/1557687356620826746032640.0
 C116=PI/3115374713241653492065280.0
 C117=PI/6230749426483306984130560.0
 C118=PI/12461498852966513968261120.0
 C119=PI/24922997705933027936522240.0
 C120=PI/49845995411866055873044480.0
 C121=PI/99691990823732111746088960.0
 C122=PI/199383981647462223492177920.0
 C123=PI/398767963294924446984355840.0
 C124=PI/797535926589848893968711680.0
 C125=PI/1595071853179697787937423360.0
 C126=PI/3190143706359395575874846720.0
 C127=PI/6380287412718791151749693440.0
 C128=PI/12760574825437982303498966880.0
 C129=PI/25521149650875964606997933760.0
 C130=PI/51042299301751939213995867520.0
 C131=PI/102084598603503878427991750400.0
 C132=PI/204169197207007756855983500800.0
 C133=PI/408338394414015513711967001600.0
 C134=PI/816676788828031027423934003200.0
 C135=PI/163335357765606205484767006400.0
 C136=PI/326670715531212410969534012800.0
 C137=PI/653341430562424821939068025600.0
 C138=PI/1306682861124849643878136051200.0
 C139=PI/2613365722249699287756272102400.0
 C140=PI/5226731444499398575512544204800.0
 C141=PI/10453462888996977151025288409600.0
 C142=PI/20906925777993954302050576819200.0
 C143=PI/41813851555987908604101153638400.0
 C144=PI/83627703111975817208202257356800.0
 C145=PI/167255406223951634416404514713600.0
 C146=PI/334510812447903268832808529427200.0
 C147=PI/669021624895806537665617058854400.0
 C148=PI/1338043249791613075331234117708800.0
 C149=PI/2676086499583226150662468235417600.0
 C150=PI/5352172999166452301324936470835200.0
 C151=PI/10704345998332946602649689541670400.0
 C152=PI/21408691996665893205299379083340800.0
 C153=PI/42817383993331786410598758166681600.0
 C154=PI/85634767986663572821197516333363200.0
 C155=PI/171269539833317445642395032666726400.0
 C156=PI/342539079666634891284790065333452800.0
 C157=PI/685078159333269782569580130666855600.0
 C158=PI/1370156318666539565131602603333711200.0
 C159=PI/2740312637333079130263205206667422400.0
 C160=PI/5480625274666158260526410413334844800.0
 C161=PI/1096125054933235652105282082666969600.0
 C162=PI/2192250109866471304210564165333939200.0
 C163=PI/4384500219733942608421128330667878400.0
 C164=PI/8769004439467885216844256661335756800.0
 C165=PI/1753800887893577043368851322667513600.0
 C166=PI/3507601775787154086737702645335027200.0
 C167=PI/7015203551574308173475405290667054400.0
 C168=PI/14030407103586516348558010581334108800.0
 C169=PI/28060814207173032697116021162668217600.0
 C170=PI/56121628414346065394232042325336435200.0
 C171=PI/11224325682869212678846084465067286400.0
 C172=PI/22448651365738425357692168930134576800.0
 C173=PI/44897302731476850715384337860269153600.0
 C174=PI/89794605462953701430768675720538307200.0
 C175=PI/179589210925867402661537351441076614400.0
 C176=PI/359178421851734805323074702882153228800.0
 C177=PI/718356843703469610646149405764306557600.0
 C178=PI/143671368740693922129239881152861115200.0
 C179=PI/287342737481387844258479762305722230400.0
 C180=PI/574685474962775688516995324611444460800.0
 C181=PI/114937094931551377033990648922888921600.0
 C182=PI/229874189863102654067981297845777843200.0
 C183=PI/459748379726205308135962595691555686400.0
 C184=PI/919496759452410616271925191383111372800.0
 C185=PI/1838993598904821232543850382766226545600.0
 C186=PI/3677987197809642465087700765532452911200.0
 C187=PI/7355974395619284930175401531064855822400.0
 C188=PI/1471194679123857986035082306212911648800.0
 C189=PI/2942389358247715972070014612425823297600.0
 C190=PI/5884778716495431944140029224851764655200.0
 C191=PI/1176955633298586388280058544960352910400.0
 C192=PI/2353911266597172776560017858920705820800.0
 C193=PI/4707822533194345553120035777841411617600.0
 C194=PI/9415645066388691106240071555682823235200.0
 C195=PI/18831280132777382212480143113365656670400.0
 C196=PI/37662560265554764424960286226731313340800.0
 C197=PI/75325120531109528849200572453462666681600.0
 C198=PI/15065024106221905769400144906925313323200.0
 C199=PI/30130048212443811538800289038950666646400.0
 C200=PI/60260096424887623077600578077851333292800.0
 C201=PI/120520192497753260153201156155706666585600.0
 C202=PI/241040384995506520306402311231413333171200.0
 C203=PI/482080769991013040612804622462826666342400.0
 C204=PI/964161539982026081225609244925653333284800.0
 C205=PI/1928323079840452162512184889811066666569600.0
 C206=PI/3856646159680854325024369779622133333139200.0
 C207=PI/7713292319361708650048739559244266666678400.0
 C208=PI/15426584638723573200974791118485333333356800.0
 C209=PI/30853169277447146401949582236970666666673600.0
 C210=PI/61706338554894292803899164473941333333347200.0
 C211=PI/123412677109788585607793328947826666666694400.0
 C212=PI/246825354219577171215586657895653333333388800.0
 C213=PI/493650708439154342431173315791306666666777600.0
 C214=PI/987301416878308684862346631582613333333555200.0
 C215=PI/197460283375661736932693326365226666666710400.0
 C216=PI/394920566751323473865386652670453333333402400.0
 C217=PI/789841133502646947730773305340906666666704800.0
 C218=PI/1579682267005293955415466510681813333333401600.0
 C219=PI/3159364534001047910830933021363626666666703200.0
 C220=PI/6318729068002095821661866042727253333333406400.0
 C221=PI/1263745813600419164333733008554453333333403200.0
 C222=PI/2527491627200838328667466017108906666666706400.0
 C223=PI/5054983254401676657334933034217813333333403200.0
 C224=PI/10109966588803353314667866068435626666666706400.0
 C225=PI/20219933177606706629335733136871253333333406400.0
 C226=PI/4043986635521341325867146627374453333333403200.0
 C227=PI/80879732710426826517342933314493125333333403200.0
 C228=PI/16175946542085365303485866662886253333333403200.0
 C229=PI/32351893084170730606971733333177253333333403200.0
 C230=PI/64703786168341461213943466666634525333333403200.0
 C231=PI/129407572336682924267868933333334525333333403200.0
 C232=PI/258815144673365848535737866666668525333333403200.0
 C233=PI/517630289346731697071475733333334525333333403200.0
 C234=PI/1035260578693463394143514666666668525333333403200.0
 C235=PI/2070521157386926788287029333333334525333333403200.0
 C236=PI/4141042314773853576574058666666668525333333403200.0
 C237=PI/8282084629547707153148117333333334525333333403200.0
 C238=PI/16564169259095414306282234666666668525333333403200.0
 C239=PI/33128338518190828612564468666666668525333333403200.0
 C240=PI/662566770363816572251289346666666668525333333403200.0
 C241=PI/132513354072763144448578686666666668525333333403200.0
 C242=PI/2650267081455262888915573466666666668525333333403200.0
 C243=PI/5300534162910525777831146866666666668525333333403200.0
 C244=PI/10601068325821051555662893466666666668525333333403200.0
 C245=PI/21202136651642103111335786866666666668525333333403200.0
 C246=PI/424042733032842062226715734666666666668525333333403200.0
 C247=PI/848085466065684124453431486666666666668525333333403200.0
 C248=PI/16961709321313682489066589346666666666668525333333403200.0
 C249=PI/3392341864262736497813317866666666666668525333333403200.0
 C250=PI/678468372852547299562663573466666666666668525333333403200.0
 C251=PI/135693674564509459125331146666666666666668525333333403200.0
 C252=PI/2713873491290188118256622934666666666666668525333333403200.0
 C253=PI/5427746982580376236513325866666666666666668525333333403200.0
 C254=PI/10855493965607532730266511466666666666666668525333333403200.0
 C255=PI/217109879312150654605334229346666666666666668525333333403200.0
 C256=PI/434219758624301309210668458666666666666666668525333333403200.0
 C257=PI/868439517248602618421336914666666666666666668525333333403200.0
 C258=PI/17368790344972052368426738293466666666666666668525333333403200.0
 C259=PI/34737580689944104736885476586666666666666666668525333333403200.0
 C260=PI/694751613798882094737709531734666666666666666668525333333403200.0
 C261=PI/1389503275977764189475419063466666666666666666668525333333403200.0
 C262=PI/27790065519555283789508381268666666666666666666668525333333403200.0
 C263=PI/55580131039110567578901665346666666666666666666668525333333403200.0
 C264=PI/1111602620782211455780333106866666666666666666666668525333333403200.0
 C265=PI/22232052415644229115406662134666666666666666666666668525333333403200.0
 C266=PI/444641048312884582308133242686666666666666666666666668525333333403200.0
 C267=PI/889282096625769164616266485346666666666666666666666668525333333403200.0
 C268=PI/1778564193251538329232531706866666666666666666666666668525333333403200.0
 C269=PI/35571283865030766584650634134666666666666666666666666668525333333403200.0
 C270=PI/71

FEC: JHJ

PAGE 6005

PAGE 5008


```

      I=I+1
      J=J+1
      ECCC 000100
      Z=0.0
      N=0
      **** TO COMPUTE MEAN JET CENTER-LINE G AND NO. OF TRANSVERSE GRID POINT
      **** Z=0.0
      J1=INT(I)
      J2=J1+1
      NMAX=NPA(1)
      F(I,J1,2)/G(I,J,2),GT./3.0P,APS(G(I,J+1,2)),GT./2)
      J=J+1
      Z=G(I,J,2)
      ECCC 000110
      ESEC 000111
      KPA(I)=J1
      KPA(I)=J1
      ECCC 000112
      JN=JMAX
      ECCC 000113
      NMAX=
      JN=J1-100/(NT)
      ACC=G(I,J,2)
      ACC=G(I,J,2)/(NT)
      JN=FLAT-(JN)/FLAT(NT)
      JW=0.0
      ECCC 000114
      NMAX=X=JN
      KPA(I)=JN
      CCE15 I=1,J1
      CCE16 I=1,J1,GT,APRAX)OC TO 6018
      CCE16 J=J1,UMAX
      F(I,J,2)=F(I,J,2)
      C(I,J,2)=C(I,J,2)
      C(I,J,2)=C(I,J,2)
      ECCC 000117
      **** CALCULATE AMPLITUDE OF OSCILLATION
      I:DX=1
      IMIN=1
      UMAX=G(I,J,2)
      UMIN=G(I,J,2)
      CCE18 I=1,J1
      IF(G(I,J,2)<=UMAX)OC TO 6020
      UMAX=G(I,J,2)
      I=MAX=1
      G(I,J,2)=0.0
      IF(G(I,J,2)>UMAX)OC TO 6030
      UMAX=G(I,J,2)
      IMIN=1
      ECCC 000119
      CALL OSC1(VMAX,VMIN)
      CALL OSC1(VMAX,VMIN)
      P=F(I,J,2)-(VMAX-VMIN)/AGC
      **** 17 COMPUTE MEAN PROFILES
      CCE15 I=1,J1
      KJ=NPA(1)
      IF(JW<=KJ)OC TO 6115
      KJ=KJ+1
      F(I,J,2)=F(I,J,2)
      F(I,J,2)=F(I,J,2)
      C(I,J,2)=C(I,J,2)
      C(I,J,2)=C(I,J,2)
      ECCC 000120
      CCE15 I=1,JW
      AVP(I,J)=F(I,J,2)

```

PAGE 111

600
601
602
603
604
605
606
607
608
609
610
611
612
613
614
615
616
617
618
619
620
621
622
623
624
625
626
627
628
629
630
631
632
633
634
635
636
637
638
639
640
641
642
643
644
645
646
647
648
649
650
651
652
653
654
655
656
657
658
659
660
661
662
663
664
665
666
667
668
669
670
671
672
673
674
675
676
677
678
679
680
681
682
683
684
685
686
687
688
689
690
691
692
693
694
695
696
697
698
699
700
701
702
703
704
705
706
707
708
709
7010
7011
7012
7013
7014
7015
7016
7017
7018
7019
7020
7021
7022
7023
7024
7025
7026
7027
7028
7029
7030
7031
7032
7033
7034
7035
7036
7037
7038
7039
7040
7041
7042
7043
7044
7045
7046
7047
7048
7049
7050
7051
7052
7053
7054
7055
7056
7057
7058
7059
7060
7061
7062
7063
7064
7065
7066
7067
7068
7069
7070
7071
7072
7073
7074
7075
7076
7077
7078
7079
7080
7081
7082
7083
7084
7085
7086
7087
7088
7089
7090
7091
7092
7093
7094
7095
7096
7097
7098
7099
70100
70101
70102
70103
70104
70105
70106
70107
70108
70109
70110
70111
70112
70113
70114
70115
70116
70117
70118
70119
70120
70121
70122
70123
70124
70125
70126
70127
70128
70129
70130
70131
70132
70133
70134
70135
70136
70137
70138
70139
70140
70141
70142
70143
70144
70145
70146
70147
70148
70149
70150
70151
70152
70153
70154
70155
70156
70157
70158
70159
70160
70161
70162
70163
70164
70165
70166
70167
70168
70169
70170
70171
70172
70173
70174
70175
70176
70177
70178
70179
70180
70181
70182
70183
70184
70185
70186
70187
70188
70189
70190
70191
70192
70193
70194
70195
70196
70197
70198
70199
70200
70201
70202
70203
70204
70205
70206
70207
70208
70209
70210
70211
70212
70213
70214
70215
70216
70217
70218
70219
70220
70221
70222
70223
70224
70225
70226
70227
70228
70229
70230
70231
70232
70233
70234
70235
70236
70237
70238
70239
70240
70241
70242
70243
70244
70245
70246
70247
70248
70249
70250
70251
70252
70253
70254
70255
70256
70257
70258
70259
70260
70261
70262
70263
70264
70265
70266
70267
70268
70269
70270
70271
70272
70273
70274
70275
70276
70277
70278
70279
70280
70281
70282
70283
70284
70285
70286
70287
70288
70289
70290
70291
70292
70293
70294
70295
70296
70297
70298
70299
70300
70301
70302
70303
70304
70305
70306
70307
70308
70309
70310
70311
70312
70313
70314
70315
70316
70317
70318
70319
70320
70321
70322
70323
70324
70325
70326
70327
70328
70329
70330
70331
70332
70333
70334
70335
70336
70337
70338
70339
70340
70341
70342
70343
70344
70345
70346
70347
70348
70349
70350
70351
70352
70353
70354
70355
70356
70357
70358
70359
70360
70361
70362
70363
70364
70365
70366
70367
70368
70369
70370
70371
70372
70373
70374
70375
70376
70377
70378
70379
70380
70381
70382
70383
70384
70385
70386
70387
70388
70389
70390
70391
70392
70393
70394
70395
70396
70397
70398
70399
70400
70401
70402
70403
70404
70405
70406
70407
70408
70409
70410
70411
70412
70413
70414
70415
70416
70417
70418
70419
70420
70421
70422
70423
70424
70425
70426
70427
70428
70429
70430
70431
70432
70433
70434
70435
70436
70437
70438
70439
70440
70441
70442
70443
70444
70445
70446
70447
70448
70449
70450
70451
70452
70453
70454
70455
70456
70457
70458
70459
70460
70461
70462
70463
70464
70465
70466
70467
70468
70469
70470
70471
70472
70473
70474
70475
70476
70477
70478
70479
70480
70481
70482
70483
70484
70485
70486
70487
70488
70489
70490
70491
70492
70493
70494
70495
70496
70497
70498
70499
70500
70501
70502
70503
70504
70505
70506
70507
70508
70509
70510
70511
70512
70513
70514
70515
70516
70517
70518
70519
70520
70521
70522
70523
70524
70525
70526
70527
70528
70529
70530
70531
70532
70533
70534
70535
70536
70537
70538
70539
70540
70541
70542
70543
70544
70545
70546
70547
70548
70549
70550
70551
70552
70553
70554
70555
70556
70557
70558
70559
70560
70561
70562
70563
70564
70565
70566
70567
70568
70569
70570
70571
70572
70573
70574
70575
70576
70577
70578
70579
70580
70581
70582
70583
70584
70585
70586
70587
70588
70589
70590
70591
70592
70593
70594
70595
70596
70597
70598
70599
70600
70601
70602
70603
70604
70605
70606
70607
70608
70609
70610
70611
70612
70613
70614
70615
70616
70617
70618
70619
70620
70621
70622
70623
70624
70625
70626
70627
70628
70629
70630
70631
70632
70633
70634
70635
70636
70637
70638
70639
70640
70641
70642
70643
70644
70645
70646
70647
70648
70649
70650
70651
70652
70653
70654
70655
70656
70657
70658
70659
70660
70661
70662
70663
70664
70665
70666
70667
70668
70669
70670
70671
70672
70673
70674
70675
70676
70677
70678
70679
70680
70681
70682
70683
70684
70685
70686
70687
70688
70689
70690
70691
70692
70693
70694
70695
70696
70697
70698
70699
70700
70701
70702
70703
70704
70705
70706
70707
70708
70709
70710
70711
70712
70713
70714
70715
70716
70717
70718
70719
70720
70721
70722
70723
70724
70725
70726
70727
70728
70729
70730
70731
70732
70733
70734
70735
70736
70737
70738
70739
70740
70741
70742
70743
70744
70745
70746
70747
70748
70749
70750
70751
70752
70753
70754
70755
70756
70757
70758
70759
70760
70761
70762
70763
70764
70765
70766
70767
70768
70769
70770
70771
70772
70773
70774
70775
70776
70777
70778
70779
70780
70781
70782
70783
70784
70785
70786
70787
70788
70789
70790
70791
70792
70793
70794
70795
70796
70797
70798
70799
70800
70801
70802
70803
70804
70805
70806
70807
70808
70809
70810
70811
70812
70813
70814
70815
70816
70817
70818
70819
70820
70821
70822
70823
70824
70825
70826
70827
70828
70829
70830
70831
70832
70833
70834
70835
70836
70837
70838
70839
70840
70841
70842
70843
70844
70845
70846
70847
70848
70849
70850
70851
70852
70853
70854
70855
70856
70857
70858
70859
70860
70861
70862
70863
70864
70865
70866
70867
70868
70869
70870
70871
70872
70873
70874
70875
70876
70877
70878
70879
70880
70881
70882
70883
70884
70885
70886
70887
70888
70889
70890
70891
70892
70893
70894
70895
70896
70897
70898
70899
70900
70901
70902
70903
70904
70905
70906
70907
70908
70909
70910
70911
70912
70913
70914
70915
70916
70917
70918
70919
70920
70921
70922
70923
70924
70925
70926
70927
70928
70929
70930
70931
70932
70933
70934
70935
70936
70937
70938
70939
70940
70941
70942
70943
70944
70945
70946
70947
70948
70949
70950
70951
70952
70953
70954
70955
70956
70957
70958
70959
70960
70961
70962
70963
70964
70965
70966
70967
70968
70969
70970
70971
70972
70973
70974
70975
70976
70977
70978
70979
70980
70981
70982
70983
70984
70985
70986
70987
70988
70989
70990
70991
70992
70993
70994
70995
70996
70997
70998
70999
70100
70101
70102
70103
70104
70105
70106
70107
70108
70109
70110
70111
70112
70113
70114
70115
70116
70117
70118
70119
70120
70121
70122
70123
70124
70125
70126
70127
70128
70129
70130
70131
70132
70133
70134
70135
70136
70137
70138
70139
70140
70141
70142
70143
70144
70145
70146
70147
70148
70149
70150
70151
70152
70153
70154
70155
70156
70157
70158
70159
70160
70161
70162
70163
70164
70165
70166
70167
70168
70169
70170
70171
70172
70173
70174
70175
70176
70177
70178
70179
70180
70181
70182
70183
70184
70185
70186
70187
70188
70189
70190
70191
70192
70193
70194
70195
70196
70197
70198
70199
70200
70201
70202
70203
70204
70205
70206
70207
70208
70209
70210
70211
70212
70213
70214
70215
70216
70217
70218
70219
70220
70221
70222
70223
70224
70225
70226
70227
70228
70229
70230
70231
70232
70233
70234
70235
70236
70237
70238
70239
70240
70241
70242
70243
70244
70245
70246
70247
70248
70249
70250
70251
70252
70253
70254
70255
70256
70257
70258
70259
70260
70261
70262
70263
70264
70265
70266
70267
70268
70269
70270
70271
70272
70273
70274
70275
70276
70277
70278
70279
70280
70281
70282
70283
70284
70285
70286
70287
70288
70289
70290
70291
70292
70293
70294
70295
70296
70297
70298
70299
70300
70301
70302
70303
70304
70305
70306
70307
70308
70309
70310
70311
70312
70313
70314
70315
70316
70317
70318
70319
70320
70321
70322
70323
70324
70325
70326
70327
70328
70329
70330
70331
70332
70333
70334
70335
70336
70337
70338
70339
70340
70341
70342
70343
70344
70345
70346
70347
70348
70349
70350
70351
70352
70353
70354
70355
70356
70357
70358
70359
70360
70361
70362
70363
70364
70365
70366
70367
70368
70369
70370
70371
70372
70373
70374
70375
70376
70377
70378
70379
70380
70381
70382
70383
70384
70385
70386
70387
70388
70389
70390
70391
70392
70393
70394
70395
70396
70397
70398
70399
70400
70401
70402
70403
70404
70405
70406
70407
70408
70409
70410
70411
70412
70413
70414
70415
70416
70417
70418
70419
70420
70421
70422
70423
70424
70425
70426
70427
70428
70429
70430
70431
70432
70433
70434
70435
70436
70437
70438
70439
70440
70441
70442
70443
70444
70445
70446
70447
70448
70449
70450
70451
70452
70453
70454
70455
70456
70457
70458
70459
70460
70461
70462
70463
70464
70465
70466
70467
70468
70469
70470
70471
70472
70473
70474
70475
70476
70477
70478
70479
70480
70481
70482
70483
70484
70485
70486
70487
70488
70489
70490
70491
70492
70493
70494
70495
70496
70497
70498
70499
70500
70501
70502
70503
70504
70505
70506
70507
70508
70509
70510
70511
70512
70513
70514
70515
70516
70517
70518
70519
70520
70521
70522
70523
70524
70525
70526
70527

Page 14

COMMUNICATIONAL
 LOGICAL LOGIC
 C**** THIS SUBRITES THE V-LIMITY GRADIENT PROFILE
 C
 IF(X,Y,LT,MAXCC TO 3600
 3605 T=1,J=1,I=1
 3610
 3615
 3620
 3625
 3630
 3635
 3640
 3645
 3650
 3655
 3660
 3665
 3670
 3675
 3680
 3685
 3690
 3695
 3700
 3705
 3710
 3715
 3720
 3725
 3730
 3735
 3740
 3745
 3750
 3755
 3760
 3765
 3770
 3775
 3780
 3785
 3790
 3795
 3800
 3805
 3810
 3815
 3820
 3825
 3830
 3835
 3840
 3845
 3850
 3855
 3860
 3865
 3870
 3875
 3880
 3885
 3890
 3895
 3900
 3905
 3910
 3915
 3920
 3925
 3930
 3935
 3940
 3945
 3950
 3955
 3960
 3965
 3970
 3975
 3980
 3985
 3990
 3995
 4000
 4005
 4010
 4015
 4020
 4025
 4030
 4035
 4040
 4045
 4050
 4055
 4060
 4065
 4070
 4075
 4080
 4085
 4090
 4095
 4100
 4105
 4110
 4115
 4120
 4125
 4130
 4135
 4140
 4145
 4150
 4155
 4160
 4165
 4170
 4175
 4180
 4185
 4190
 4195
 4200
 4205
 4210
 4215
 4220
 4225
 4230
 4235
 4240
 4245
 4250
 4255
 4260
 4265
 4270
 4275
 4280
 4285
 4290
 4295
 4300
 4305
 4310
 4315
 4320
 4325
 4330
 4335
 4340
 4345
 4350
 4355
 4360
 4365
 4370
 4375
 4380
 4385
 4390
 4395
 4400
 4405
 4410
 4415
 4420
 4425
 4430
 4435
 4440
 4445
 4450
 4455
 4460
 4465
 4470
 4475
 4480
 4485
 4490
 4495
 4500
 4505
 4510
 4515
 4520
 4525
 4530
 4535
 4540
 4545
 4550
 4555
 4560
 4565
 4570
 4575
 4580
 4585
 4590
 4595
 4600
 4605
 4610
 4615
 4620
 4625
 4630
 4635
 4640
 4645
 4650
 4655
 4660
 4665
 4670
 4675
 4680
 4685
 4690
 4695
 4700
 4705
 4710
 4715
 4720
 4725
 4730
 4735
 4740
 4745
 4750
 4755
 4760
 4765
 4770
 4775
 4780
 4785
 4790
 4795
 4800
 4805
 4810
 4815
 4820
 4825
 4830
 4835
 4840
 4845
 4850
 4855
 4860
 4865
 4870
 4875
 4880
 4885
 4890
 4895
 4900
 4905
 4910
 4915
 4920
 4925
 4930
 4935
 4940
 4945
 4950
 4955
 4960
 4965
 4970
 4975
 4980
 4985
 4990
 4995
 5000
 5005
 5010
 5015
 5020
 5025
 5030
 5035
 5040
 5045
 5050
 5055
 5060
 5065
 5070
 5075
 5080
 5085
 5090
 5095
 5100
 5105
 5110
 5115
 5120
 5125
 5130
 5135
 5140
 5145
 5150
 5155
 5160
 5165
 5170
 5175
 5180
 5185
 5190
 5195
 5200
 5205
 5210
 5215
 5220
 5225
 5230
 5235
 5240
 5245
 5250
 5255
 5260
 5265
 5270
 5275
 5280
 5285
 5290
 5295
 5300
 5305
 5310
 5315
 5320
 5325
 5330
 5335
 5340
 5345
 5350
 5355
 5360
 5365
 5370
 5375
 5380
 5385
 5390
 5395
 5400
 5405
 5410
 5415
 5420
 5425
 5430
 5435
 5440
 5445
 5450
 5455
 5460
 5465
 5470
 5475
 5480
 5485
 5490
 5495
 5500
 5505
 5510
 5515
 5520
 5525
 5530
 5535
 5540
 5545
 5550
 5555
 5560
 5565
 5570
 5575
 5580
 5585
 5590
 5595
 5600
 5605
 5610
 5615
 5620
 5625
 5630
 5635
 5640
 5645
 5650
 5655
 5660
 5665
 5670
 5675
 5680
 5685
 5690
 5695
 5700
 5705
 5710
 5715
 5720
 5725
 5730
 5735
 5740
 5745
 5750
 5755
 5760
 5765
 5770
 5775
 5780
 5785
 5790
 5795
 5800
 5805
 5810
 5815
 5820
 5825
 5830
 5835
 5840
 5845
 5850
 5855
 5860
 5865
 5870
 5875
 5880
 5885
 5890
 5895
 5900
 5905
 5910
 5915
 5920
 5925
 5930
 5935
 5940
 5945
 5950
 5955
 5960
 5965
 5970
 5975
 5980
 5985
 5990
 5995
 6000
 6005
 6010
 6015
 6020
 6025
 6030
 6035
 6040
 6045
 6050
 6055
 6060
 6065
 6070
 6075
 6080
 6085
 6090
 6095
 6100
 6105
 6110
 6115
 6120
 6125
 6130
 6135
 6140
 6145
 6150
 6155
 6160
 6165
 6170
 6175
 6180
 6185
 6190
 6195
 6200
 6205
 6210
 6215
 6220
 6225
 6230
 6235
 6240
 6245
 6250
 6255
 6260
 6265
 6270
 6275
 6280
 6285
 6290
 6295
 6300
 6305
 6310
 6315
 6320
 6325
 6330
 6335
 6340
 6345
 6350
 6355
 6360
 6365
 6370
 6375
 6380
 6385
 6390
 6395
 6400
 6405
 6410
 6415
 6420
 6425
 6430
 6435
 6440
 6445
 6450
 6455
 6460
 6465
 6470
 6475
 6480
 6485
 6490
 6495
 6500
 6505
 6510
 6515
 6520
 6525
 6530
 6535
 6540
 6545
 6550
 6555
 6560
 6565
 6570
 6575
 6580
 6585
 6590
 6595
 6600
 6605
 6610
 6615
 6620
 6625
 6630
 6635
 6640
 6645
 6650
 6655
 6660
 6665
 6670
 6675
 6680
 6685
 6690
 6695
 6700
 6705
 6710
 6715
 6720
 6725
 6730
 6735
 6740
 6745
 6750
 6755
 6760
 6765
 6770
 6775
 6780
 6785
 6790
 6795
 6800
 6805
 6810
 6815
 6820
 6825
 6830
 6835
 6840
 6845
 6850
 6855
 6860
 6865
 6870
 6875
 6880
 6885
 6890
 6895
 6900
 6905
 6910
 6915
 6920
 6925
 6930
 6935
 6940
 6945
 6950
 6955
 6960
 6965
 6970
 6975
 6980
 6985
 6990
 6995
 7000
 7005
 7010
 7015
 7020
 7025
 7030
 7035
 7040
 7045
 7050
 7055
 7060
 7065
 7070
 7075
 7080
 7085
 7090
 7095
 7100
 7105
 7110
 7115
 7120
 7125
 7130
 7135
 7140
 7145
 7150
 7155
 7160
 7165
 7170
 7175
 7180
 7185
 7190
 7195
 7200
 7205
 7210
 7215
 7220
 7225
 7230
 7235
 7240
 7245
 7250
 7255
 7260
 7265
 7270
 7275
 7280
 7285
 7290
 7295
 7300
 7305
 7310
 7315
 7320
 7325
 7330
 7335
 7340
 7345
 7350
 7355
 7360
 7365
 7370
 7375
 7380
 7385
 7390
 7395
 7400
 7405
 7410
 7415
 7420
 7425
 7430
 7435
 7440
 7445
 7450
 7455
 7460
 7465
 7470
 7475
 7480
 7485
 7490
 7495
 7500
 7505
 7510
 7515
 7520
 7525
 7530
 7535
 7540
 7545
 7550
 7555
 7560
 7565
 7570
 7575
 7580
 7585
 7590
 7595
 7600
 7605
 7610
 7615
 7620
 7625
 7630
 7635
 7640
 7645
 7650
 7655
 7660
 7665
 7670
 7675
 7680
 7685
 7690
 7695
 7700
 7705
 7710
 7715
 7720
 7725
 7730
 7735
 7740
 7745
 7750
 7755
 7760
 7765
 7770
 7775
 7780
 7785
 7790
 7795
 7800
 7805
 7810
 7815
 7820
 7825
 7830
 7835
 7840
 7845
 7850
 7855
 7860
 7865
 7870
 7875
 7880
 7885
 7890
 7895
 7900
 7905
 7910
 7915
 7920
 7925
 7930
 7935
 7940
 7945
 7950
 7955
 7960
 7965
 7970
 7975
 7980
 7985
 7990
 7995
 8000
 8005
 8010
 8015
 8020
 8025
 8030
 8035
 8040
 8045
 8050
 8055
 8060
 8065
 8070
 8075
 8080
 8085
 8090
 8095
 8100
 8105
 8110
 8115
 8120
 8125
 8130
 8135
 8140
 8145
 8150
 8155
 8160
 8165
 8170
 8175
 8180
 8185
 8190
 8195
 8200
 8205
 8210
 8215
 8220
 8225
 8230
 8235
 8240
 8245
 8250
 8255
 8260
 8265
 8270
 8275
 8280
 8285
 8290
 8295
 8300
 8305
 8310
 8315
 8320
 8325
 8330
 8335
 8340
 8345
 8350
 8355
 8360
 8365
 8370
 8375
 8380
 8385
 8390
 8395
 8400
 8405
 8410
 8415
 8420
 8425
 8430
 8435
 8440
 8445
 8450
 8455
 8460
 8465
 8470
 8475
 8480
 8485
 8490
 8495
 8500
 8505
 8510
 8515
 8520
 8525
 8530
 8535
 8540
 8545
 8550
 8555
 8560
 8565
 8570
 8575
 8580
 8585
 8590
 8595
 8600
 8605
 8610
 8615
 8620
 8625
 8630
 8635
 8640
 8645
 8650
 8655
 8660
 8665
 8670
 8675
 8680
 8685
 8690
 8695
 8700
 8705
 8710
 8715
 8720
 8725
 8730
 8735
 8740
 8745
 8750
 8755
 8760
 8765
 8770
 8775
 8780
 8785
 8790
 8795
 8800
 8805
 8810
 8815
 8820
 8825
 8830
 8835
 8840
 8845
 8850
 8855
 8860
 8865
 8870
 8875
 8880
 8885
 8890
 8895
 8900
 8905
 8910
 8915
 8920
 8925
 8930
 8935
 8940
 8945
 8950
 8955
 8960
 8965
 8970
 8975
 8980
 8985
 8990
 8995
 9000
 9005
 9010
 9015
 9020
 9025
 9030
 9035
 9040
 9045
 9050
 9055
 9060
 9065
 9070
 9075
 9080
 9085
 9090
 9095
 9100
 9105
 9110
 9115
 9120
 9125
 9130
 9135
 9140
 9145
 9150
 9155
 9160
 9165
 9170
 9175
 9180
 9185
 9190
 9195
 9200
 9205
 9210
 9215
 9220
 9225
 9230
 9235
 9240
 9245
 9250
 9255
 9260
 9265
 9270
 9275
 9280
 9285
 9290
 9295
 9300
 9305
 9310
 9315
 9320
 9325
 9330
 9335
 9340
 9345
 9350
 9355
 9360
 9365
 9370
 9375
 9380
 9385
 9390
 9395
 9400
 9405
 9410
 9415
 9420
 9425
 9430
 9435
 9440
 9445
 9450
 9455
 9460
 9465
 9470
 9475
 9480
 9485
 9490
 9495
 9500
 9505
 9510
 9515
 9520
 9525
 9530
 9535
 9540
 9545
 9550
 9555
 9560
 9565
 9570
 9575
 9580
 9585
 9590
 9595
 9600
 9605
 9610
 9615
 9620
 9625
 9630
 9635
 9640
 9645
 9650
 9655
 9660
 9665
 9670
 9675
 9680
 9685
 9690
 9695
 9700
 9705
 9710
 9715
 9720
 9725
 9730
 9735
 9740
 9745
 9750
 9755
 9760
 9765
 9770
 9775
 9780
 9785
 9790
 9795
 9800
 9805
 9810
 9815
 9820
 9825
 9830
 9835
 9840
 9845
 9850
 9855
 9860
 9865
 9870
 9875
 9880
 9885
 9890
 9895
 9900
 9905
 9910
 9915
 9920
 9925
 9930
 9935
 9940
 9945
 9950
 9955
 9960
 9965
 9970
 9975
 9980
 9985
 9990
 9995
 10000

Appendix B. Figures

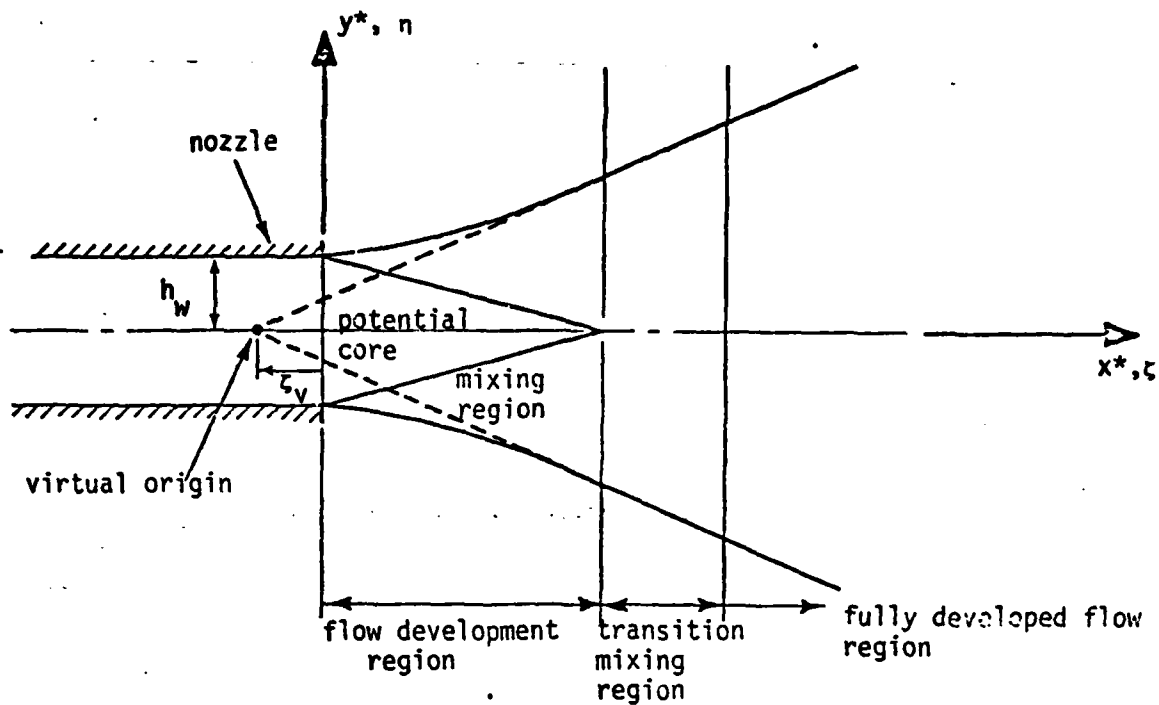


Figure 1. Configuration of the Plane Jet

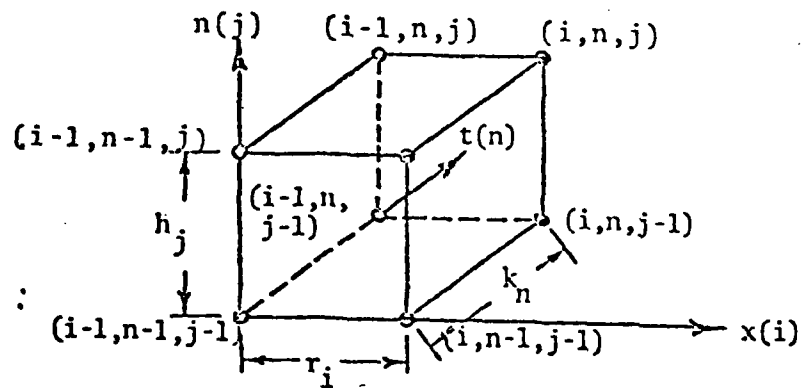


FIGURE 2. Net cube for the difference equations for Eq (21).

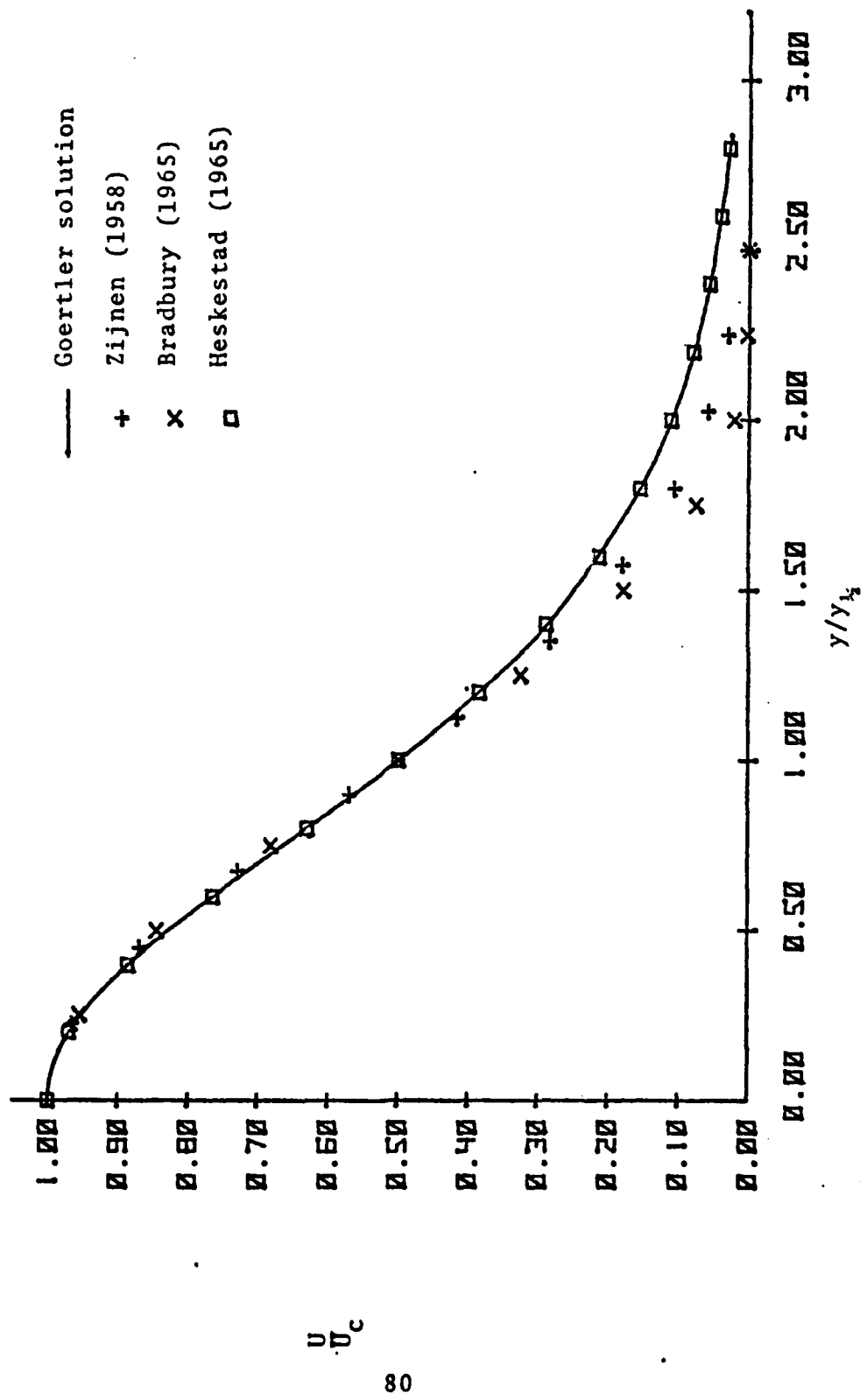


Figure 3. Non-Dimensional Self-Preserved Velocity Profile of the Steady Jet

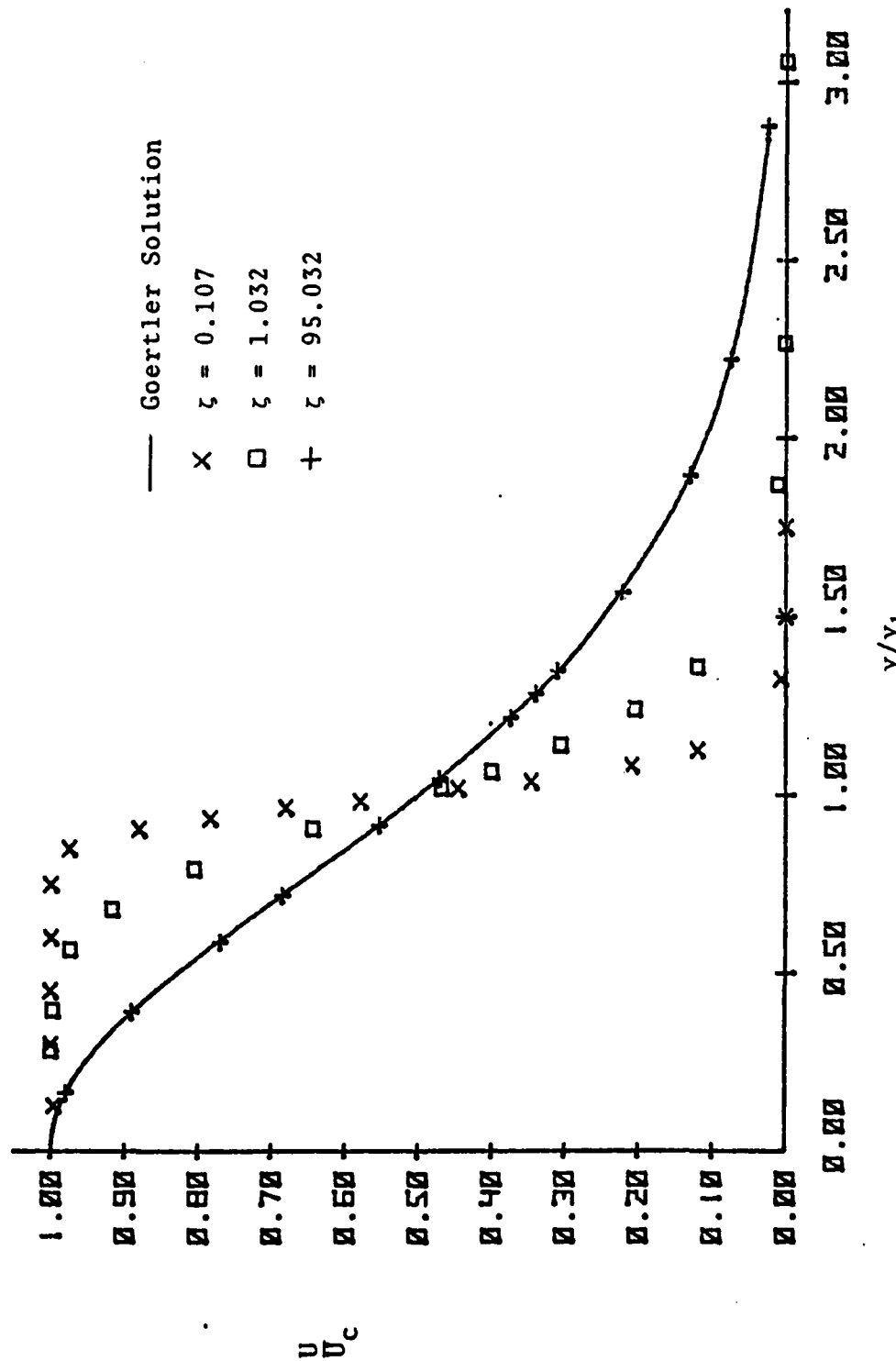


Figure 4 (a) Non-Dimensional Velocity Distribution of the Steady Jet

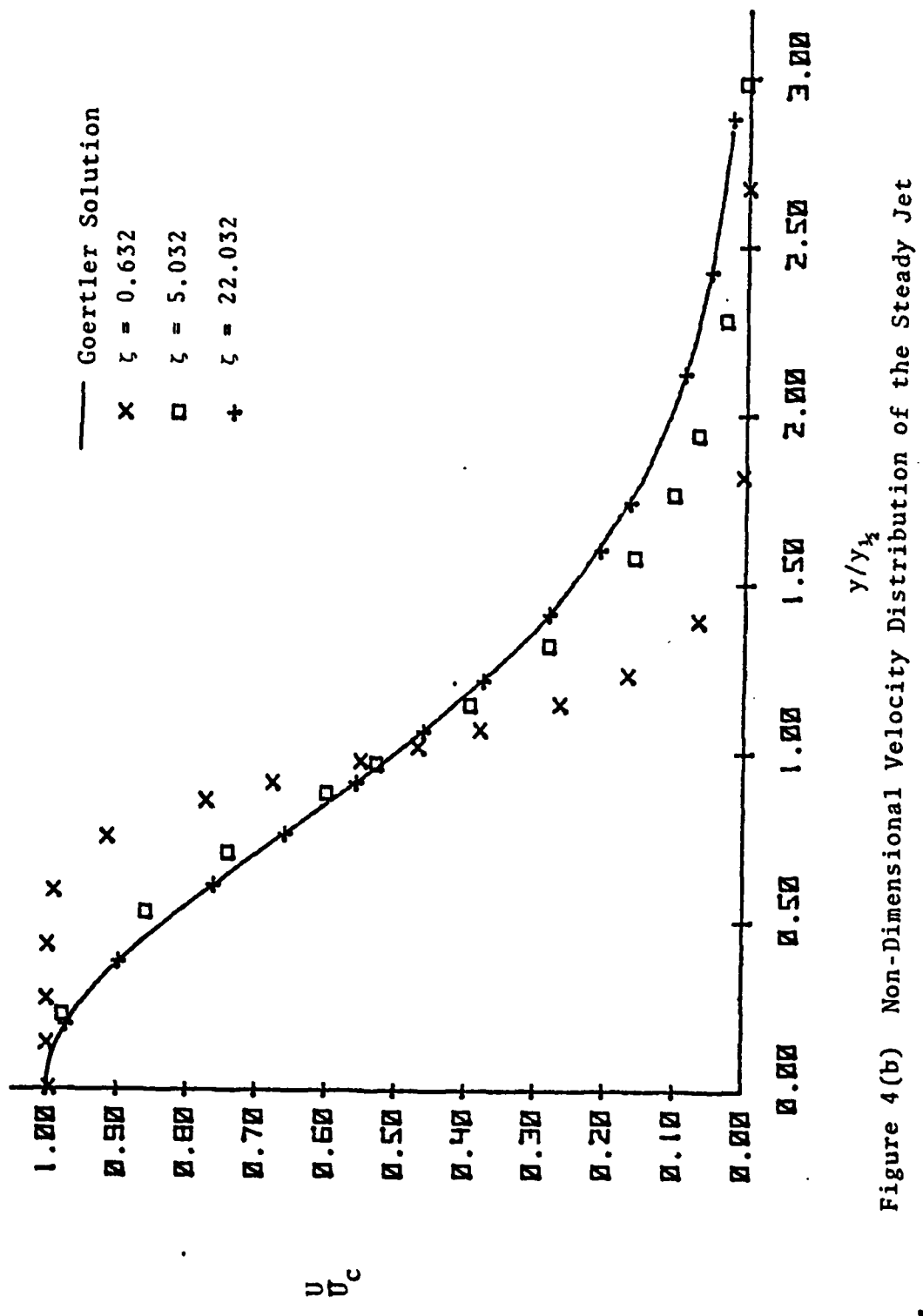
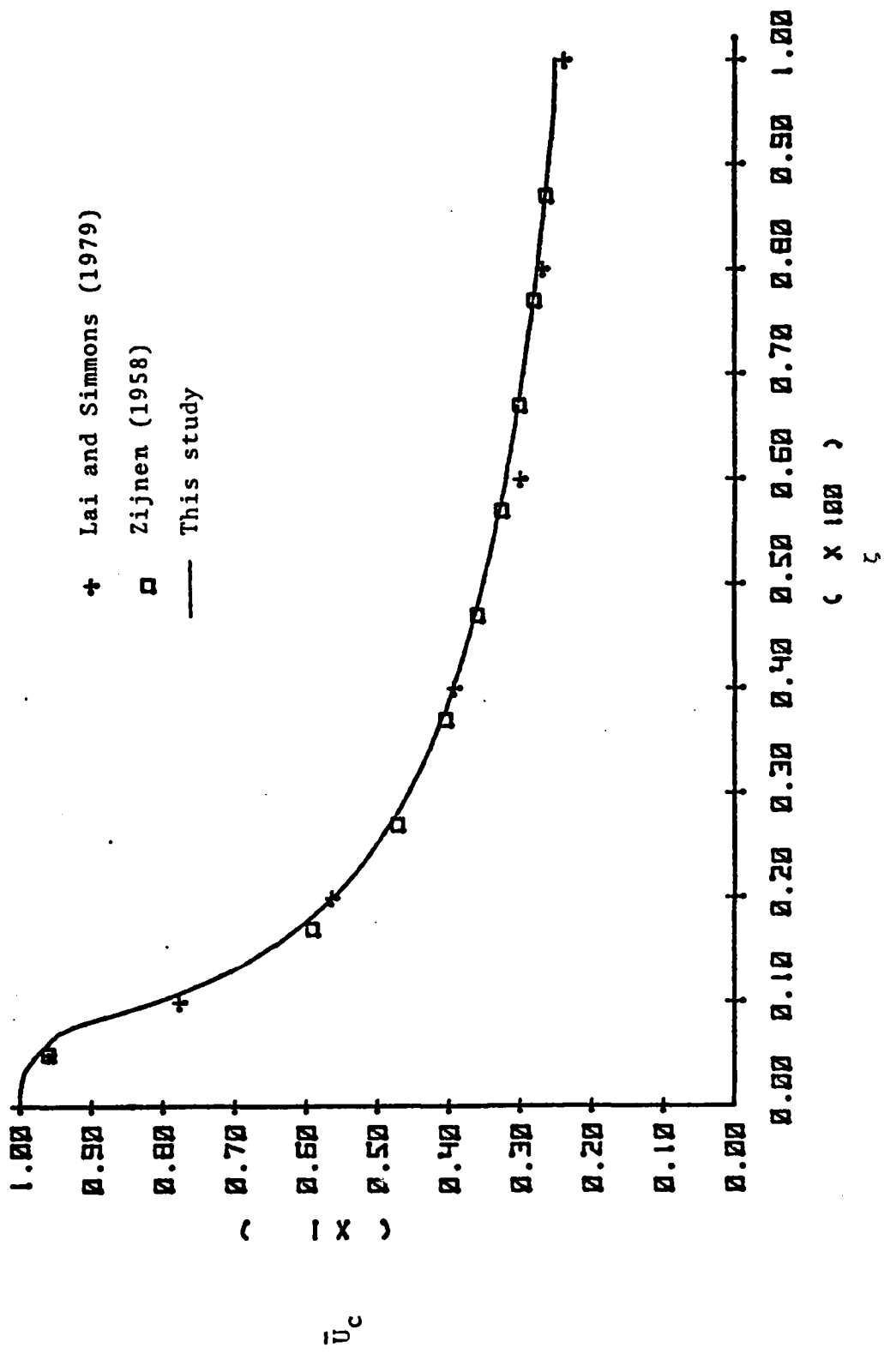
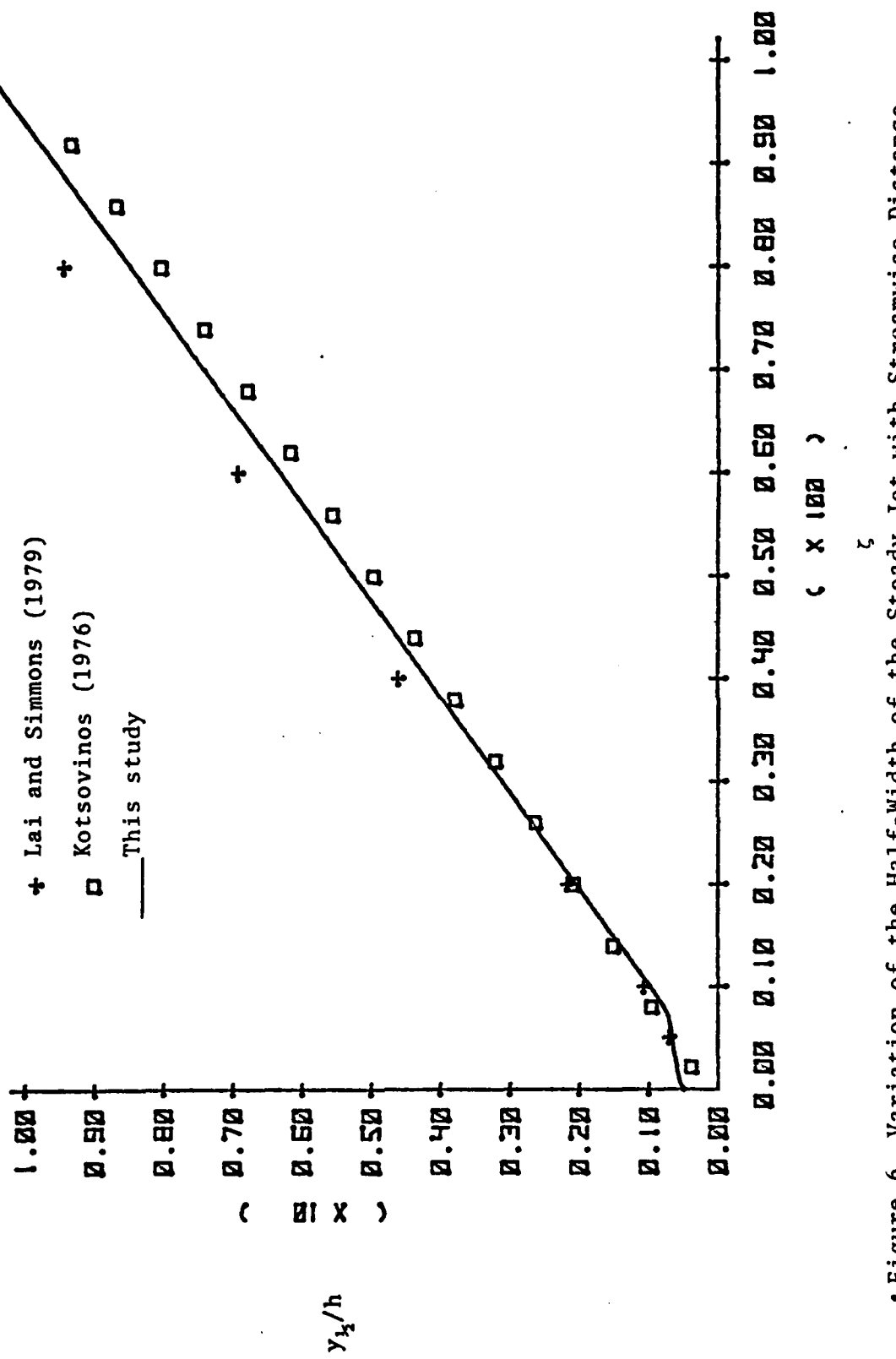


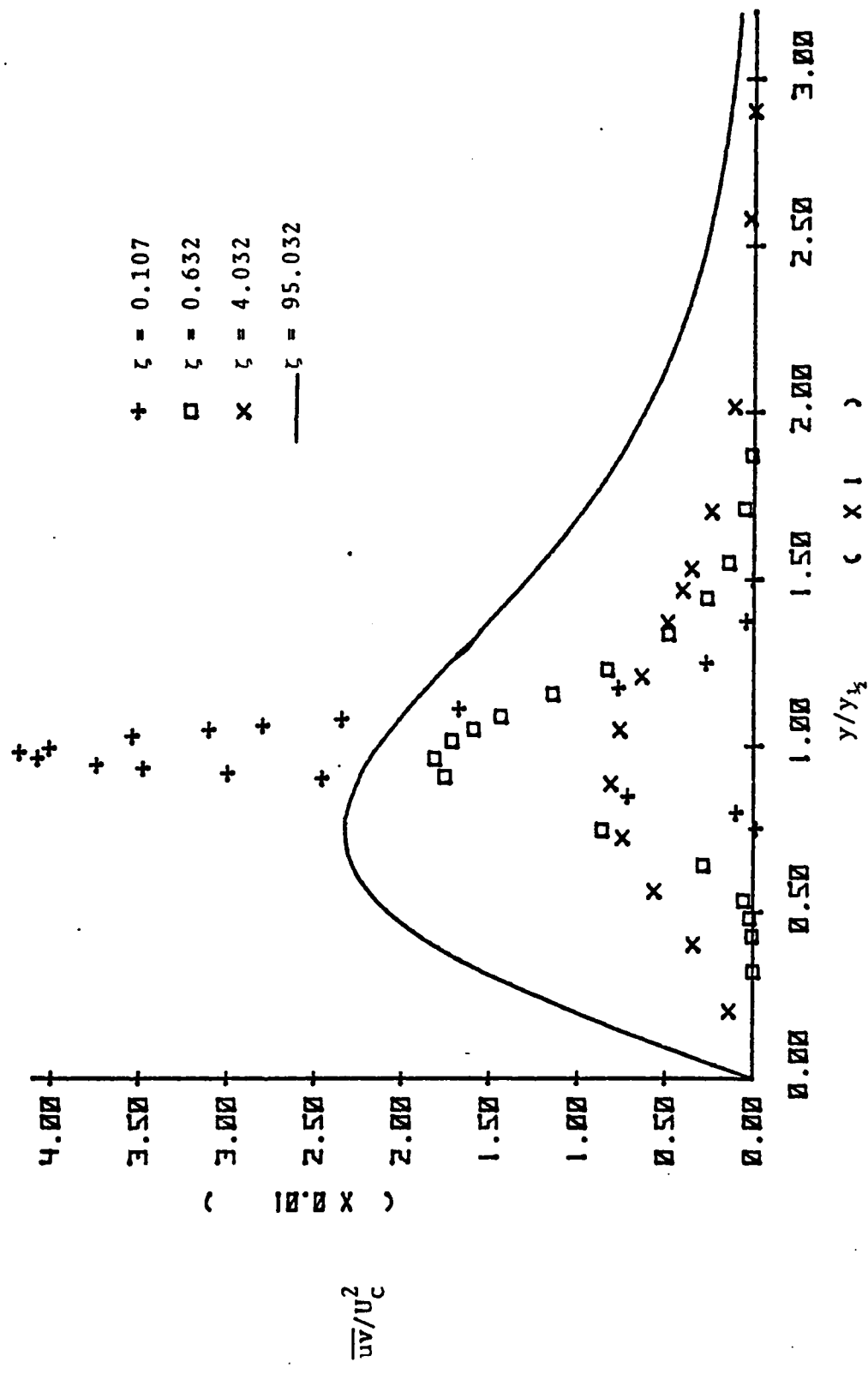
Figure 4(b) Non-Dimensional Velocity Distribution of the Steady Jet



• Figure 5 Variation of Centre-Line Velocity of the Steady Jet with Streamwise Distance



• Figure 6 Variation of the Half-Width of the Steady Jet with Streamwise Distance
 ξ



• Figure 7 (a) Nondimensional Shear Stress Profile for the Steady Jet

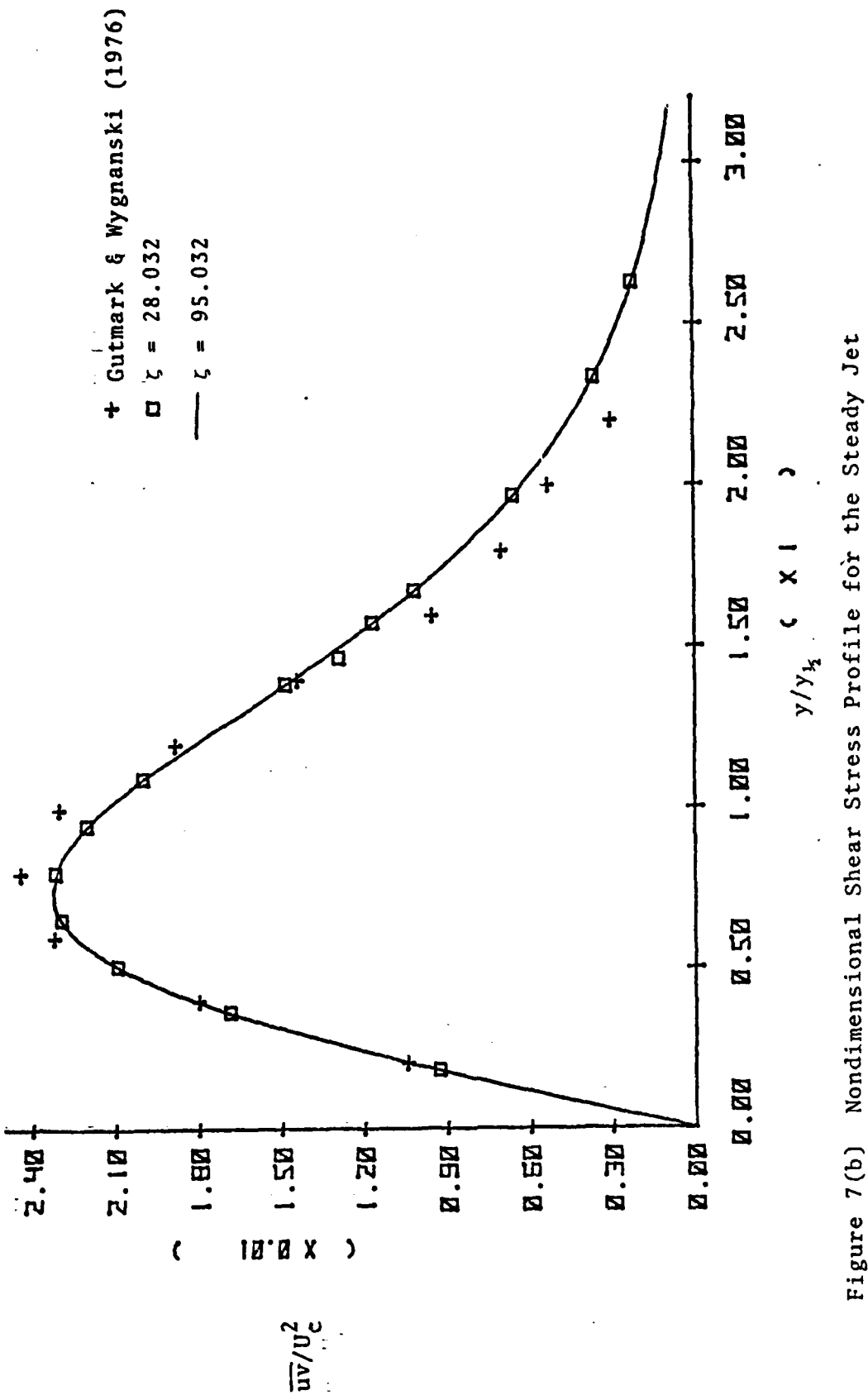


Figure 7(b) Nondimensional Shear Stress Profile for the Steady Jet

AD-A094 614

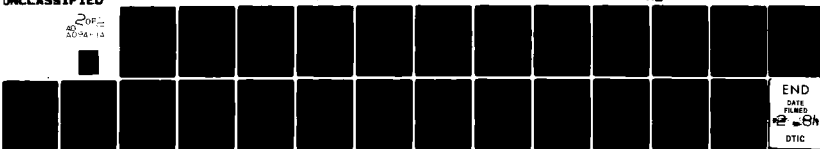
NAVAL POSTGRADUATE SCHOOL MONTEREY CA
NUMERICAL SOLUTION OF STEADY AND PERIODICALLY PULSED TWO-DIMENS--ETC(U)
APR 80 J C LAI, J M SIMMONS

F/6 20/4

NL

UNCLASSIFIED

20P12
20-14-12



END
1
FILED
2 - 8h
DTIC

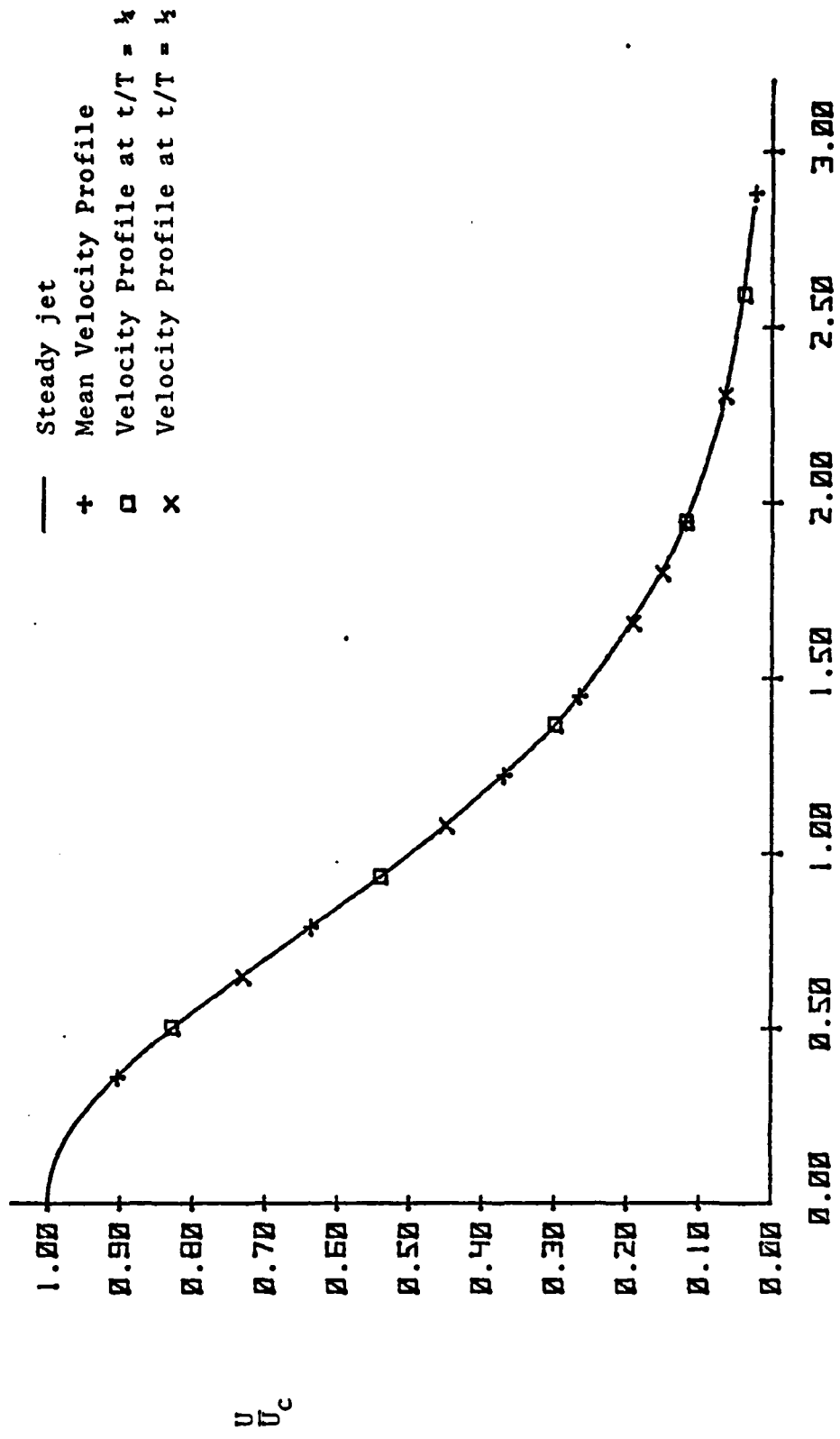


Figure 8(a) Non-dimensional Velocity Distribution for $\xi = 40.032$,
 $\omega = 0.000871$,
 $\epsilon = 0.1$

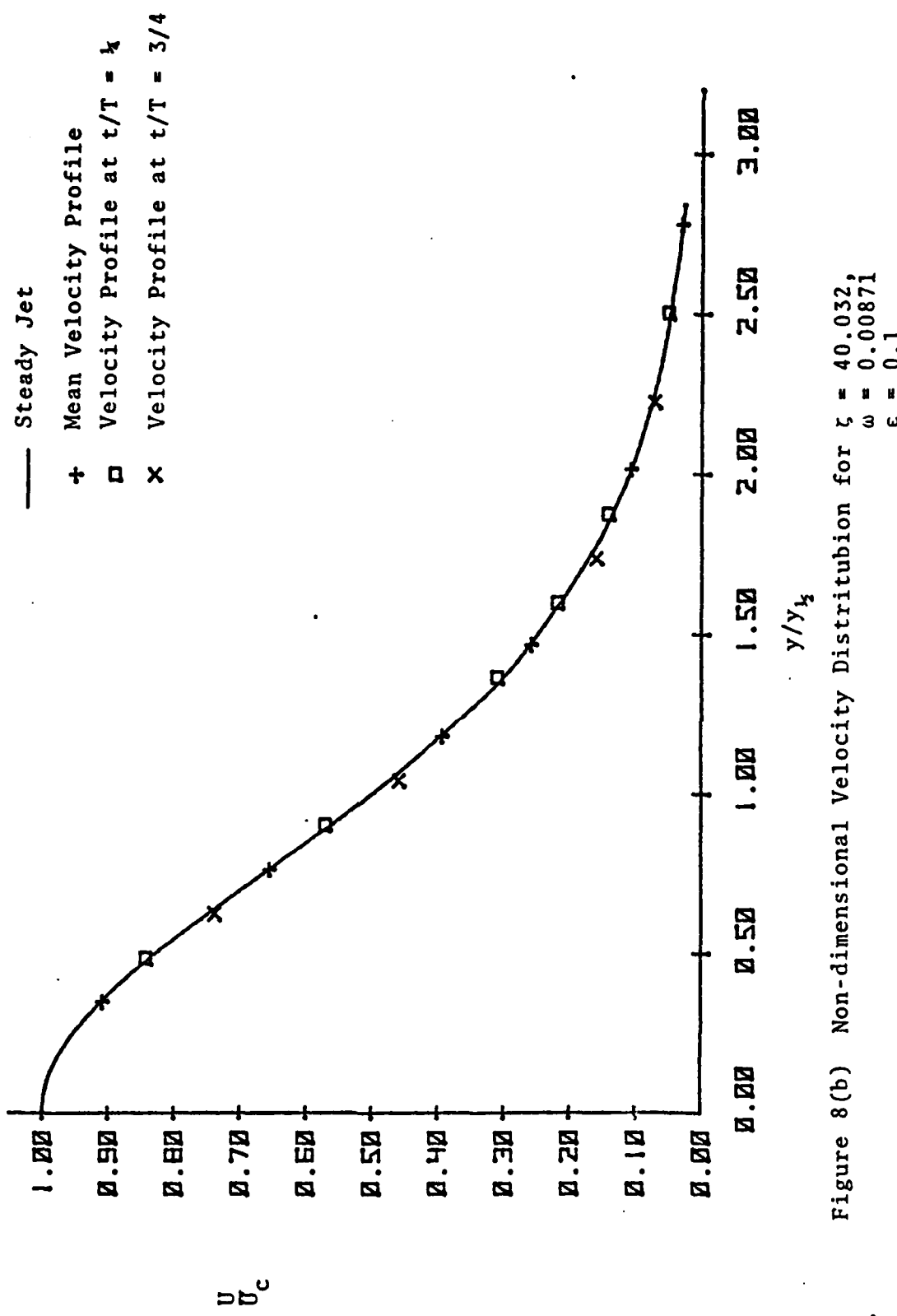


Figure 8(b) Non-dimensional Velocity Distribution for $\xi = 40.032$,
 $\omega = 0.00871$,
 $\epsilon = 0.1$

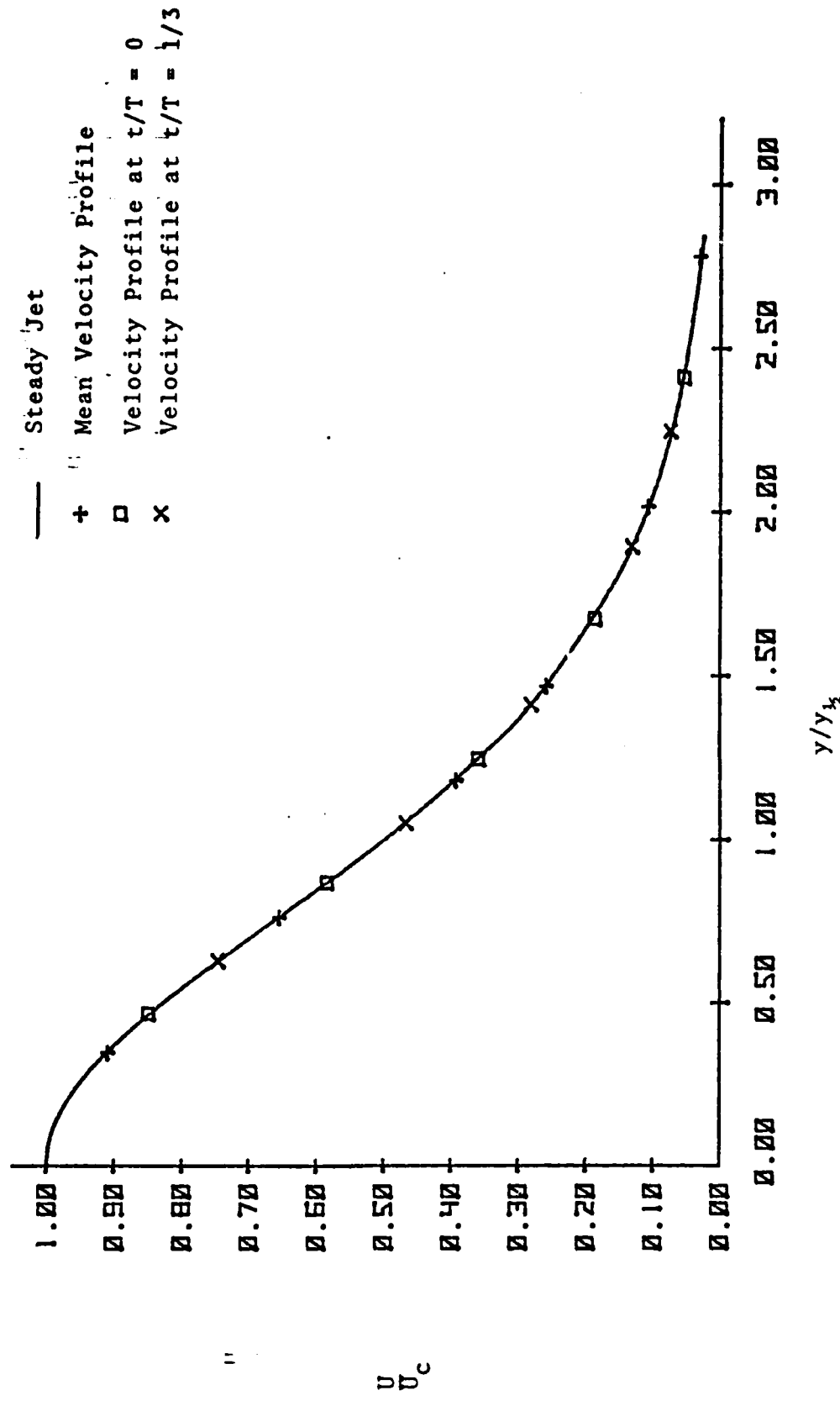


Figure 8(c) Non-dimensional Velocity Distribution for $\xi = 40.032$
 $\omega = 0.0871$
 $\epsilon = 0.1$

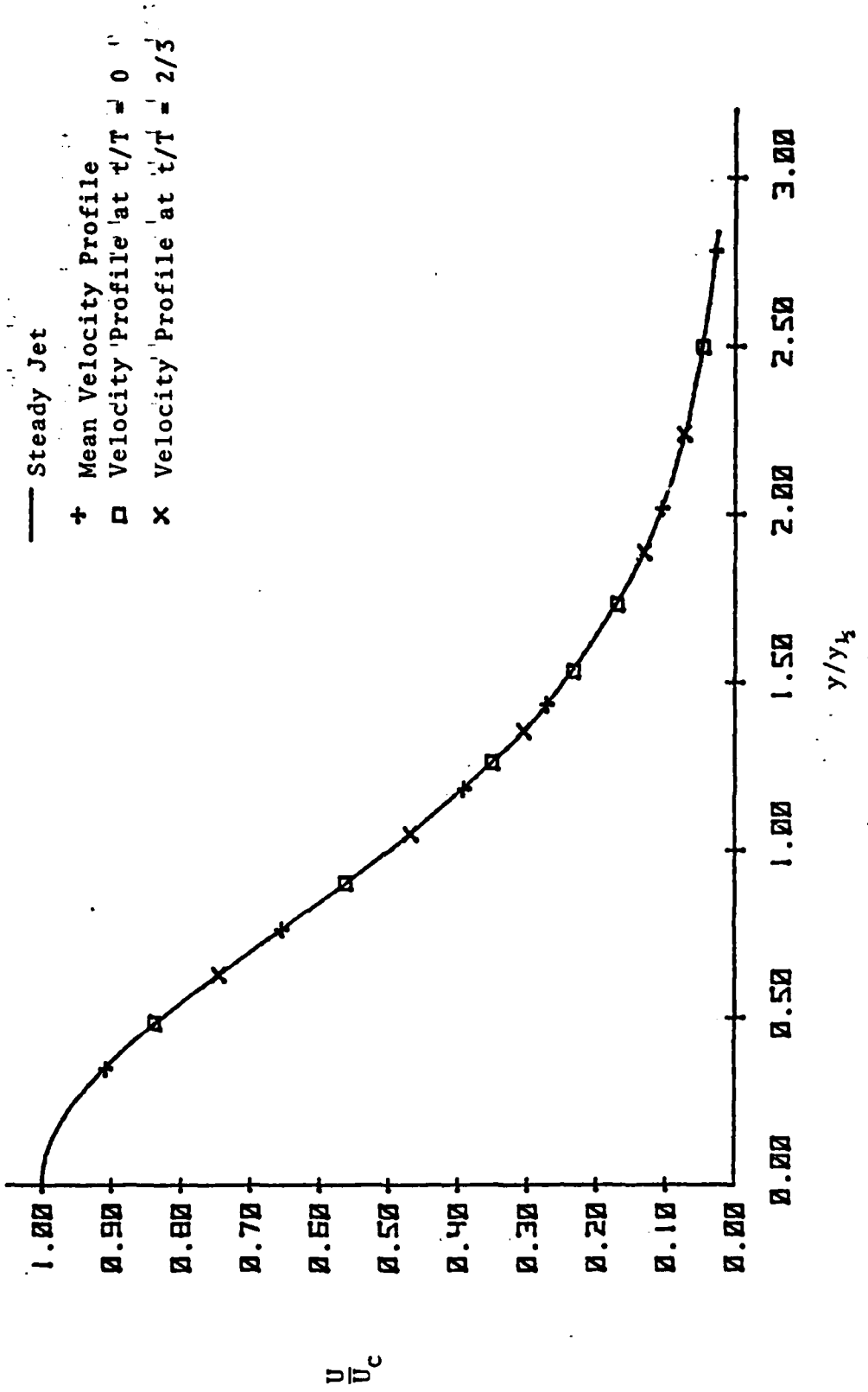


Figure 8(d) Non-dimensional Velocity distribution for $\xi = 40.032$
 $\omega = 0.000871$
 $\epsilon = 0.15$

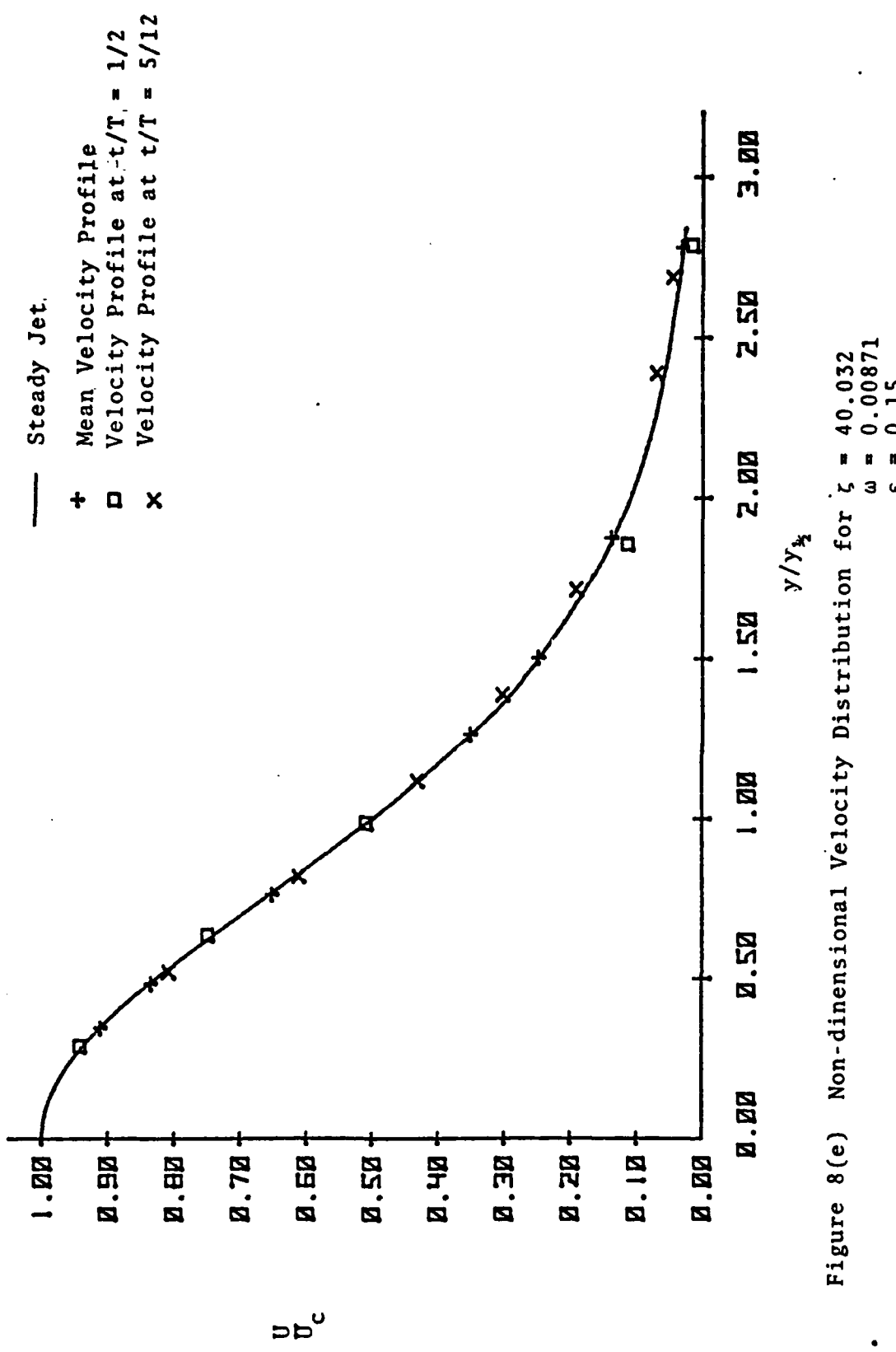


Figure 8(e) Non-dimensional Velocity Distribution for $\xi = 40.032$
 $\omega = 0.00871$
 $\epsilon = 0.15$

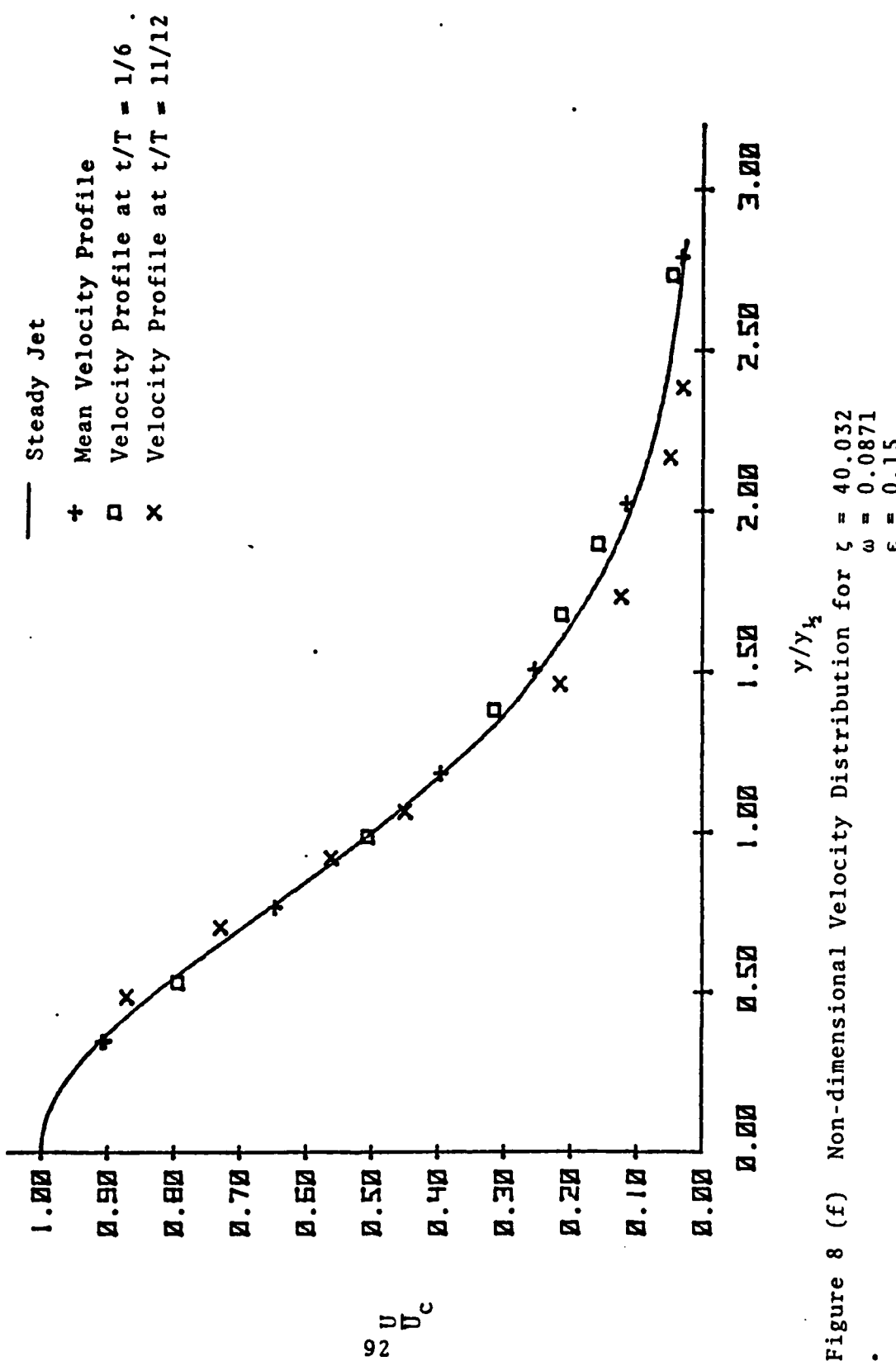


Figure 8 (f) Non-dimensional Velocity Distribution for $\xi = 40.032$, $\omega = 0.081$, $\epsilon = 0.15$.

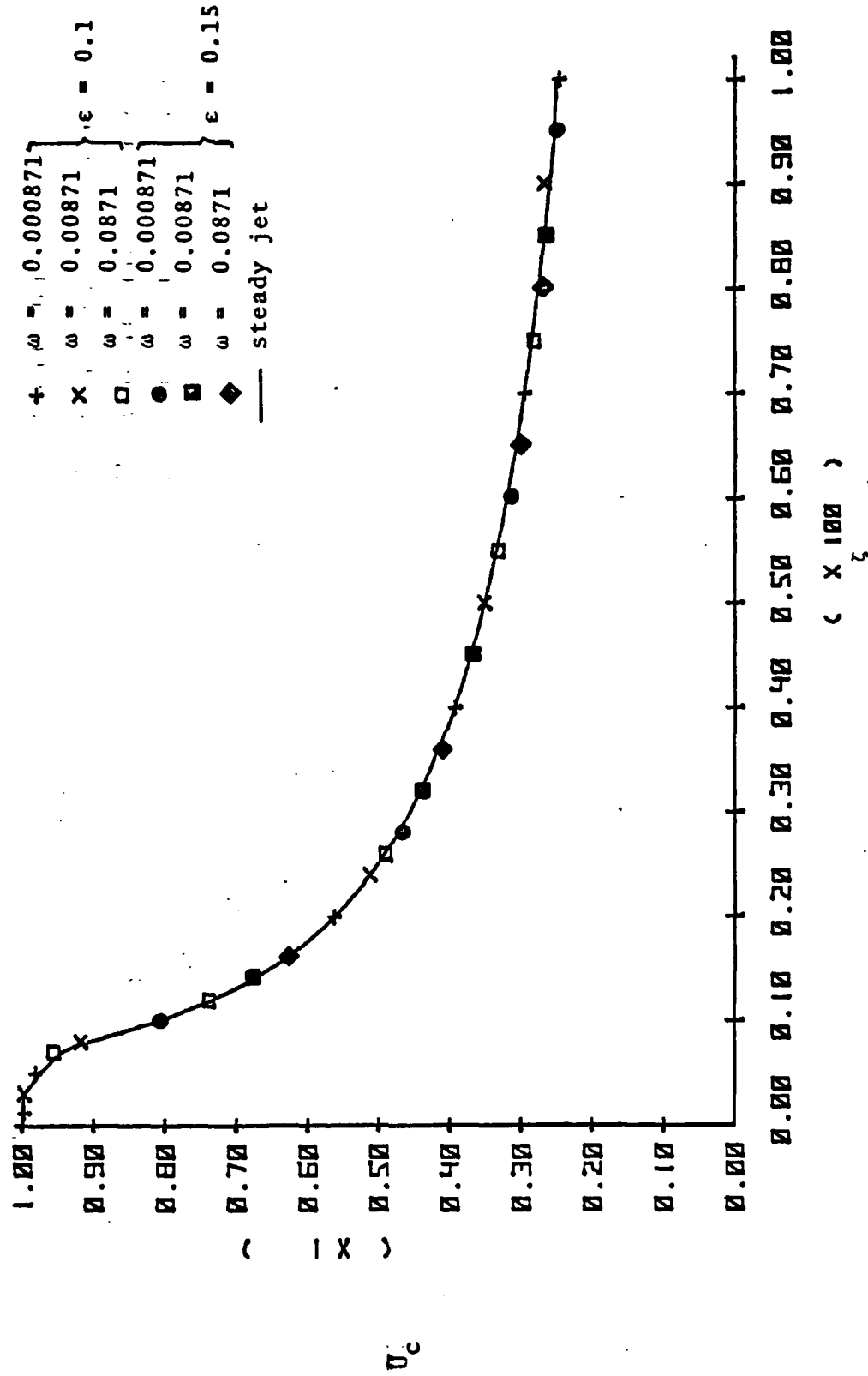


Figure 9 Variation of Mean Centre-Line Velocity with Streamwise Distance

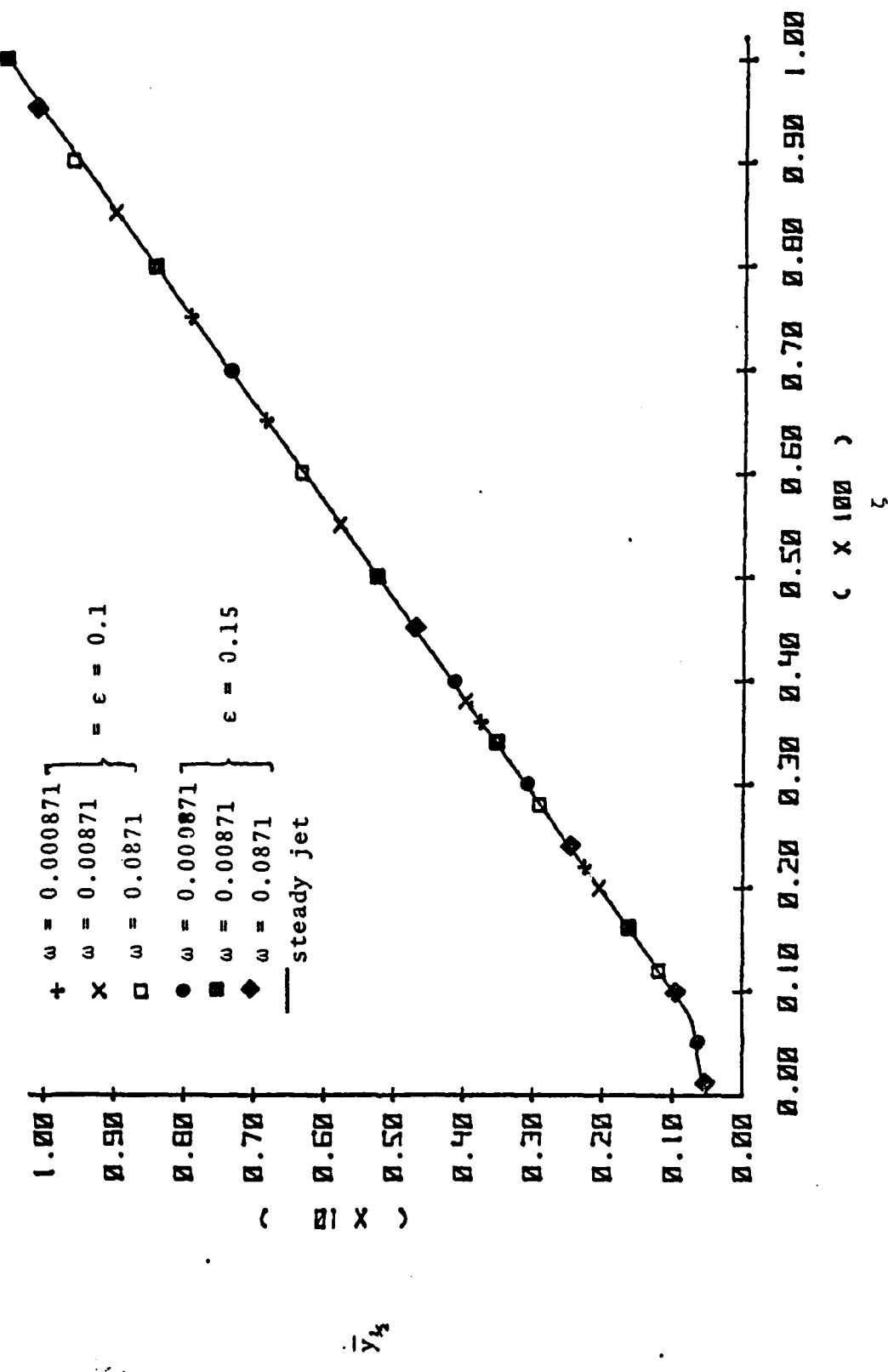
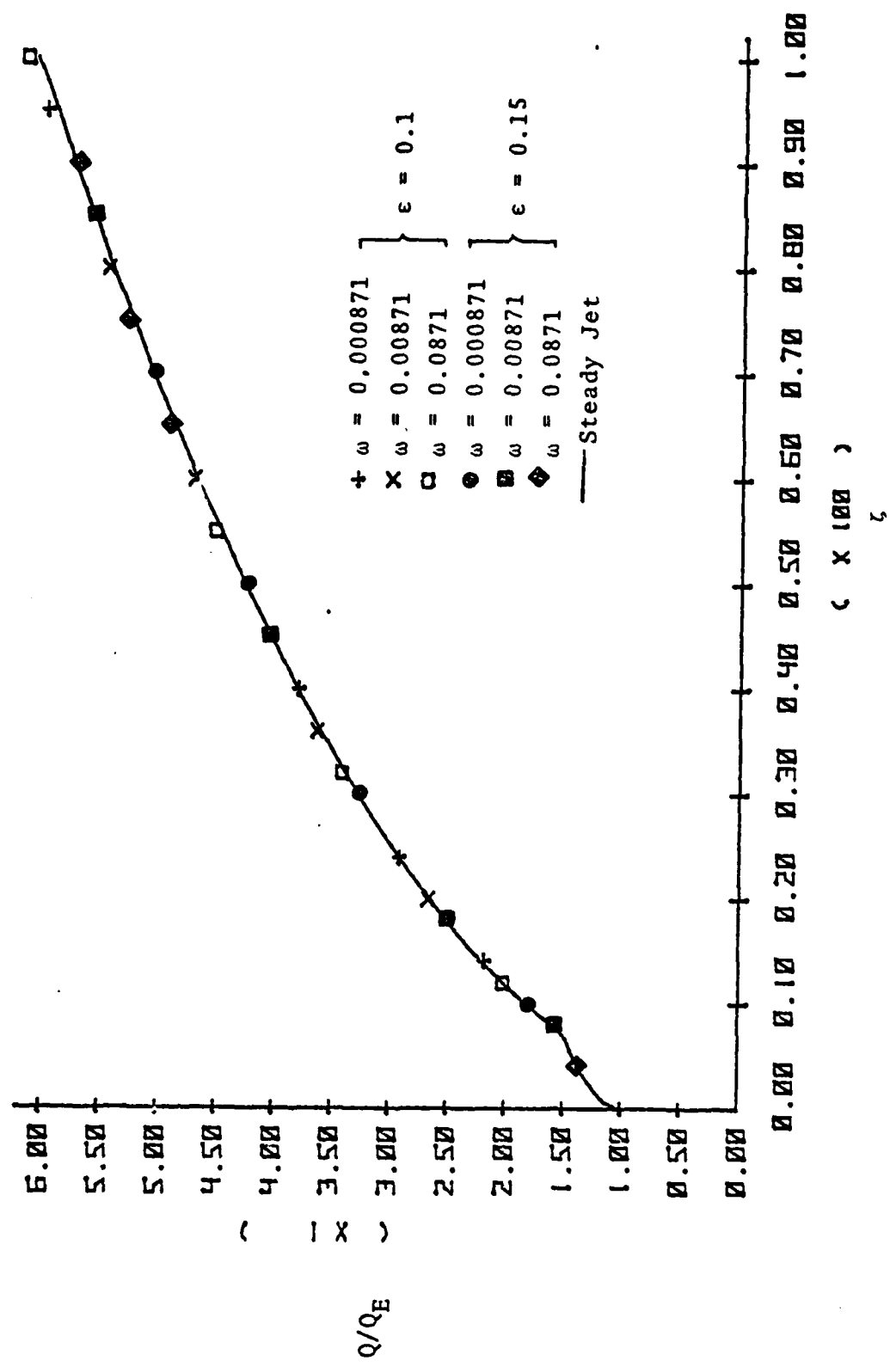


Figure 10 Variation of Mean Jet Half-with Streamwise Distance



• Figure 11 Variation of Non-Dimensional Mass Flow with Streamwise Distance

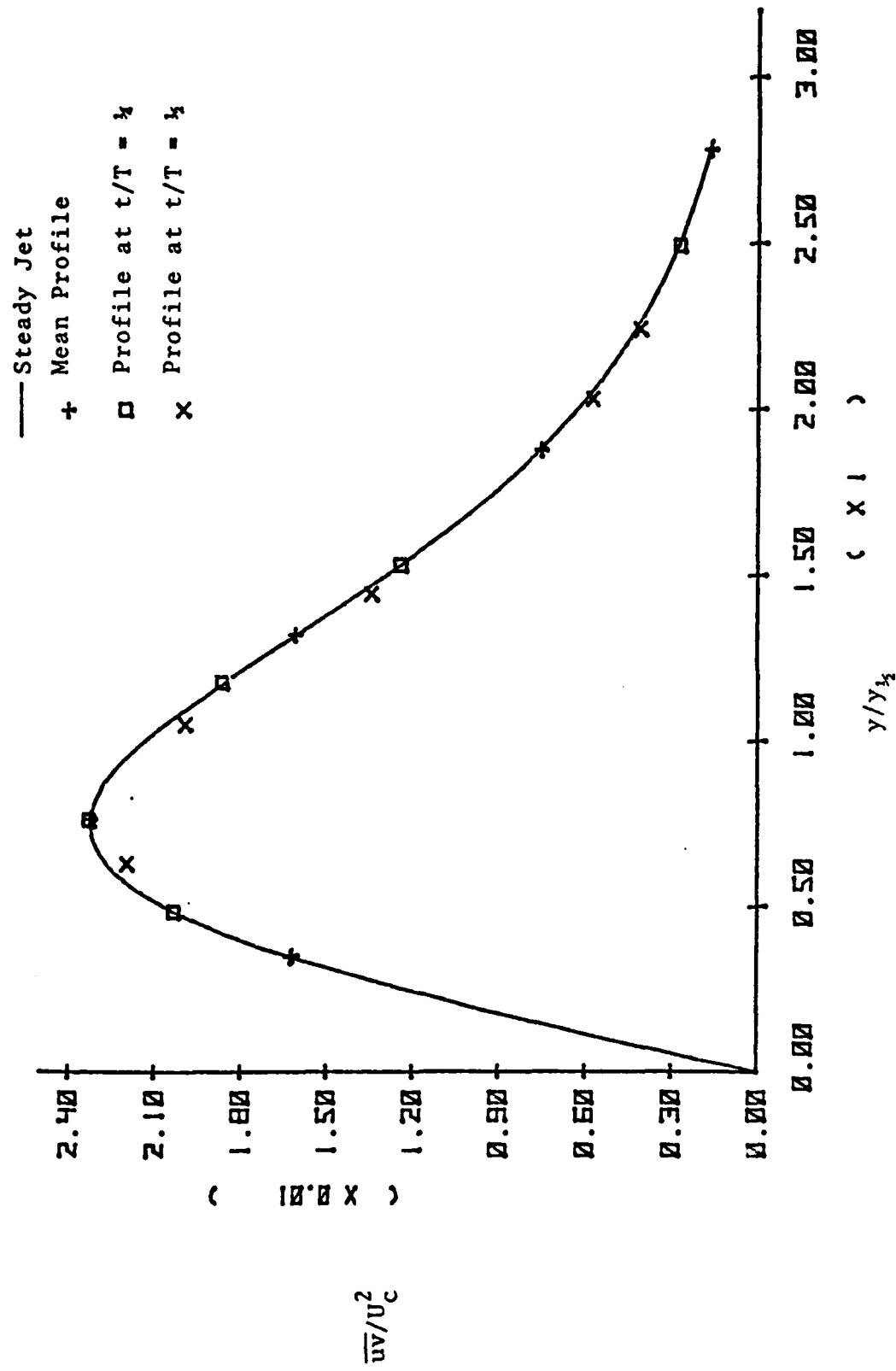


Figure 12(a) Non-Dimensional Shear Stress Profile for $\zeta = 40.032$, $\omega = 0.000871$, $\epsilon = 0.1$

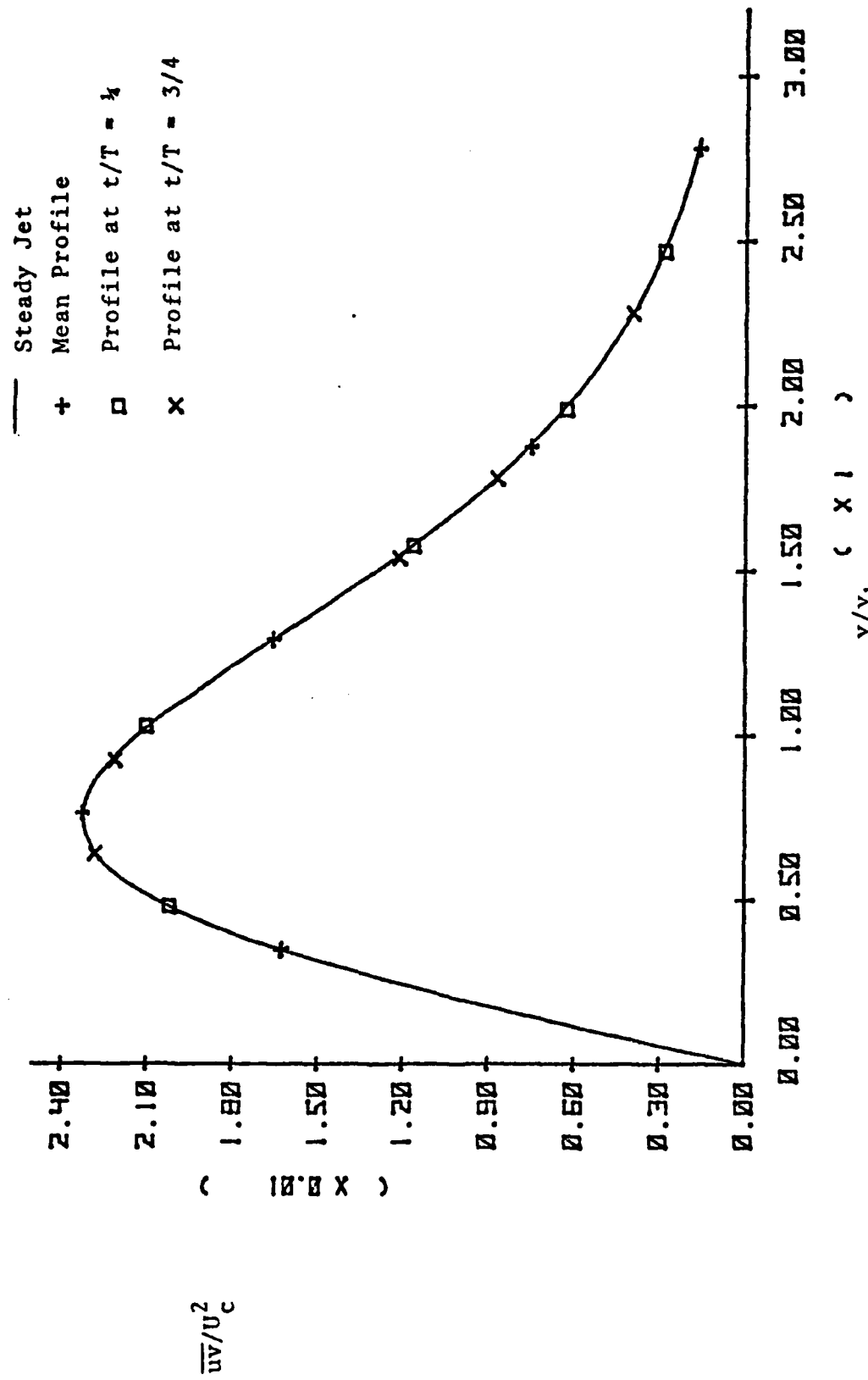


Figure 12(b) Non-dimensional Shear Stress Profile for $\xi = 40.032$, $\omega = 0.00871$, $\epsilon = 0.1$

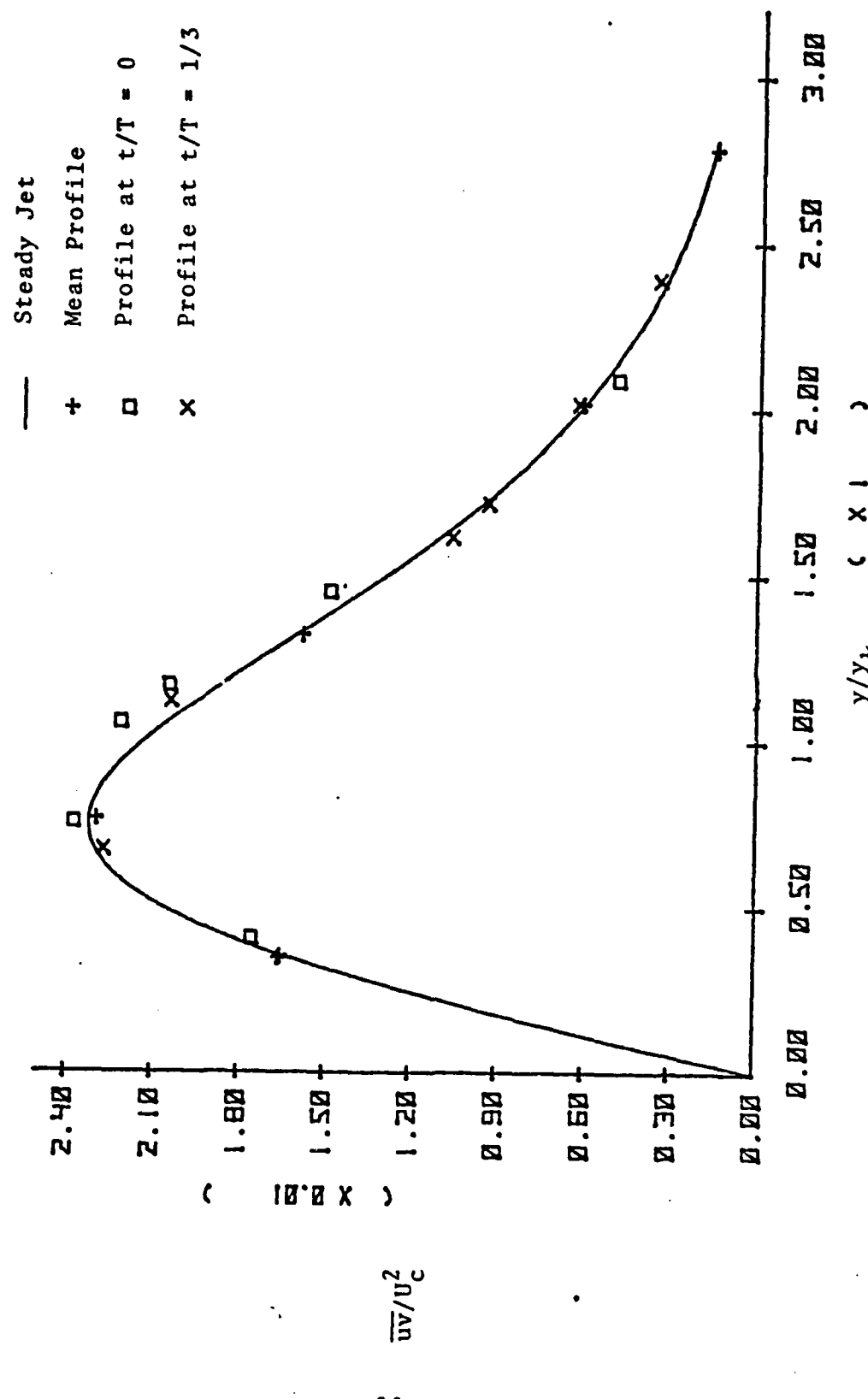


Figure 12(c) Non-dimensional Shear Stress Profile for $\zeta = 40.032$, $\omega = 0.0871$, $\epsilon = 0.1$

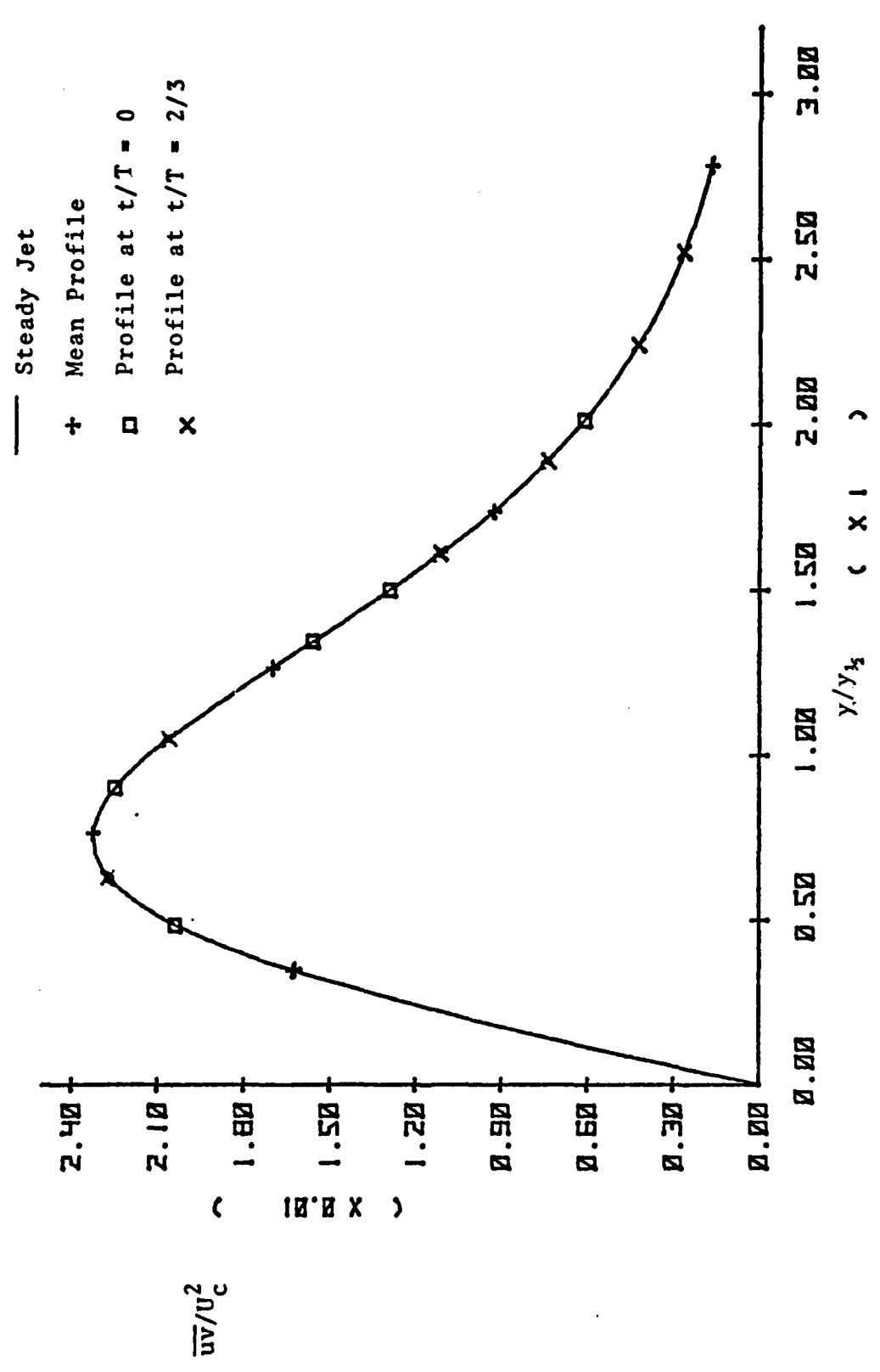


Figure 12(d) Non-Dimensional Shear Stress Profile for $\xi = 40.032$, $\omega = 0.000871$, $\epsilon = 0.15$

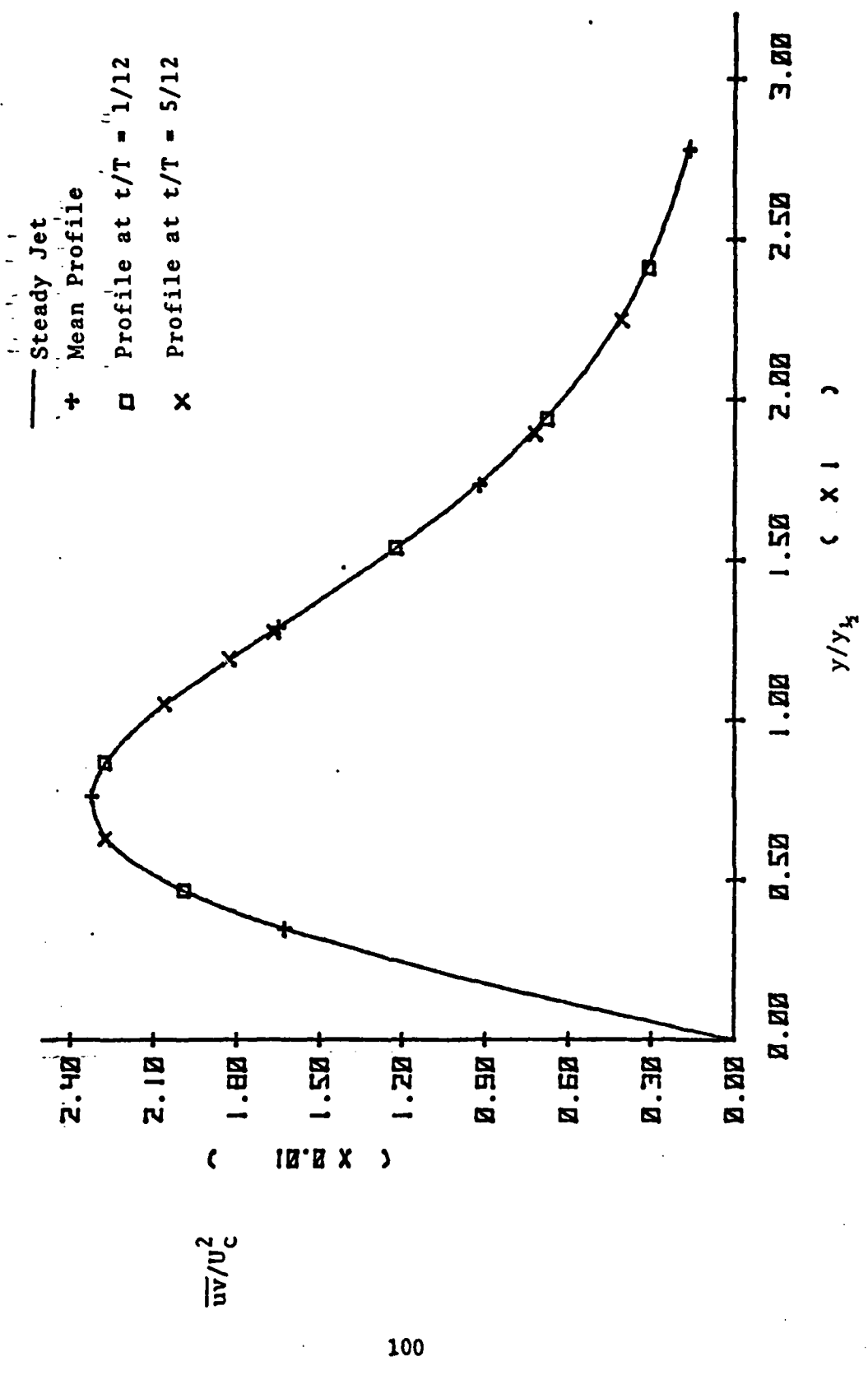


Figure 12(e) Non-Dimensional Shear Stress Profile for $\zeta = 40.032$, $\omega = 0.00671$, $\epsilon = 0.15$

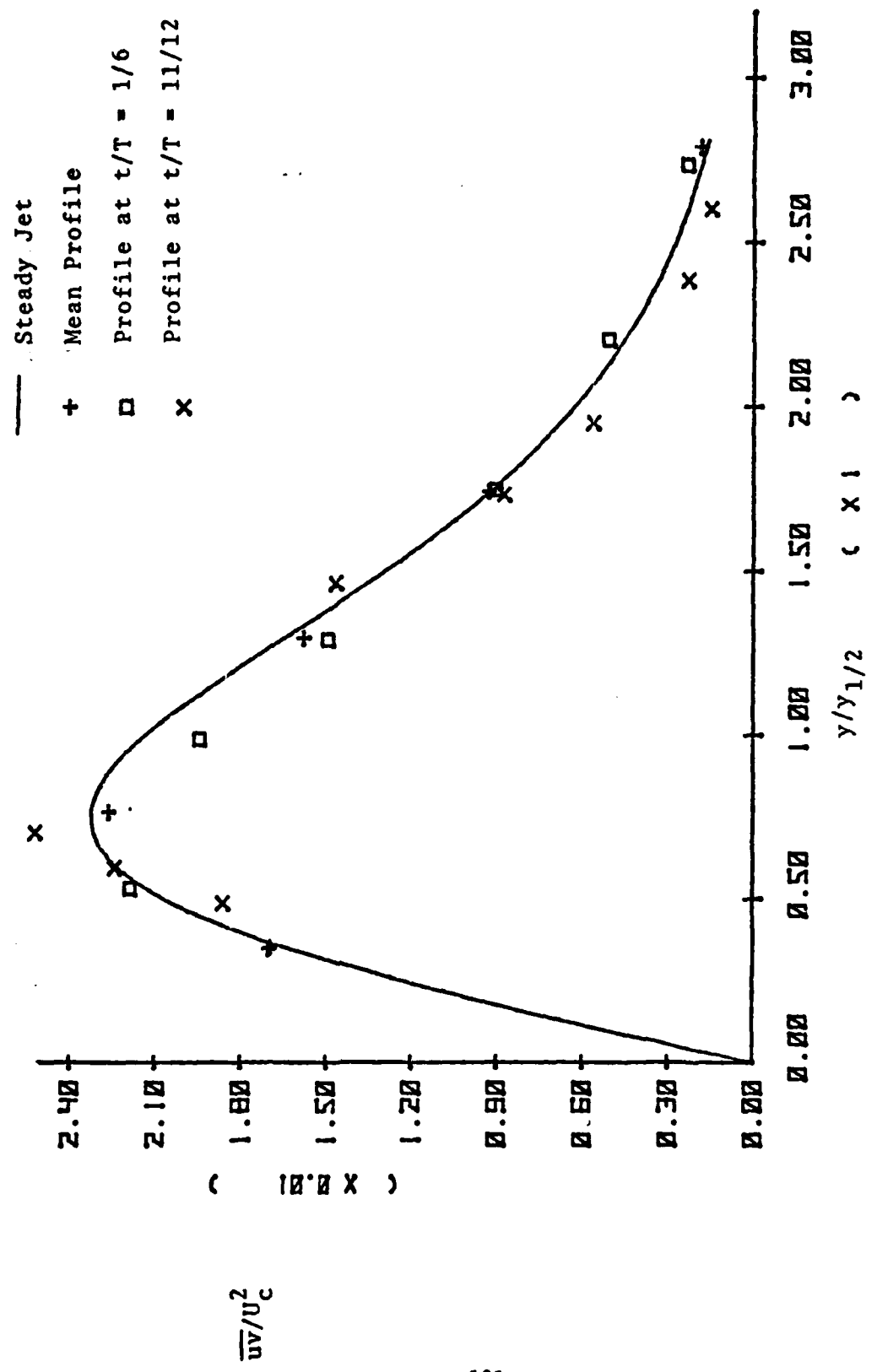


Figure 12(f) Non-Dimensional Shear Stress Profile for $\zeta = 4.0.032$, $\omega = 0.0871$, $\epsilon = 0.15$

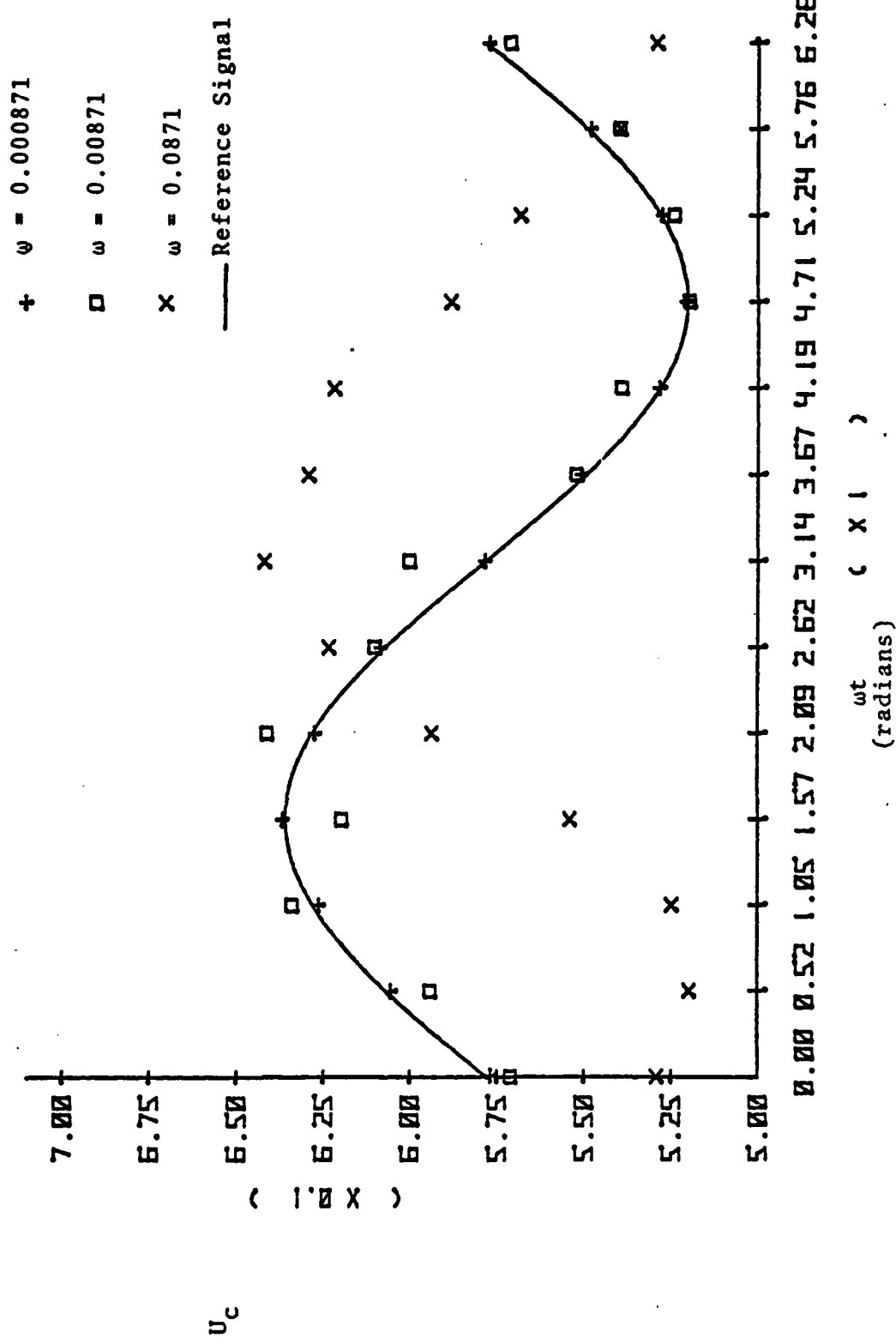
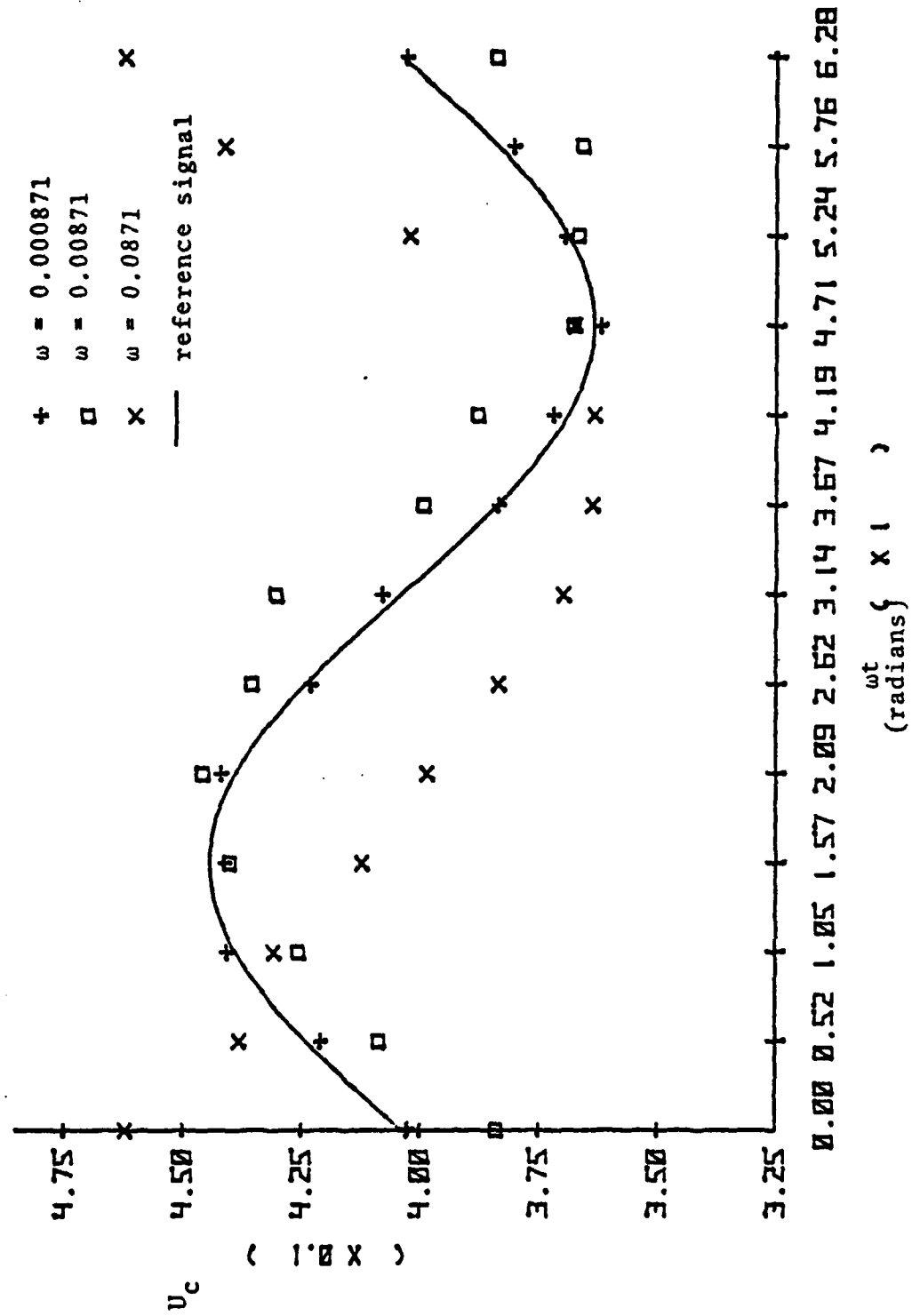


Figure 13(a) Variation of Instantaneous Centre-Line Velocity with Time for $\xi_c = 69.1032$



103

Figure 13(b) Variation of Instantaneous Centre-Line Velocity with Time for $\epsilon = 38.032$

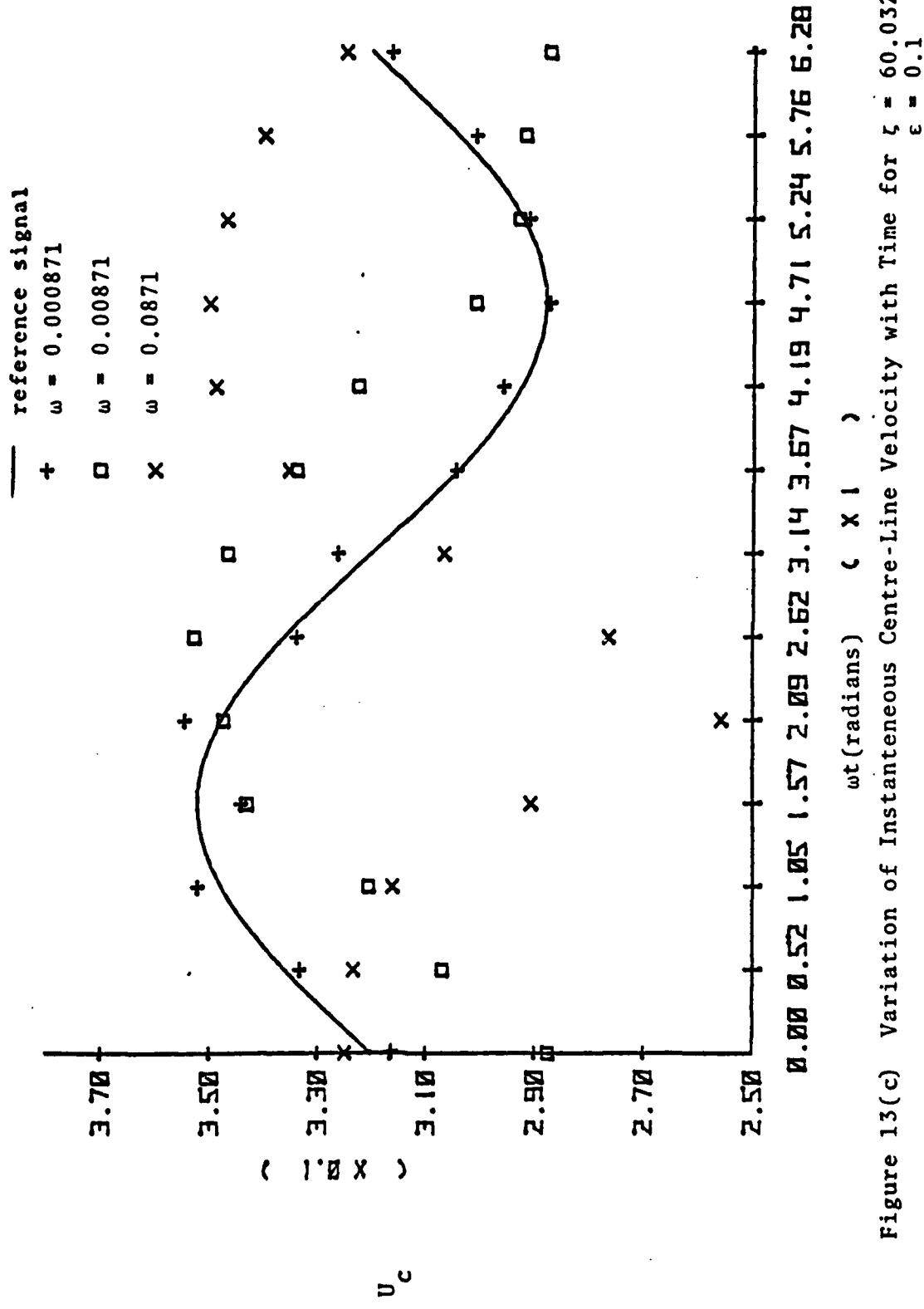


Figure 13(c) Variation of Instantaneous Centre-Line Velocity with Time for $\xi = 60.032$
 $\epsilon = 0.1$

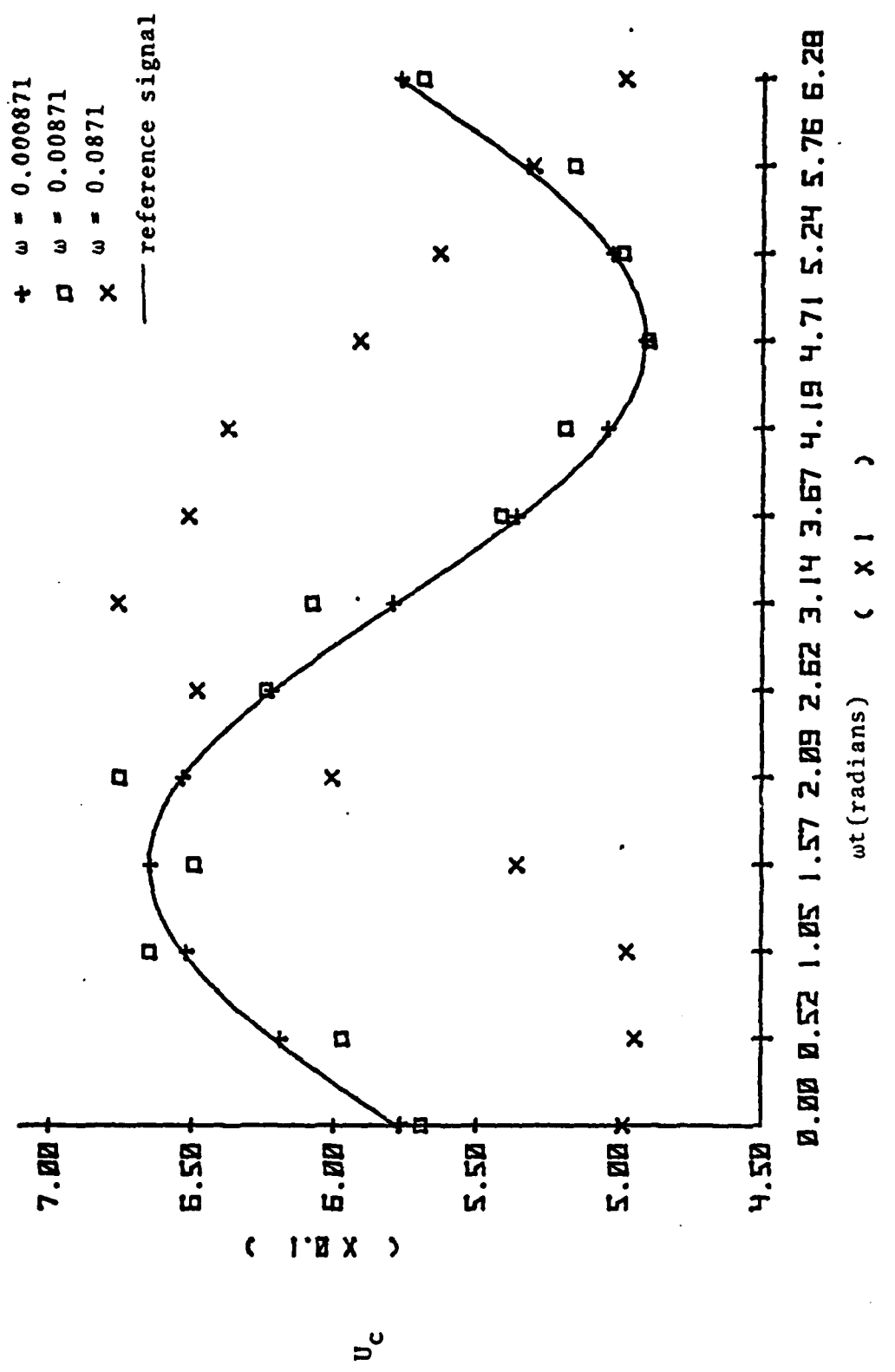


Figure 13(d) Variation of Instantaneous Centre-Line Velocity with Time for $\xi = 19.032$
 $\epsilon = 0.15$

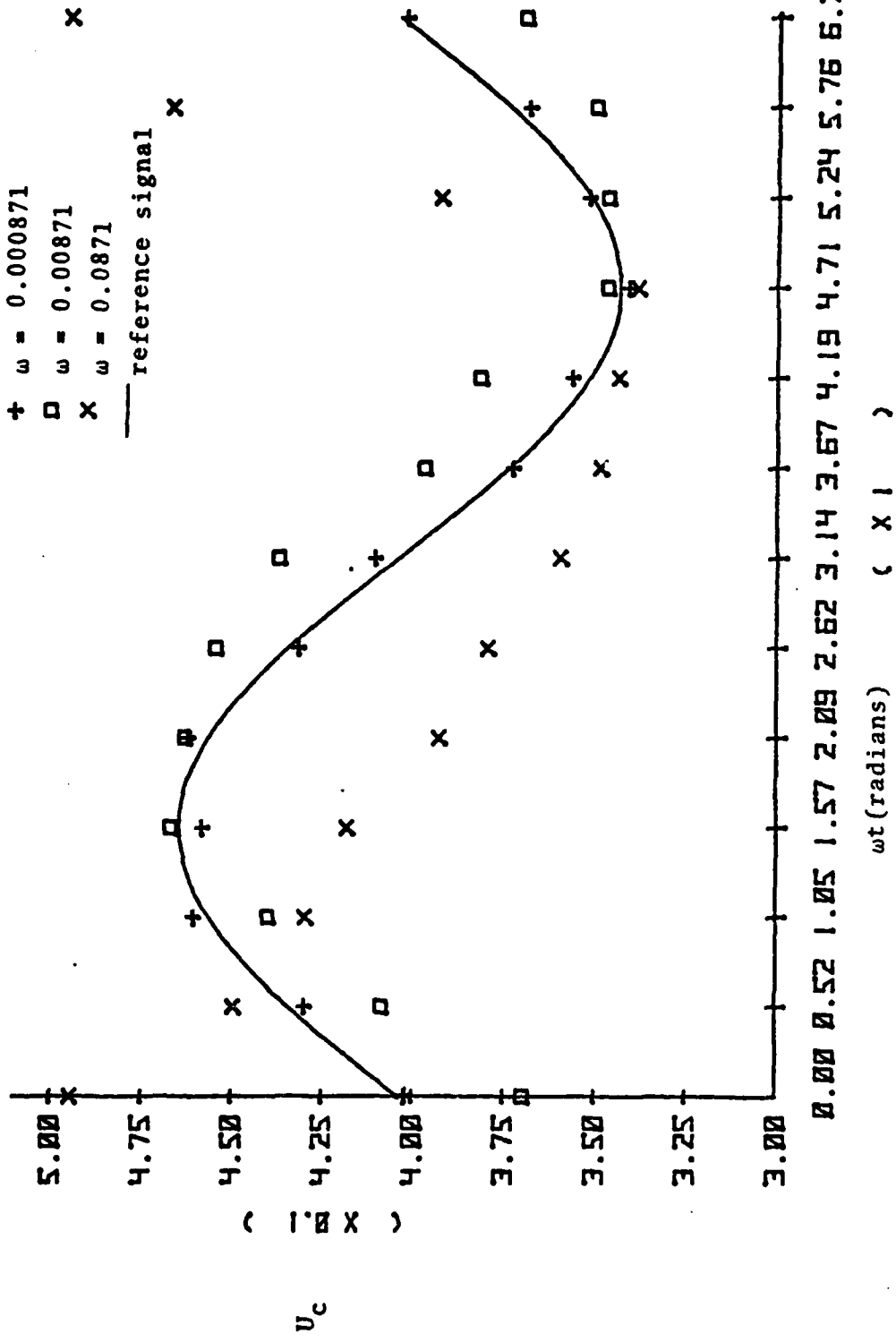


Figure 13(e) Variation of Instantaneous Centre-Line Velocity with Time for $\xi = 38.032$
 $\epsilon = 0.15$

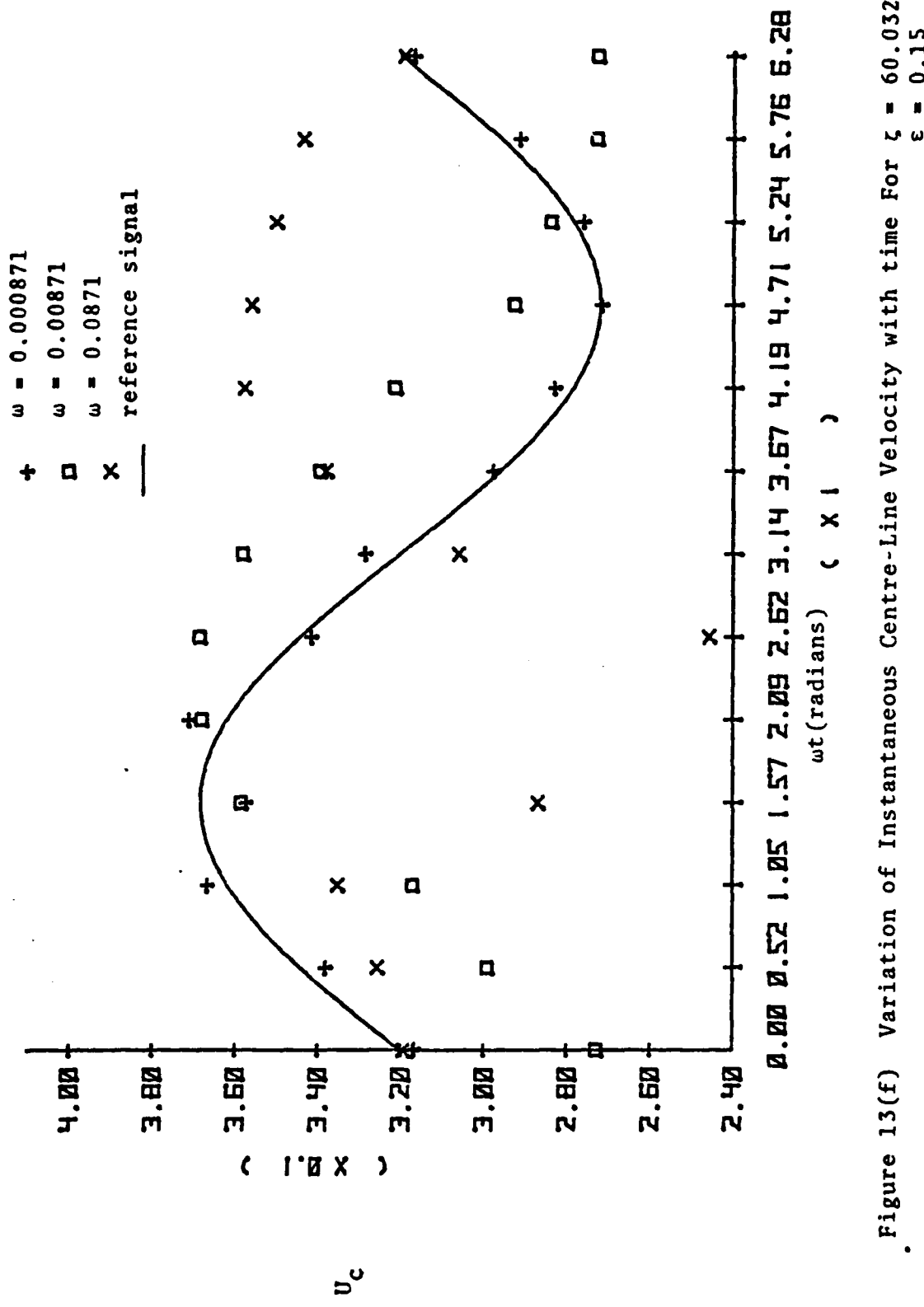


Figure 13(f) Variation of Instantaneous Centre-Line Velocity with time For $\zeta = 60.032$
 $\epsilon = 0.15$

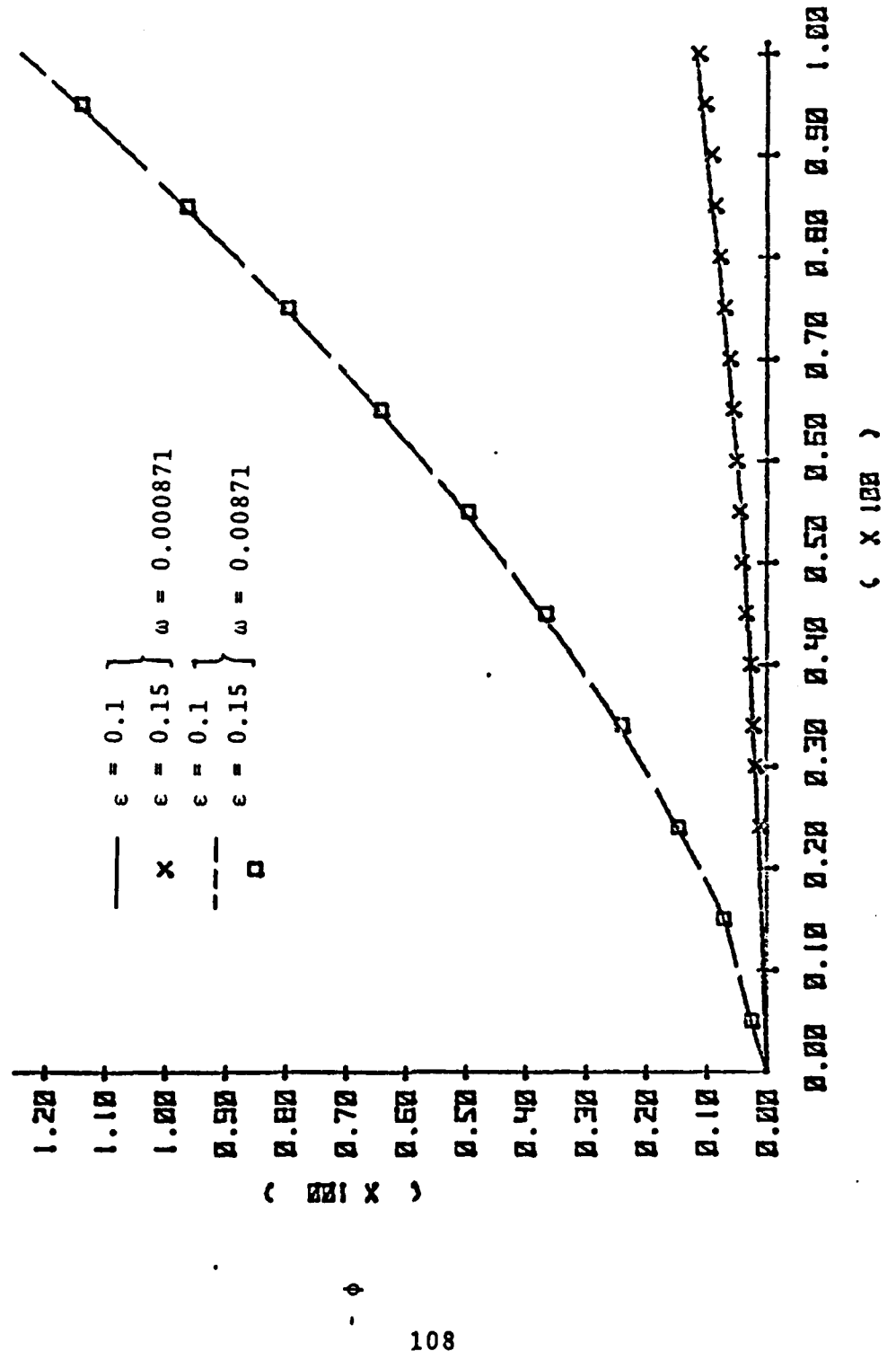


Figure 14(a) Variation of Phase Angle with Streamwise Distance

ζ

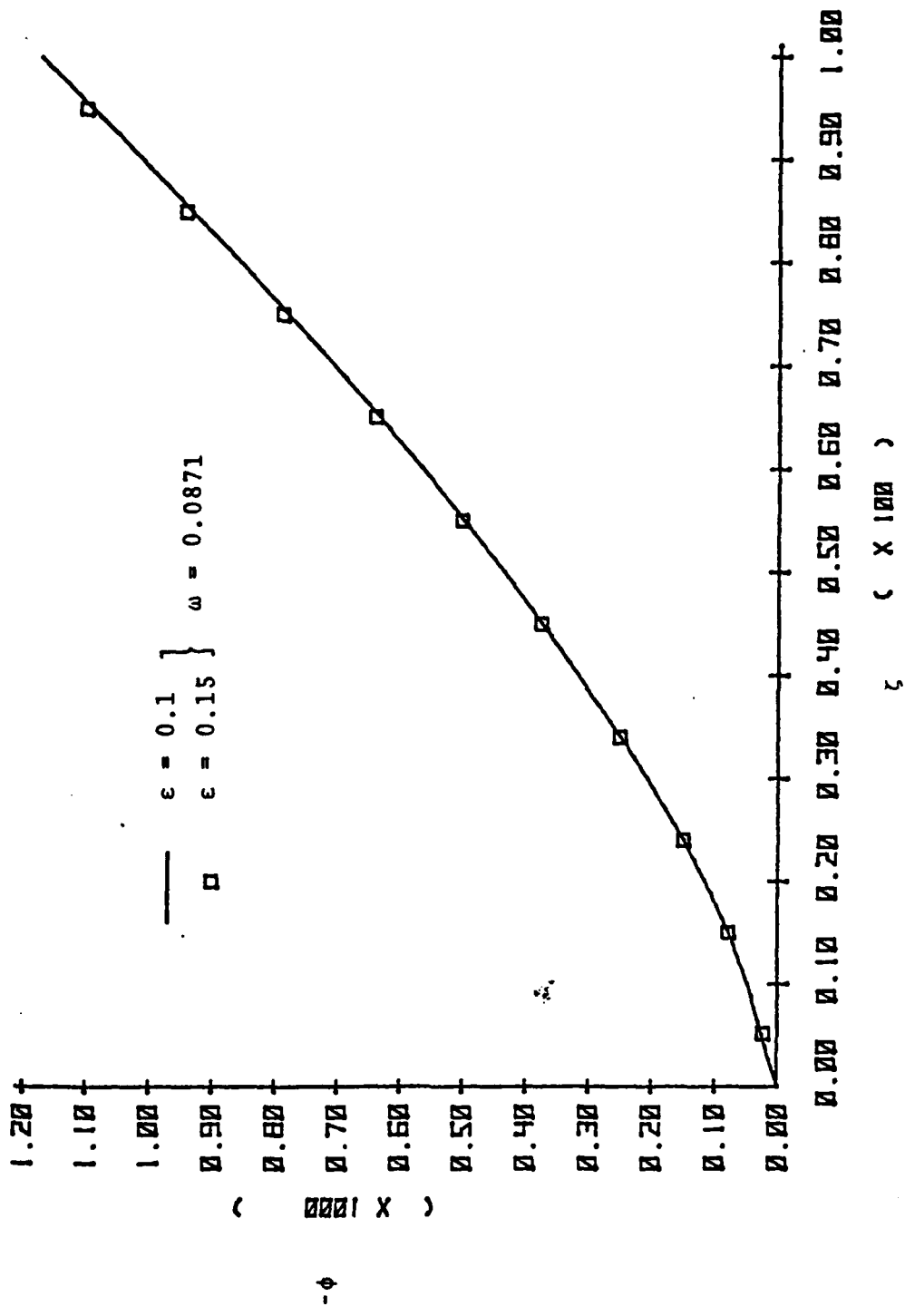


Figure 14(b) Variation of Phase Angle with Streamwise Distance

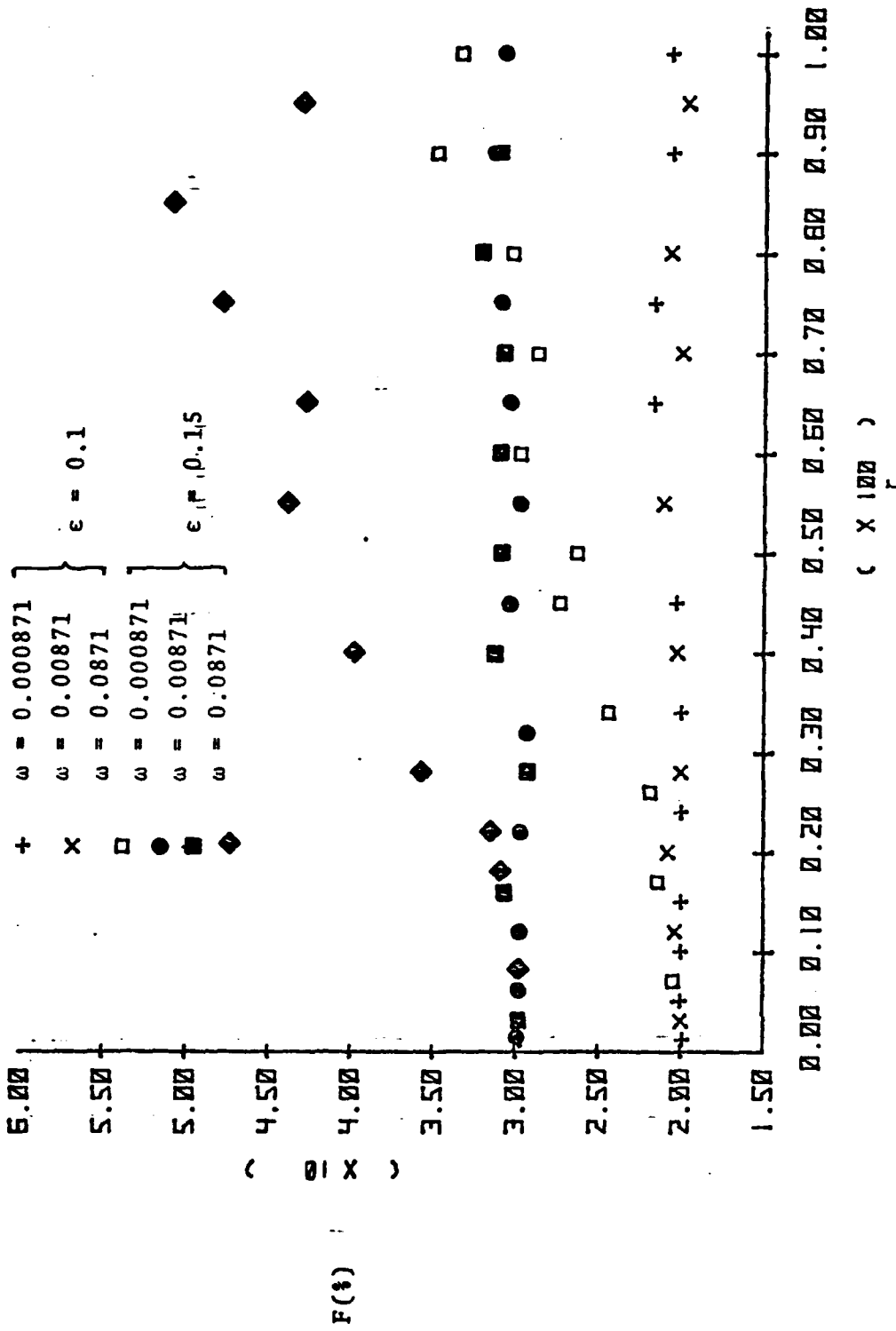


Figure 15 Variation of Peak-to-Peak Oscillation of Centre-Line Velocity with Streamwise Distance

DISTRIBUTION LIST

	No. of Copies
1. Defense Technical Information Center Cameron Station Alexandria, VA 22314	2
2. Library, Code 0142 Naval Postgraduate School Monterey, CA 93940	2
3. Professor K. J. Bullock Department of Mechanical Engineering University of Queensland St. Lucia, Brisbane Australia 4067	1
4. Dr. J. M. Simmons Department of Mechanical Engineering University of Queensland St. Lucia, Brisbane Australia 4067	5
5. Mr. J. C. S. Lai Department of Mechanical Engineering University of Queensland St. Lucia, Brisbane Australia 4067	5
6. DR. T. Cebeci Distinguished Professor Mechanical Engineering Department Cal State University Long Beach, CA	1
7. Professor H. H. Korst Mechanical Engineering Department University of Illinois Urbana, Illinois	1
8. Professor M. F. Platzer Chairman, Department of Aeronautics Naval Postgraduate School Monterey, CA 93940	5
9. Professor R. P. Shreeve Department of Aeronautics Naval Postgraduate School Monterey, CA 93940	1

